5-2016

# Simulation of conservation practice effects on water quality under current and future climate scenarios

Carlington W. Wallace
*Purdue University*

*Graduate School Form*
*30 Updated 12/26/2015*

**PURDUE UNIVERSITY**
**GRADUATE SCHOOL**
**Thesis/Dissertation Acceptance**

This is to certify that the thesis/dissertation prepared

By Carlington W. Wallace

Entitled
Simulation of Conservation Practice Effects on Water Quality under Current and Future Climate Scenarios

For the degree of Doctor of Philosophy

Is approved by the final examining committee:

Dr. Bernard A. Engel
Chair

Dr. Dennis C. Flanagan

Dr. Keith Cherkauer

Dr. Venkatesh Merwade

To the best of my knowledge and as understood by the student in the Thesis/Dissertation Agreement, Publication Delay, and Certification Disclaimer (Graduate School Form 32), this thesis/dissertation adheres to the provisions of Purdue University's "Policy of Integrity in Research" and the use of copyright material.

Approved by Major Professor(s): Drs. Bernard A. Engel and Dennis C. Flanagan

Approved by: Dr. Bernard A. Engel 4/22/2016

Head of the Departmental Graduate Program Date

# SIMULATION OF CONSERVATION PRACTICE EFFECTS ON WATER QUALITY UNDER CURRENT AND FUTURE CLIMATE SCENARIOS

A Dissertation

Submitted to the Faculty of

Purdue University

by

Carlington W. Wallace

In Partial Fulfillment of the

Requirements for the Degree

of

Doctor of Philosophy

May 2016

Purdue University

West Lafayette, Indiana

This dissertation is in honor to my parents, the late Leebert and Eugennie Wallace, and to the Accompong Maroon community of St. Elizabeth, Jamaica.

# ACKNOWLEDGEMENTS

I owe thanks to many people whose assistance was indispensable throughout my graduate studies to this point of completing my research. Firstly, I thank my advisors Dr. Bernard A. Engel and Dr. Dennis C. Flanagan for accepting me as their student, for their guidance, thoroughness and promptness in reviewing my work. Without their patience, constructive comments and feedback, it would have been impossible to handle a research project of this magnitude. I would also like to extend my sincere thanks to my committee members Dr. Keith Cherkauer and Dr. Venkatesh Merwade for their participation in my dissertation committee and their valued feedbacks.

I would like to thank the staff at the USDA Agricultural Research Service National Soil Erosion Research Laboratory, West Lafayette, Indiana for accommodating me, for providing a pleasant working environment, and for providing the data used in this study.

I would also like to thank my brother Cadien Wallace, and my mentor Dr. Godfrey Gayle, for believing in me, and for being there every step of the way. Finally, I would like to say special thanks to my wife Ogechi Wallace and our daughter Chelsea for providing me with motivation and inspiration. None of this would have been possible without your love and patience.

TABLE OF CONTENTS

Page

Page

Page

# LIST OF TABLES

Table Page

# LIST OF FIGURES

Figure Page

Figure Page

# ABSTRACT

Wallace, Carlington W. Ph.D., Purdue University, May 2016. Simulation of Conservation Practice Effects on Water Quality under Current and Future Climate Scenarios. Major Professors: Bernard A. Engel and Dennis C. Flanagan

Analysis of the effects of implementing different conservation practices, as well as increased levels of conservation practices under existing and projected future climate, will determine if current conservation practice recommendations will be sufficient to maintain soil and water resources. The Soil and Water Assessment Tool (SWAT) was used to study four watersheds of different sizes (CCW = 680 $km^2$, F34 = 183 $km^2$, AXL = 42 $km^2$ and ALG = 20 $km^2$) located in Northeastern Indiana. The overarching goal of this study was to evaluate the effect of various agricultural practices on runoff and agricultural chemical losses under current and future climate conditions, using an appropriately calibrated SWAT model.

The results indicated calibrating SWAT at one watershed size and applying the optimized parameters to watersheds of different sizes with similar physiographic features produced satisfactory predictions of streamflow, nitrogen and phosphorus losses. Between the baseline period (1961-90) and the end of this century (2099), average annual precipitation for the watershed is expected to increase by approximately 8.5%, average daily solar radiation will increase by approximately 2.4% and average annual maximum and

minimum temperatures will increase by approximately 3.9 and 4.0$^{o}$ C, respectively. Based on SWAT simulations, changes in future climate resulted in decreased surface runoff (9% to 22%) and increased tile flow (20% to 25%) because more precipitation occurred in smaller events, allowing more infiltration to occur. There was an increase in sediment loss for all four watersheds (ranging from 6% to 30%), while average annual soluble P loss decreased for the CCW (10%) and F34 (25%) watersheds between the baseline period and the end of this century. Changes in atrazine, soluble N, total N and total P losses were not significant at $\alpha = 0.05$

Given the changes in projected future climate, the long-term impacts of both individual and combined conservation practices were assessed in the AXL watershed. The estimated average annual reductions for each decade of future climate due to conservation practices implementation ranged from 15% to 25% for surface runoff, 32% to 68% for sediment, 37% to 60% for atrazine, 5% to 13% for soluble N, 12% to 35% for total N, 9% to 41% for soluble P, and 33% to 60% for total P. Results of the study indicated that individual conservation practices were effective in reducing a targeted pollutant load, but combined practices were more effective in reducing multiple pollutant loadings simultaneously. No-till was the most effective individual conservation practice, while a combination of five conservation practices was most effective in reducing runoff, sediment, atrazine, and nitrogen and phosphorus losses.

***Keywords***: *Climate change, MarkSim, nutrients, surface flow, SWAT, tile flow*

# CHAPTER 1. GENERAL INTRODUCTION

One of the biggest water quality problems in agricultural watersheds stems from surface runoff that transports a variety of pollutants from various sources into rivers, streams and lakes (USEPA, 1994). These pollutants vary from sediment, pesticides, and nutrients to oil and pathogens (USEPA, 1994). Pollutant source areas may include agricultural lands, mining and construction sites, residential streets, lawns and parking lots (USEPA, 1994).

The Great Lakes, which consist of Lake Superior, Lake Michigan, Lake Huron, Lake Erie and Lake Ontario, are the largest system of fresh surface water on earth, by area, yet despite their large size, the Great Lakes are sensitive to the effects of a wide range of environmental pollutants from agricultural and urban runoff (USEPA, 2014). Lake Erie, the smallest of the five lakes (by volume) is the most significantly stressed from agriculture (USEPA, 2014). It receives agricultural runoff from southwest Ontario and portions of Indiana, Michigan, and Ohio.

The St. Joseph River Watershed Initiative (SJRWI) assessed water quality in the St. Joseph River, Indiana, USA, and identified pesticide and nutrient runoff from agricultural lands as primary stressors of surface water quality in the region (SJRWI, 2005). The St. Joseph River transports agricultural runoff from northeastern Indiana to the Maumee

River that eventually drains into Lake Erie (SJRWI, 2005), resulting in significant algal growth and poor water quality conditions. The overabundance of algae, which was primarily due to excess loading of nutrients, such as , into the lake, resulted in anoxic conditions that subsequently led to large fish kills during the 1970's (Rawls et al., 1980) and harmful toxic algal blooms that resulted in a ban on regional drinking water supply to the City of Toledo, Ohio as recently as August 2014 (Fitzsimmons, 2014).

The St. Joseph River also supplies drinking water to approximately 250,000 people in the City of Fort Wayne, Indiana. In 1995, high concentrations of atrazine (a pesticide used in corn production) above the EPA recommendations resulted in an extensive and costly treatment of source water in order to meet the required safe drinking water standards for atrazine (Cohen et al., 1995).

In an effort to mitigate these problems, the Environmental Protection Agency's (EPA) national water program is focused on conservation practices that are based on water quality controls implemented at the watershed scale (the Healthy Watershed Initiative) (USEPA, 2011). The healthy watershed strategy involves the development of Total Maximum Daily Loads (TMDLs) for polluted water bodies, which are followed by an implementation plan to address the load allocations established by TMDLs.

In an implementation plan, the required reductions needed to achieve water quality standards are usually accomplished through a combination of conservation practices. Conservation practices are sets of land management practices implemented to control soil losses, nutrients and other chemical losses that often lead to degradation of water quality

in rivers, streams and lakes. Conservation practices also help to improve agricultural lands, protect natural resources, forests and wildlife habitats. In 2002, Congress passed the Farm Security and Rural Investment Act (2002 Farm Bill Act), which resulted in a significant increase in funding for conservation programs throughout the country above the level set under the 1996 Farm Bill (Mausbach and Dedrick, 2004). Subsequently, the 2014 Farm Bill Act consolidated 23 overlapping conservation programs into 13, tightened eligibility rules for funding of these programs, and streamlined means tests to make farm programs more accountable.

Despite protecting millions of hectares, the environmental benefits of conservation practices have not been quantified to the extent that they can be reported at the national scale (Mausbach and Dedrick, 2004). As a result, the Conservation Effects Assessment Project (CEAP) was launched in an effort to provide accountability on how the millions of dollars being spent on conservation programs are benefiting the environment.

This study will address portions of the USDA ARS CEAP Watershed Assessment Study (WAS) Project Plan objectives, specifically, objectives two and three. Objective two of the plan seeks to quantify the effects of conservation practices on water quality and other environmental parameters, while objective three seeks to validate water quality models such as the Soil and Water Assessment Tool (SWAT) and determine their uncertainty at predictions of water quality parameters in 14 benchmark watersheds (Heathman et al., 2009).

Based on a review of available literature, several studies conducted using SWAT concluded that future climate changes tend to have significant influence on watershed processes (Ficklin et al., 2009; Gosain et al., 2006; Narsimlu et al., 2013). However, the extent to which watershed size affects future climate-change assessments is not clearly understood. Therefore, a quantitative analysis of the uncertainty in SWAT calibration parameters, and the effect of different agricultural practices on streamflow and chemical losses will be evaluated at four watersheds under current and future climate conditions using SWAT.

## 1.1. Research Goal

The overall goal of this study was to evaluate the effect of various agricultural practices on runoff and chemical losses under current and future climate conditions using the Soil and Water Assessment Tool (SWAT). First, SWAT was calibrated for streamflow, $NO_3$+$NO_2$ (soluble N), total nitrogen (total N), soluble phosphorus (soluble P) and total phosphorus (total P) losses at four watersheds (varying in size) under current management practices and climate conditions. Second, the MarkSim weather generator downscaling program developed by the International Centre for Tropical Agriculture (Jones and Thornton, 1999, 2000) was used to project future climate conditions, thus producing new climate inputs to SWAT, which were used to quantify the effect of future climate conditions on runoff and agricultural chemical losses.

Third, the effects of different types and levels of conservation practice implementation on predicted runoff and chemical losses were evaluated under current and future climate

conditions. Each objective and their related hypothesis are further defined in the following sections.

### 1.1.1. Quantifying the Effects of Watershed Size on SWAT Calibration

SWAT has been calibrated in many watersheds of various sizes and physiographic features. However, the relationship between model parameters optimization and the size at which SWAT was calibrated is not clearly understood. Understanding the influence of watershed size on SWAT model calibration will allow users to determine the validity of using such an assessment tool at various watershed sizes. Results of this objective were interpreted and used to select an appropriate watershed-calibration size to evaluate the effect of different types and levels of conservation practices, and future climate conditions on streamflow and chemical losses.

The specific objective was to evaluate the effect of watershed size on SWAT model calibration for streamflow, soluble N, total N, soluble P, and total P losses under current management practices and climate conditions. The size at which the model best represents watershed processes limits the successful application of watershed scale models in environmental studies and land and water resources management.

*Hypothesis*

Optimizing SWAT calibration parameters at one watershed size and then applying said optimized parameters at a different watershed size with similar physiographic features and management practices will not result in satisfactory predictions of streamflow, soluble N, total N, soluble P, and total P losses at the different watershed sizes.

### 1.1.2 Quantifying the Effects of Future Climate Conditions on Runoff, Sediment and Chemical Losses

Future climate conditions may greatly influence national and regional hydrologic conditions and subsequently affect runoff volume and chemical losses. The implications on future water resources and water quality may be severe; therefore, a more in-depth assessment is required especially in agricultural watersheds.

The specific objective of this portion of the study was to evaluate the effects of future climate conditions on runoff, sediment, atrazine, soluble N, total N, soluble P, and total P losses under current management practices using SWAT. The MarkSim weather generator was used to project future climate conditions and create new weather input files for SWAT. MarkSim has been used to project future climate conditions and generate new climate files for crop modeling and risk assessment in Africa, South America and the US (Jones and Thornton, 1999, 2000).

*Hypothesis*

Future climatic conditions in northeastern Indiana will have a significant influence on runoff, sediment, atrazine, soluble nitrogen, total nitrogen, soluble phosphorus and total phosphorus losses under current management practices.

### 1.1.3 Quantifying the Effects of Conservation Practice Implementation on Predicted Runoff and Chemical Losses

Quantifying the impact of long-term conservation practice implementation given current and future climate conditions can provide insight into the long-term effectiveness of best management practices (BMPs). The specific tasks required to complete this objective were:

1) Modify SWAT model parameters and algorithms in order to represent blind inlets as conservation practices in SWAT. A blind inlet is a filtration system installed in closed depressions (potholes) that traps sediment and other contaminants, thus reducing pollutants entering subsurface tiles.

2) Evaluate the impact of no-tillage, vegetative buffer strips, grassed waterways, blind inlets and nutrient management on runoff, sediment, pesticide, and nutrient reduction under current and future climate conditions. The methods for representing these conservation practices were based on published literature pertaining to BMP simulation in hydrologic models, and considering the hydrologic and water quality processes simulated in SWAT.

*Hypothesis*

Given future climate conditions for northeastern Indiana, the implementation of best management practices will result in significant reductions of pesticide, sediment and nutrient losses at the watershed scale there.

# CHAPTER 2. QUANTIFYING THE EFFECTS OF WATERSHED SIZE ON SWAT CALIBRATION

## 2.1 Synopsis

The Soil and Water Assessment Tool (SWAT) has been calibrated in many watersheds of various sizes and physiographic features. However, the relationship between model calibration parameters and the watershed size at which SWAT was calibrated is not clearly understood. Understanding the influence of watershed size on SWAT model calibration parameters will allow users to determine the validity of using such an assessment tool at various sized watersheds. Additionally, this will allow users with limited data to determine whether it is appropriate to calibrate SWAT in one watershed and implement the optimized parameters in a different watershed with similar physiographic features. In this study, SWAT was used to investigate the influence of watershed size on SWAT model calibration on four watersheds (CCW = 680 $km^2$, F34 = 183 $km^2$, AXL = 42 $km^2$ and ALG = 20 $km^2$) located in Northeastern Indiana. The results show that calibrating SWAT at one size and applying the optimized parameters at different watershed sizes of similar physiographic features will produce satisfactory simulation results. The size at which the model was calibrated had little effect on streamflow simulations. The predictions of soluble nitrogen loss were improved when calibration was performed at the larger CCW watershed, while calibrating SWAT at the

smaller AXL and ALG watersheds produced improved NSE, $R^2$ and PBIAS values for soluble P and total P when applied to the larger CCW and F34 watersheds. Due to the physical characteristics of the F34 watershed, SWAT parameters optimized at the F34 level did not always result in satisfactory results when applied to the CCW, AXL and ALG watershed configurations.

## 2.2 Introduction

Growing concerns over water quality in agricultural watersheds continue to be the topic of many discussions. Agricultural runoff is considered a primary cause of nonpoint source pollution in the United States (Yu et al., 2004) because it often transports pesticides, nutrients and sediment from agricultural fields and other areas to rivers and streams. This may have serious implications for the chemical, physical and biological integrity of the nation's water bodies (USEPA, 1994). The Farm Security and Rural Investment Act provide significant financial assistance for farmers to construct and improve watershed management structures, and to implement conservation practices that will control soil erosion and improve water quality. The primary pollutants affecting water quality in northeastern Indiana and much of the Midwest Corn Belt Region are nitrogen and phosphorus, particularly soluble phosphorus (Lake Erie LAMPs, 2011) that are transported in agricultural runoff.

An effective watershed management program is one that minimizes the loss of agricultural chemicals and maintains water quality standards. However, developing an effective watershed management program requires comprehensive understanding of the

hydrologic and chemical processes within the watershed (Larose et al., 2007). These processes are usually examined at the watershed scale using computer simulation models such as the Soil and Watershed Assessment Tool (SWAT) (Arnold et al., 1998). SWAT is also used to assess the effect of various management practices, and for developing and improving watershed management programs (Spruill et al., 2000).

SWAT is useful for providing long-term analysis of watershed processes and does not model individual storm events effectively. It was developed for use in large ungauged watersheds and can be used without calibration (Neitsch, 2002). However, SWAT model parameters vary in sensitivity during different flow regimes and for different simulation periods, therefore requiring dynamic updating of parameters during the simulation. As a result, several researchers recommend that SWAT be calibrated in cases where measured data are available, because calibration will improve the model's performance thus resulting in more accurate simulations (Kirsch et al., 2002; Santhi et al., 2001).

In recent years, several procedures have been developed to perform calibration and uncertainty analysis of hydrologic models such as SWAT. The SWAT Calibration and Uncertainty Program (SWAT-CUP) (Abbaspour et al., 2007), as described below, links several of these processes to SWAT in order to provide an automated calibration and uncertainty analysis tool that may be tailored to a specific project.

Several studies (Bingner et al., 1997; FitzHugh and Mackay, 2000; Kumar and Merwade, 2009; Muleta and Nicklow, 2005) have evaluated the effects of spatial scale on SWAT streamflow simulations and have concluded that streamflow predictions are not very

sensitive to spatial scale. An earlier study (Jha et al., 2004) also suggested that spatial scale had very little effect on streamflow simulations, but will definitely impact the simulation of nitrogen and  loss simulations. Heathman et al. (2007) attempted to explore the influence of scale on SWAT model calibration when they compared observed versus simulated streamflow for SWAT model calibration at the 2810 $km^2$ St. Joseph River Basin (SJRW) in Indiana (one of the 14 Conservation Effects Assessment Project benchmark watersheds) and at the 679.2 $km^2$ Cedar Creek watershed (largest tributary in SJRW). They concluded that the scale at which the model was calibrated had little impact on SWAT simulated streamflow for the watersheds. This conclusion was supported by (Thampi et al., 2010) based on a study in the Chaliyar River Basin (Kerala, India). Srinivasan et al. (1998) also calibrated SWAT in the 5,157 $km^2$ Richland and Chambers Creek watershed in Upper Trinity Basin, Texas, and validated it at the smaller Mill Creek watershed (282 $km^2$), and concluded that the model explained at least 84 percent of the variability in the observed streamflow data.

Despite being calibrated in many watersheds of various sizes and physiographic features, the relationship between SWAT calibration parameters and the size at which SWAT was calibrated is still not clearly understood, especially for nitrogen and phosphorus simulations. Understanding the influence of watershed size on SWAT model calibration parameters will provide insight into the validity of using such an assessment tool at various watershed sizes. This will also help to determine whether it is acceptable to

calibrate the model in one watershed and apply the optimized parameters in a watershed with a different size, assuming both watersheds have similar physiographic properties.

### 2.2.1 SWAT Model Description

SWAT is a lumped, semi-distributed hydrologic model developed by USDA ARS to study the effects of management decisions on water quality "with reasonable accuracy" on large ungauged watersheds (Arnold et al., 1998). SWAT is capable of operating on a daily time step or annual time steps for long-term simulations (Arnold et al., 1998). SWAT uses a two-level "disaggregation" scheme to represent large complex watersheds. First, it divides the watershed into sub basins based on topographic features, and then further discretizes those sub basins into Hydrologic Response Units (HRUs) based on unique combinations of land use, soil type and slope classes. Computations are then performed at the HRU level, which are assumed homogeneous in hydrologic response to land use/land cover change. The major components of the model include hydrology, land management, nutrients, pathogens and bacteria, pesticides, plant growth, soil properties and weather (Arnold et al., 2012).

### 2.2.2 Uses and Limitations

SWAT is a public domain model that is often used for predicting and interpreting the effects of agricultural management practices and climate variability on water quality, and in assessing the environmental efficiency of conservation practices in very complex watersheds (Arnold and Fohrer, 2005; Arnold et al., 1998; Van Liew et al., 2003). It is widely used by government agencies, research institutions, universities, and private

corporations worldwide to assess the influence of climate change, land management, and other processes on a wide range of water resources or “exploratory assessments of model capabilities for potential future applications” (Gassman et al., 2007). Since its conception in the early 1990s, SWAT has gained worldwide acceptance with applications in places such as the United States, European Union, Africa, South America, Asia, Middle East and the Caribbean.

The integration of SWAT with ArcGIS (ArcSWAT) provides a user-friendly interface that simplifies model inputs and parameterization. Advanced users can easily modify SWAT to simulate additional processes and conditions, as well as incorporate other simulation models such as the Agricultural Policy Environmental EXtender (APEX) model. SWAT and APEX are currently being used to support CEAP and for landscape and watershed environmental analysis. Other strengths of the model include its ability to analyze both point and nonpoint sources of pollution.

While SWAT was developed for use on ungauged watersheds, extensive calibration is often required to improve model performance. Overall, SWAT offers the most comprehensive representation of environmental processes that can be used to assess land use and management alternatives that may affect water quality, and support decision making at national and regional levels.

### 2.2.3 Hydrologic Processes

In order to simulate hydrologic processes, SWAT requires climate inputs such as daily precipitation, maximum/minimum air temperatures and solar radiation. These climate

data drive the hydrologic cycle and provide moisture and energy inputs that control the water balance. The water balance is the primary driver of the hydrologic processes, fate and transport of nutrients and pesticides, plant growth, and sediment processes in the watershed (Arnold et al., 2012). SWAT separates watershed hydrology into two main phases; the land phase controls the amount of water, nutrients, pesticides, and sediments being transported from the land surface to the main channel in each subbasin; and the routing phase controls the transport of water, nutrients, pesticides, and sediments through the channel network of the watershed to the outlet (Arnold et al., 2012). Hydrologic processes simulated by SWAT include evapotranspiration (ET), infiltration, lateral shallow aquifer and deep aquifer flow, percolation losses, redistribution of water within the soil profile, surface runoff, tile drainage, return flow, and recharge by seepage from surface water bodies, ponds, and tributary channels (Arnold et al., 2012). SWAT provides multiple options for estimating potential evapotranspiration (Penman-Monteith method, Priestley-Taylor or Hargreaves method) and runoff (Soil Conservation Service runoff curve number (CN) or the Green-Ampt infiltration model (Green and Ampt, 1911). The Penman-Monteith method (Monteith, 1995) as described in Equation (2.1), captures the effects of wind and relative humidity, thus accounting for vegetation shading, wind resistance, and transpiration through leaves, which makes it suitable for application in highly vegetated watersheds. Therefore, given the vegetated nature of the study watersheds, the Penman-Monteith method was selected over the Priestley-Taylor and Hargreaves methods for estimating evapotranspiration.

$$\lambda E = \frac{\Delta*(H_{net}-G)+\rho_{air}*c_p*\frac{[e_z^o-e_z]}{ra}}{\Delta+\gamma*\left(1-\frac{r_c}{r_a}\right)} \quad (2.1)$$

where λE is the latent heat flux density (MJ/m$^2$/d), Δ is the slope of the saturation vapor pressure temperature curve (kPa/$^o$C). $H_{net}$ is the net radiation (MJ/m$^2$/d), G is the heat flux density to the ground (MJ/m$^2$/d), $\rho_{air}$ is the air density (kg/m$^3$), $c_p$ is the specific heat at constant pressure (MJ/kg/°C), $e_z^o$ is the saturation vapor pressure of air at height z (kPa), $e_z$ is the water vapor pressure of air at height z (kPa), $\gamma$ is the psychrometric constant (kPa/°C), $r_c$ is the plant canopy resistance (s/m), and $r_a$ is the diffusive resistance of the air layer (s/m).

The CN method (USDA-SCS, 1986) as described in Equation (2.2) was selected instead of the Green and Ampt equation in this study for its simplicity, predictability and stability. It does not require rainfall intensity and duration data, rather only total daily rainfall depth is required when estimating surface runoff. Despite the fact that the CN method fails to account for the spatial and temporal variability of infiltration and other abstractive losses, it is believed to simulate the saturation overland flow mode of runoff generation sufficiently, especially on agricultural lands for which it was originally intended (Ponce and Hawkins, 1996). King et al. (1999) compared the Green-Ampt method versus the SCS CN method using SWAT and concluded that no significant advantage was gained by using Green-Ampt to estimate surface runoff in a large pasture dominated watershed. SCS CN is an empirical model developed by the USDA Natural Resources Conservation

Service (formerly the Soil Conservation Service) to provide consistent estimates of runoff from various land use and soil types. The equation is as follows:

$$Q_{sruf} = \frac{(P_{day} - 0.2S)^2}{(P_{day} + 0.8S)} \quad (2.2)$$

where $Q_{surf}$ is the accumulated runoff depth (mm), $P_{day}$ is the precipitation depth (plus snowmelt) for the day (mm), and $S$ is the potential maximum retention (mm) that may be defined using Equation (2.3):

$$S = 25.4\left(\frac{1000}{CN} - 10\right) \quad (2.3)$$

where CN is the curve number for the day.

The channel water routing needed to predict the changes in the magnitude of the peak and the corresponding stage of flow as a flood wave moves downstream was based on the variable storage coefficient method (Arnold et al., 2012). The change in volume of storage during the time step is the difference between the inflow volume and the outflow volume in this simple continuous model.

### 2.2.4 Nitrogen Processes

Nitrogen (N) processes are simulated in SWAT using a typical nitrogen cycle to track the transport and fate of various forms of N throughout the watershed (Arnold et al., 1998). The portion of N used by plants is estimated using the supply and demand approach. Nitrates and organic N are also removed from the soil through mass flow of water. Nitrate loading is estimated as the product of average nitrate concentration and the volume of

water present in a particular layer (Arnold et al., 1998). The amount of N loss through surface runoff is calculated using Equations (2.4) and (2.5):

$$NO3_{conc} = \frac{NO3_{lyr} * \left(1 - \exp\left[\frac{-w_{mobile}}{(1-\theta_e) * SAT_{lyr}}\right]\right)}{w_{mobile}} \quad (2.4)$$

$$NO3_{surf} = \beta_{NO3} * NO3_{conc} * Q_{surf} \quad (2.5)$$

where $NO3_{conc}$ is the concentration of nitrate in the water (kg N/mm), $NO3_{lyr}$ is the amount of nitrate in the layer, and $w_{mobile}$ is the amount of mobile water in the layer (mm). $\theta_e$ is the fraction of porosity excluding anions, $SAT_{lyr}$ is the saturated water content of the soil layer (mm), $NO3_{surf}$ is the nitrate removed in surface runoff (kg N/ha), $\beta_{NO3}$ is the nitrate percolation coefficient, and $Q_{surf}$ is the surface runoff generated on a given day (mm). Nitrate loss through lateral flow and percolation are also calculated using similar equations. The amount of organic N transported with sediment to the stream is calculated using the Williams and Hann (1978) loading function, Equation (2.6):

$$orgN_{surf} = 0.001 * orgN_{conc} * \frac{S_{day}}{A_{hru}} * \epsilon_{Nsday} \quad (2.6)$$

where $orgN_{surf}$ is the amount of organic N transported to the main channel in surface runoff (kg N/ha), $orgN_{conc}$ is the concentration of organic N in the top 10 mm (g N/ton), $S_{day}$ is the sediment yield on a given day (tons), $\epsilon_{Nsday}$ is the N enrichment ratio, and $A_{hru}$ is the area of the specific HRU (km$^2$).

### 2.2.5 Processes

(P) processes are simulated in SWAT using a typical cycle to track the transport and fate of various forms of P throughout the watershed (Arnold et al., 1998). The portion of P used by plants is estimated using the supply and demand approach. Soluble P and organic P are also removed from the soil through mass flow of water. Soluble P loading is estimated using the solution P concentration in the top 10 mm of the soil, runoff volume and a partitioning factor (Arnold et al., 1998), Equation (2.7):

$$P_{surf} = \frac{P_{solution,surf} * Q_{surf}}{\rho_b * depth_{surf} * k_{d,surf}} \quad (2.7)$$

where $P_{surf}$ is the amount of soluble P loss in surface runoff (kg P/ha), and $P_{solution,surf}$ is the amount of dissolved P in the top 10 mm of the soil (kg P/ha). $Q_{surf}$ is the amount of surface runoff on a given day (mm), $\rho_b$ is the bulk density of the top soil layer (Mg/m$^3$), $depth_{surf}$ is the depth of the surface layer (10 mm), and $k_{d,surf}$ ( soil partitioning coefficient) is the ratio of soluble P concentration in the first 10 mm of soil to the concentration of soluble P in surface runoff (m$^3$/Mg). The amount of organic P transported with sediment to the stream is calculated using the Williams and Hann (1978) loading function, similar to organic nitrogen transport.

### 2.2.6 Closed Depressions and Tile Drainage Processes

Isolated closed depressions with no natural outlet are often filled with water, especially after heavy storm events or snowmelt. The potholes can have a significant effect on the hydrologic balance, and can reduce crop yields when they fill with water (Smith and

Livingston, 2013). Therefore, in order to maximize crop production, closed depressions are often drained using surface tile inlets. These surface tile inlets are usually plastic pipes extending approximately one meter above the soil surface with one to two centimeter diameter-holes, or a metal cage that extends 0.25 to 0.4 m above the ground, placed at the lowest point of the depression to drain the ponded surface water (Feyereisen et al., 2015). The tile inlets are attached to subsurface drain tiles that transfer water from the field directly to the stream network.

The water balance for a pothole is represented in Equation (2.8) (Du et al., 2005) as:

$$V = V_{pcp} + V_{flowin} + V_{stored} - V_{evap} - V_{seep} - V_{flowout} \quad (2.8)$$

where V is the volume of water in the impoundment at the end of the day ($m^3$), and $V_{pcp}$ is the volume of precipitation falling in the pothole during the day ($m^3$). For surface area and precipitation volume calculations, the potholes are assumed to be cone-shaped (Du et al., 2005). $V_{flowin}$ is surface runoff and lateral subsurface water flow from upland HRUs in the subbasin during the day ($m^3$), and $V_{stored}$ is the volume of water stored in the pothole at the beginning of the day ($m^3$). $V_{evap}$ is the volume of water removed from the pothole by evaporation during the day ($m^3$), $V_{seep}$ is the volume of water lost from the pothole by seepage ($m^3$), and $V_{flowout}$ is the volume of water flowing out of the pothole during the day ($m^3$). In previous versions of SWAT, all HRU flow was assumed to contribute directly to the channel system without interacting with other HRUs. However, with recent modifications (Du et al., 2005), the user is able to specify the fraction of flow

from upland HRUs that contributes to the pothole HRU (*pot_fr*), with the remainder flowing directly into the channel system.

When surface tile inlets are installed in a pothole, the pothole will contribute water to channels through tile flow. The pothole outflow originating from surface inlets is as follows:

$$\text{if } V > pot\_tile * 86400,\ V_{flowout} = pot\_tile * 86400 \quad (2.9)$$

$$\text{if } V \leq pot\_tile * 86400,\ V_{flowout} = V \quad (2.10)$$

and if overflow and surface tile inlet-led flow in a pothole occur at the same time,

$$V_{flowout} = pot\_tile * 86400 + V - pot\_volx \quad (2.11)$$

where $V_{flowout}$ is the volume of water flowing out of the water body during the day ($m^3$), $pot\_tile$ is the average daily tile flow rate ($m^3\ s^{-1}$), $V$ is the volume of water entering the pothole ($m^3$), and $pot\_volx$ is the maximum amount of water that can be stored in the pothole ($m^3$) (Du et al., 2005).

Tile flow is predicted on days when the simulated height of the water table over the impervious layer is greater than the height of the tile above the impervious layer. In other words, tile flow occurs when the water table height exceeds the height of the tile drains. Simulation of tile drainage in an HRU is indicated by the presence of a DDRAIN parameter greater than zero, and a design drawdown time (TDRAIN) is used to determine the "rate" of flow. Du et al. (2005) introduced a new drainage coefficient (tiletime), which determines the portion of the flow from the tile drains into the streams on a daily basis, essentially smoothing the drain flow hydrograph (Equation 2.12):

$$tiletime = 1 - e^{\left(-\frac{24}{GDRAIN}\right)} \quad (2.12)$$

where GDRAIN is the drain tile lag time (h). The depth from the soil surface to the impervious layer is represented by DEP_IMP (mm), which can be varied between drained and undrained HRUs. The DEP_IMP parameter defines the depth to the impervious layer in the soil profile and is required if perched water tables, closed depressions (potholes) or tile drainage are being modeled in an HRU.

## 2.3 Objective

This study examines the influence of watershed size on SWAT calibrations for streamflow, nitrogen and phosphorus losses from four watersheds within the St. Joseph River Watershed (SJRW) in northeastern Indiana. Watershed characteristics such as land use, soil type, climate and other physiographic features are approximately the same at the different watershed sizes considered here, which therefore conforms to the concept of downscaling rather than regionalization. However, more area-specific land management data required by SWAT for parameterization are available for the smaller watersheds where farm management records are available. Usually in larger watersheds, management information for SWAT is generalized based on countywide averages (Heathman et al., 2007; Larose et al., 2007).

## 2.4 Methodology

### 2.4.1 Study Area Description

The St. Joseph River Watershed is a 2,810-km$^2$ catchment that intersects the states of Indiana, Michigan and Ohio (Figure 2.1). The headwaters of the St. Joseph River originate in Michigan, and the river flows through Ohio and Indiana before joining the St. Mary's River near Ft. Wayne, Indiana to form the Maumee River. The Maumee River flows into the Maumee Bay of Lake Erie in Toledo, Ohio. The Cedar Creek watershed (CCW = 679 km$^2$) located in northeastern Indiana (85°19'28.101" to 84°54'12.364"W and 41°11'47.494" to 41°32'8.776"N) is the largest tributary to the St. Joseph River, intersecting the counties of Allen, DeKalb and Noble. Cedar Creek is predominantly an agricultural watershed (68%) with approximately 15% forest (Table 2.1).

The majority of soils in the watersheds are comprised of the Eel-Martinsville-Genesee and Morley-Blount associations. The Eel-Martinsville-Genesee association consists of deep, moderately well drained, nearly level, and medium to moderately fine-textured soils on low lands and stream terraces (Larose et al., 2007; SJRWI, 2004). The Morley-Blount association occurs mostly in the upland and consists of deep, moderately to poorly drained soils with nearly level to deep medium-textured soils (USDA, 2014). Tile drainage systems are used to drain water from many of these soils into managed drainage ditches, which resulted in alteration of the watershed hydrology and the transport of pesticide and nutrients across the landscape (Pappas and Smith, 2007; Smith et al., 2008). CCW is the largest of the four calibration watersheds analyzed in this study. The three

remaining watersheds (F34 = 182.5 km$^2$, AXL = 41.5 km$^2$ and ALG =19.7 km$^2$) are nested within the upper Cedar Creek (Figure 2.1) and share similar physiographic features to that of Cedar Creek (Table 2.1).

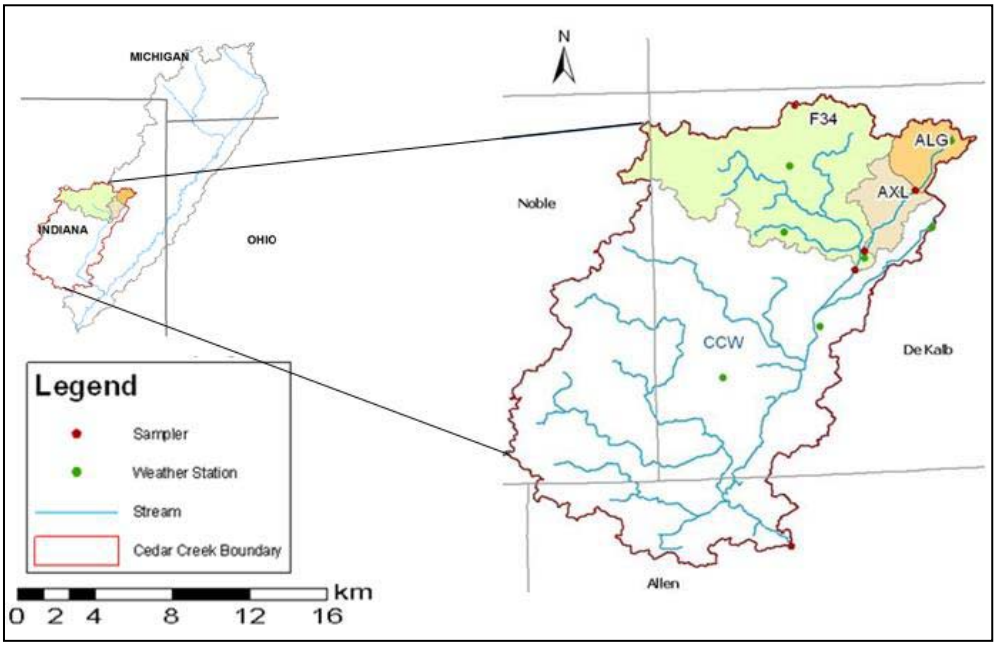


Figure 2.1. Location map of the study areas (CCW, F34, AXL and ALG).

Table 2.1. Description of watershed characteristics (land use distribution, topography and average annual climate conditions).

| Land use (NASS, 2011) | CCW | F34 | AXL | ALG |
|---|---|---|---|---|
| Corn (%) | 21.0 | 27.2 | 23.9 | 18.8 |
| Soybean (%) | 23.7 | 25.6 | 37.9 | 44.1 |
| Winter Wheat (%) | 3.2 | 3.1 | 5.3 | 7.7 |
| Pasture (%) | 19.4 | 16.2 | 12.8 | 12.0 |
| Forest-Mixed (%) | 14.8 | 11.5 | 10.1 | 8.8 |
| Residential (%) | 10.5 | 7.5 | 5.8 | 4.7 |
| Other (%) | 7.5 | 8.9 | 4.3 | 4.0 |
| Watershed area (km$^2$) | 679.2 | 182.5 | 41.5 | 19.7 |
| % of watershed area contributing to farmed-closed depressions (%) | 5.1 | 8.2 | 10.0 | 8.7 |
| Average depth of farmed closed depression (m) | 0.94 | 0.82 | 0.91 | 0.90 |
| Average slope (%) | 1.5 | 1.9 | 1.0 | 1.2 |
| Average annual rainfall (2001 to 2013) (mm) | 960 | 948 | 948 | 948 |
| Average temperature during crop growth season ($^o$C) | | 10 to 23 | | |

### 2.4.2 Model Input and Setup

The ArcSWAT version 2012.10.5a interface was used to expedite SWAT model input and output display. To obtain suitable flow paths, the stream delineation from the National Hydrograph Dataset (NHD) was used to burn in the location of the streams in a 10-m Digital Elevation Model (DEM) obtained from USGS at a map scale of 1:24,000. The USGS National Water Quality Assessment Program (NAWQA) water quality/streamflow gauge station located near Cedarville, Allen County, Indiana was used as the watershed outlet for CCW. The USDA Agricultural Research Service (ARS) National Soil Erosion Research Laboratory (NSERL) water quality/streamflow gauge stations were used to specify the location of the F34, AXL and ALG outlets. The Soil Survey Geographic Database (SSURGO) spatial data at a scale of 1:12,000 and the USDA National Agricultural Statistics Service (USDA-NASS, 2011) Indiana Cropland Layer were used to determine hydrologic response units (HRUs) for SWAT.

HRUs (also referred to as modeling units) are unique combinations of land use, soils, and slope classes within each sub-basin, whereby, the model establishes management practices. In order to establish modeling units, SWAT must first divide the watershed into smaller subbasins based on a specified critical source area (CSA) threshold for stream generation. CSA is specified as a percentage of the total watershed area that determines the minimum upstream drainage area required to form a channel. The second division occurs when each subwatershed is further divided into HRUs using a specified threshold area for land use, soil types and slope classes in each subwatershed.

Table 2.2. Model input data, sources and descriptions.

| Data Type | Source | Description |
|---|---|---|
| DEM | viewer.nationalmap.gov/viewer/ | 10-m Resolution, Digital Elevation Model (USGS ,2011) |
| Soils | soildatamart.nrcs.usda.gov/ | Soil Survey Geographic Database (SSURGO) (USDA-NRCS, 2011) |
| Land use | http://www.nass.usda.gov/ | National Agricultural Statistics Service (USDA-NASS, 2011) |
| Hydrographic | nhd.usgs.gov/data.html | National Hydrograph Dataset (NHD) (USGS, 2011) |
| Weather | ARS-CEAP Water Quality Assessment Program | Daily precipitation, solar radiation, wind, relative humidity, maximum and minimum daily temperature (2001 to 2012) |
| Weather | National Climate Data Center ncdc.noaa.gov/data-access/ | Daily precipitation, maximum and minimum daily temperature (2001 to 2012) (Diamond et al., 2013) |
| Crop Management | ARS CEAP watershed survey, DeKalb and Allen County SWCDs | Tillage operations, fertilizer and herbicide applications, crop rotation, time of planting and time of harvesting |
| Water Quality | St. Joseph River Watershed Initiative | Streamflow, bi-weekly pesticide and nutrient concentration (TP, TN, $NO_2$+$NO_3$) |
| Water Quality | ARS CEAP Water Quality Assessment Program | Streamflow, daily pesticide and nutrient concentration (TP, PO4, TN, NO2+NO3) |

Table 2.3. Minimum stream threshold values and the resulting subwatersheds and HRUs for each study watershed.

| Watershed | Stream Threshold (ha) | Sub watersheds | HRUs |
|---|---|---|---|
| CCW | 3000 (5% of watershed area) | 17 | 5474 |
| F34 | 900 (5% of watershed area) | 11 | 1954 |
| AXL | 200 (5% of watershed area) | 11 | 806 |
| ALG | 100 (5% of watershed area) | 14 | 659 |

For this research, a critical source area of 5% was specified for each watershed, which resulted in stream threshold area of 30 $km^2$, 9 $km^2$, 2 $km^2$ and 1 $km^2$ for CCW, F34, AXL and ALG, respectively (Table 2.3). The threshold for HRU definition was set to 0% land: 0% soil: 0% slope, which means that all possible land use/soil/slope combinations were assessed. This was necessary to facilitate the spatial representation of closed depressions

within the watersheds. The minimum stream threshold value and the resulting sub watersheds and HRUs for each of the study watersheds are shown in Table 2.3.

Climate data such as precipitation, maximum and minimum air temperatures, solar radiation, relative humidity, and wind speed were obtained from 10 CEAP weather stations located in the upper Cedar Creek region for the period 2003 to 2013. Daily precipitation and maximum and minimum air temperatures were also obtained from the National Climate Data Center (Diamond et al., 2013) for the Auburn, Angola, Butler, Garrett, and Waterloo stations located within or around the watershed, with records from 1980 to 2013. Missing data for a given station were estimated by averaging values for the nearest weather stations, typically within a 5 km radius. Because less than five percent of each dataset were missing, the replacement method was expected to have negligible effects on simulation results.

Area-specific land management data (Tables 2.4 and 2.5) were collected by the ARS-NSERL through the CEAP program, as well as from the DeKalb and Allen Counties Soil and Water Conservation Districts (SWCDs), and were used to represent the current management practices occurring in the Cedar Creek watershed. Conservation tillage has been widely adopted in the watershed. In DeKalb County, 34% of all corn and 77% of all soybeans planted in 2012 were under a no-till system or mulch-till system (DeKalb SWCD, 2012). Therefore, no-till and conventional tillage were used as input in the SWAT management file. The management files were constructed to simulate corn/soybeans (the predominant crops in the watershed), rotated on all lands classified as corn or soybeans.

All lands classified as wheat were simulated in a three-year rotation with corn and soybeans (corn/soybeans/wheat). The management scheme includes yearly tillage operations, nutrient and pesticide application rates, planting and harvesting dates (Tables 2.4 and 2.5).

Tile drainage was assumed for all corn, soybean and winter wheat areas. The tile drainage area was considered to have an average depth of 1.0 meter, 48 hours of drainage after a rain to reach field capacity, with a drain tile lag time of 24 hours (Du et al., 2005; Larose et al., 2007). The typical spacing between tiles (estimated based on soil type and drainage) is 20 meters (Wright and Sands, 2001).

Table 2.4. Management operations for land in corn/soybeans rotation.

| Crop | Date | Management Operation | Rate |
|---|---|---|---|
| Corn | 22-Apr | Nitrogen Application (as Anhydrous Ammonia) | 176.0 kg/ha |
| | 22-Apr | ($P_2O_5$) Application (as DAP/MAP) | 54.0 kg/ha |
| | 22-Apr | Pesticide Application (as Atrazine) | 2.2 kg/ha |
| | 6-May | Tillage - Offset disk (60% mixing) | |
| | 6-May | Planting - Row planter, double disk openers | |
| | 10-Oct | Harvest | |
| Soybeans | 10-May | ($P_2O_5$) Application (as DAP/MAP) | 40.0 kg/ha |
| | 24-May | No-tillage planting - Drills | |
| | 7-Oct | Harvest | |
| | 20-Oct | Tillage, Chisel (30% mixing) | |

Table 2.5. Management operations for land in winter wheat production (following corn/soybeans rotation in Table 2.4).

| Crop | Date | Management Operation | Rate |
|---|---|---|---|
| Wheat | 23-Oct | ($P_2O_5$) Application (as DAP) | 45.0 kg/ha |
| | 25-Oct | Tillage, Tandem disk (60% mixing) | |
| | 25-Oct | Planting – Drills, double disk openers | |
| | 1-Mar | Nitrogen Application (as Urea) | 75.0 kg/ha |
| | 1-Jul | Harvest | |

Closed depressions (potholes) and tile inlets were also addressed in the SWAT configurations. In order to represent potholes in SWAT, ArcGIS version 10.1 was used to process a 1-meter DEM of the entire study area. The processing involves: 1) identifying sink features in the elevation dataset; 2) classifying sink features as potholes based on certain criteria; 3) create pothole look-up tables that will link pothole features with SWAT HRUs, and 4) update SWAT HRU files using a simple python script. Detailed descriptions of these steps are presented in Table 2.6, which may be adjusted to suite modeling needs. The percentages of watershed area contributing flow to farmed closed depressions were estimated at 5.1%, 8.2%, 10.0% and 8.7% for CCW, F34, AXL and ALG, respectively. Average depths of potholes were 0.94 meter, 0.82 meter, 0.91 meter and 0.90 meter for CCW, F34, AXL and ALG, respectively.

SWAT was set up to run on a daily time step for the period 2001 to 2013 with a warm-up period of five years (01/2001 to 12/2005). The warm-up period is recommended for the model to initialize and approach reasonable starting values for model variables (Tolson and Shoemaker, 2007) before beginning the calibration process.

Table 2.6. Detailed methods for representing potholes in SWAT.

| Phase 1: Identifying sinks using ArcGIS |
|---|
| 1) Fill sinks in a 1-meter DEM for the entire Cedar Creek watershed.<br>2) Subtract the original DEM from the filled DEM to obtain a raster with only the sink features.<br>3) Convert sink raster to feature class.<br>4) Use the interpolate function in the 3D Analyst tool to interpolates z-values for the feature class based on the 1-meter DEM.<br>5) Add a new field to the attribute table of the new feature to calculate the average depth of the sink (subtract minimum z-value from maximum z-value).<br>6) Add another field to the attribute table of the feature class, and then use Calculate Geometry to calculate the area in hectares for each feature. |
| Phase 2: Classifying closed depressions as sink features in cultivated lands using ArcGIS |
| 7) Use the select by Attribute tool to select small polygons (e.g. features <0.2ha and features with depth < 0.5m), then delete the selected features.<br>8) Add the stream network layer to the map, and then use the Select by Location tool to select features that intersect or fall within 100 meters of the stream network. Delete the selected features.<br>9) Use a base map (aerial photo) to locate sink features that represent actual ponds and wetlands, and then manually delete them from the feature class.<br>10) Add the land use layer to the ArcGIS display, and then use the Make Feature tool to select all sink features that are within cultivated lands. The resulting feature class will consist of only closed depressions (potholes) that are likely to be tile-drained for cultivation. |
| Phase 3: Creating pothole lookup table |
| 11) Use the Drainage Area Characterization tool from the Terrain Morphology menu in ArcHydro to calculate the volume of the potholes<br>12) Add the HRU shapefile from the initial SWAT configuration to the ArcGIS display and use the spatial join tool to associate the potholes with the HRUs, and then export the new attribute table to excel.<br>13) Open the excel file and use a pivot table to summarize the data into three columns (column one contains the HRU ID, column two contains the aggregated pothole area for each HRU, and column three contains the aggregate pothole volume for each HRU). The summarized data is then saved as the pothole lookup table. |
| Phase 4: Updating SWAT HRU files using python |
| 14) A simple python script was created to add the pothole information to the respective HRU files. The script reads the lookup table and HRU files (located in the TextInOut folder), converts volume in $m^3$ to mm and updates the pot_volx parameter.<br>15) Other pothole related parameters pot_tile, pot_fr, pot_solp, pot_no3L, and pot_NSED were also updated using the python script. |

### 2.4.3 Model Calibration and Validation

Calibration is the process used to optimize parameters in a model using observed conditions in an effort to reduce the prediction uncertainty associated with the model. Parameters in SWAT were calibrated at the monthly time scale in a distributed fashion

using the SWAT-CUP autocalibration tool. Calibration was performed at the F34, AXL and ALG outlets for streamflow, $NO_3$+$NO_2$ nitrogen (soluble N), total nitrogen (total N), orthophosphate (soluble P) and total phosphorus (total P) over a 4-yr period (01/2006 to 12/2009). Due to limited data availability, SWAT was calibrated at the CCW outlet near Cedarville for streamflow (01/2006 to 12/2009), soluble N (04/2006 to 12/2009), and total P (4/2006 to 2009).

Historical measured data for streamflow, soluble N and total P concentrations were obtained from the St. Joseph River Watershed Initiative for the CCW outlet near Cedarville, while soluble N, total N, soluble P and total P concentrations were obtained from the ARS-NSERL-CEAP database for the F34, AXL and ALG outlets. Measured data for total nitrogen and total phosphorus were also obtained from the ARS-NSERL-CEAP database for the F34, AXL and ALG outlets. Concentration values for nutrients obtained from ARS were multiplied by flow on a daily time step to obtain total daily loads. Since the end goal of SWAT simulations was to evaluate long-term average annual loads, the daily loads were further aggregated into total monthly loads, which were used to perform monthly calibration and validation of the F34, AXL and ALG SWAT configurations. The nutrient data obtained from the SJRWI were biweekly grab samples (not sufficient to perform monthly calibration). Therefore, the Load Estimator (LOADEST) was used to estimate monthly constituent loads for CCW. LOADEST (Runkel et al., 2004) requires a time series of streamflow and the available constituent data, which it uses to develop a regression model for the estimation of constituent load. A summary of the average

measured streamflow and nutrient loads from each watershed during the years 2006 through 2013 is presented in Table 2.7.

The measured streamflow data obtained from the USGS and the ARS-NSERL-CEAP project are comprised of baseflow and surface runoff. Base flow is the groundwater contribution to streamflow, which needs to be separated so that measured surface flow can be compared to simulated values (Larose et al., 2007). The Web-based Hydrograph Analysis Tool (WHAT) developed by Purdue University (Lim et al., 2005) based on the (Arnold and Allen, 1999) base flow filter program was used to separate storm flow from base flow. Optimization of the SWAT configurations ensured that simulated baseflow approximated the fraction of water yield contributed by the baseflow from the measured flow estimated by WHAT.

After calibration, the next step was to validate the model performance, therefore ensuring it is able to perform simulations correctly and is suitable for use in decision-making. Validation was performed for F34, AXL and ALG configurations over a 4-year period (01/2010 to 12/2013). The CCW configuration was validated for streamflow over a 4-yr period (01/2010 to 12/2013), and soluble N and total P over a 3-yr period (01/2010 to 12/2012) due to limited data availability.

Table 2.7. Annual streamflow rate and nutrient loads measured from each watershed for the period 2006 through 2013.

| | Flow ($m^3/s$) | $NO_3+NO_2$ (kg) | Total N (kg) | Soluble P (kg) | Total P (kg) |
|---|---|---|---|---|---|
| 2006 | | | | | |
| CCW | 8.41 | 478203 | - | - | 42788 |
| F34 | 2.06 | 298063 | 304651 | 1910 | 12369 |
| AXL | 0.54 | 99056 | 100432 | 825 | 2634 |
| ALG | 0.37 | 48817 | 60293 | 305 | 1285 |
| 2007 | | | | | |
| CCW | 7.82 | 572740 | - | - | 48011 |
| F34 | 1.71 | 176556 | 193882 | 1151 | 12768 |
| AXL | 0.43 | 37172 | 55819 | 363 | 2999 |
| ALG | 0.23 | 13511 | 19260 | 151 | 1062 |
| 2008 | | | | | |
| CCW | 8.94 | 605748 | - | - | 54515 |
| F34 | 2.05 | 103213 | 139521 | 2405 | 11574 |
| AXL | 0.47 | 59888 | 77011 | 691 | 4404 |
| ALG | 0.33 | 17295 | 35422 | 495 | 2602 |
| 2009 | | | | | |
| CCW | 9.58 | 967120 | - | - | 57766 |
| F34 | 2.59 | 119270 | 205300 | 6532 | 25840 |
| AXL | 0.68 | 102327 | 145464 | 661 | 7358 |
| ALG | 0.44 | 39021 | 57820 | 423 | 2681 |
| 2010 | | | | | |
| CCW | 6.6 | 812899 | - | - | 37294 |
| F34 | 1.76 | 82465 | 106442 | 3233 | 18501 |
| AXL | 0.44 | 65783 | 86502 | 1485 | 7105 |
| ALG | 0.26 | 70639 | 39962 | 410 | 5786 |
| 2011 | | | | | |
| CCW | 11.08 | 1485662 | - | - | 73223 |
| F34 | 2.22 | 162319 | 170544 | 2627 | 28267 |
| AXL | 0.63 | 66877 | 110091 | 1077 | 12701 |
| ALG | 0.39 | 33506 | 67763 | 471 | 4719 |
| 2012 | | | | | |
| CCW | 4.01 | 342734 | - | - | 15674 |
| F34 | 0.99 | 48180 | 61144 | 919 | 2874 |
| AXL | 0.2 | 27077 | 32056 | 153 | 874 |
| ALG | 0.09 | 10501 | 14593 | 106 | 702 |
| 2013 | | | | | |
| CCW | 5.95 | - | - | - | 30147 |
| F34 | 1.54 | 175503 | 329090 | 2764 | 10361 |
| AXL | 0.47 | 75711 | 107625 | 534 | 3349 |
| ALG | 0.28 | 30702 | 32711 | 383 | 2523 |
| Average annual | | | | | |
| CCW | 7.80 | 752158 | - | - | 44927 |
| F34 | 1.87 | 145696 | 188822 | 2693 | 15319 |
| AXL | 0.48 | 66736 | 89375 | 724 | 5178 |
| ALG | 0.30 | 32999 | 40978 | 343 | 2691 |

Note: CCW pollutant values were estimated using LOADEST

In order to evaluate the effects of watershed size on SWAT model calibration, the optimized parameters for each SWAT configuration (CCW, F34, AXL and ALG) were applied to subsequent configurations. For example, parameters optimized at the CCW level during the calibration process were later implemented at the F34, AXL and ALG levels, and their effect on streamflow, nitrogen and phosphorus loss evaluated.

### 2.4.4 SWAT-CUP Calibration with SUFI-2

The calibration and uncertainty programs for SWAT (SWAT-CUP) developed by (Abbaspour et al., 2007) were used to aid in the calibration process. SWAT-CUP allows users to perform calibration, validation, sensitivity analysis (one-at-a-time, and global) and uncertainty analysis for a SWAT model simulation using either the PSO, SUFI-2, MCMC, ParaSol or GLUE algorithm. The SUFI-2 algorithm was selected in SWAT-CUP to optimize nine parameters for monthly streamflow volume, and 10 parameters directly related to sediment, nitrogen and phosphorus losses (Table 2.8). The selection of optimization parameters and the parameters' ranges were based on an extensive literature review (Arnold et al., 2012; Cibin et al., 2010; Kumar and Merwade, 2009; Larose et al., 2007; Neitsch, 2002; Parker et al., 2007; White and Chaubey, 2005) and an earlier sensitivity analysis performed for CCW (Heathman et al., 2009).

SUFI-2 was preferred because it required less iteration to achieve optimization, and it accounted for model uncertainty as well as uncertainty associated with model parameters and measured variables (e.g., discharge). It uses a P-factor and an R-factor as the means to quantify the strength of a calibration/uncertainty analysis. The P-factor, which ranges

from zero to one, is the percentage of measured data bracketed by the 95% prediction uncertainty (95PPU), calculated at the 2.5% and 97.5% levels of the cumulative distribution of output variables obtained through Latin hypercube sampling. The R-factor, which ranges from zero to infinity, is the average thickness of the 95PPU band divided by the standard deviation of the measured data. SUFI-2 seeks to bracket most of the measured data with the smallest possible uncertainty band (Abbaspour, 2012). Therefore, the P-factor would be equal to one and the R-factor equal to zero if the simulation matches the observed data exactly. The Kling–Gupta efficiency (KGE) was used as the objective function for optimizing SWAT input parameters because it optimizes from a "multi-objective" perspective (Kling and Gupta, 2009). It balances three major components of the hydrograph (mean, standard deviation, and timing/shape) with a single value (Equation 2.13).

$$KGE = 1 - \sqrt{(r-1)^2 + (\propto -1)^2 + (\beta - 1)^2} \tag{2.13}$$

where r is the linear correlation coefficient between corresponding simulated and observed values, $\propto$ is a measure of relative variability in the simulated and observed values, and $\beta$ is the bias between the mean simulated and mean observed data. Steps involved in setting up and executing SWAT-CUP are outlined in (Abbaspour, 2012).

Table 2.8. List of SWAT parameters used for calibration of CCW, F34, AXL and ALG configurations.

| Parameters | Description | Initial Value | Lower Bound | Upper Bound | Final Value | | | |
|---|---|---|---|---|---|---|---|---|
| | | | | | CCW | F34 | AXL | ALG |
| Parameters governing surface water response | | | | | | | | |
| r_CN2.mgt | SCS runoff curve number (%) | -- | -20% | +20% | -13 (2) | -9 (3) | -13 (3) | -14 (3) |
| v_ESCO.hru | Soil evaporation compensation factor | 0.95 | 0.60 | 0.95 | 0.61 (5) | 0.88 (1) | 0.76 (4) | 0.66 (4) |
| r_SOL_AWC.sol | Soil layer available water capacity (%) | -- | -50% | +50% | -30 (6) | +40 (7) | -41 (6) | -40 (5) |
| Parameters governing subsurface water response | | | | | | | | |
| v_GWQMN.gw | Depth of water for return flow to occur | 1000 | 0 | 1000 | 805 (10) | 295 (2) | 667 (10) | 608 (7) |
| v_GW_DLAY.gw | Groundwater delay (days) | 31.0 | 10.0 | 40.0 | 12.2 (4) | 32.0 (8) | 18.3 (5) | 25.2 (6) |
| v_GW_REVAP.gw | Groundwater "revap" coefficient | 0.02 | 0.02 | 0.20 | 0.03 (9) | 0.19 (10) | 0.09 (7) | 0.07 (9) |
| v_REVAPMN.gw | Depth of water for "revap" to occur | 1.0 | 0.0 | 300.0 | 99.0 (7) | 144 (4) | 99.7 (9) | 215 (8) |
| Parameters governing basin response | | | | | | | | |
| v_CH_K2.rte | Effective hydraulic conductivity (mm/h) | 0.0 | 6.0 | 150.0 | 18.5 (1) | 86.8 (9) | 11.7 (1) | 17.3 (1) |
| v_CH_N2.rte | Manning's "n" value for the main channel | .014 | 0.016 | 0.140 | .027 (3) | .064 (6) | .02 (2) | .037(2) |
| Parameters governing potholes and tile response | | | | | | | | |
| *DDRAIN | Depth to subsurface drain (mm) | 0 | 50 | 1450 | 1000 | 1000 | 1000 | 1000 |
| *GDRAIN | Drain tile lag time (h) | 0 | 0 | 94 | 48 | 48 | 48 | 48 |
| *TDRAIN | Time to drain soil to field capacity (h) | 0 | 0 | 72 | 24 | 24 | 24 | 24 |
| Parameters governing sediment response | | | | | | | | |
| v_SPCON.bsn | Sediment retention in channel | .0001 | .0001 | .0100 | .0067 (1) | .0057 (2) | .0035 (2) | .003 (2) |
| v_SPEXP.bsn | Sediment re-entrained in channel routing | 1.00 | 1.00 | 1.50 | 1.37 (2) | 1.44 (1) | 1.28 (1) | 1.22 (1) |
| Parameters governing nitrogen response | | | | | | | | |
| v_NPERCO.bsn | Nitrogen percolation coefficient | 0.2 | 0.0 | 1.0 | 0.7 (1) | 0.5 (3) | 0.6 (4) | 0.8 (4) |
| v_N_UPDIS.bsn | Nitrogen uptake distribution parameter | 20.0 | 0.0 | 100.0 | 35.6 (4) | 46.4 (1) | 33.4 (3) | 36.2 (3) |
| v_CDN.bsn | Denitrification exponential rate coefficient | 1.4 | 0.0 | 3.0 | 2.8 (2) | 2.0 (2) | 2.6 (1) | 3.0 (1) |
| v_CMN.bsn | Humus mineralization of active OM | .000 | .001 | .003 | .001 (3) | .002 (4) | .001 (2) | .001 (2) |
| Parameters governing response | | | | | | | | |
| v_PPERCO.bsn | percolation coefficient | 10.0 | 10.0 | 17.5 | 10.8 (3) | 10.7 (4) | 10.2 (3) | 10.4 (3) |
| v_PHOSKD.bsn | soil partitioning coefficient | 175.0 | 100.0 | 200.0 | 144 (2) | 199 (1) | 153 (2) | 169 (2) |
| v_PSP.bsn | sorption coefficient | 0.4 | 0.0 | 0.7 | 0.2 (4) | 0.5 (3) | 0.2 (4) | 0.5 (4) |
| v_P_UPDIS.bsn | uptake distribution parameter | 20.0 | 0.0 | 100.0 | 67.2 (1) | 48.4 (2) | 66.9 (1) | 69.9 (1) |

Note: Table includes calibration parameters, their file extensions, units; default values, lower and upper bounds selected during calibration and the final calibration values (sensitivity ranking) for each watershed.
Parameters were edited in the management files (.mgt); hru files .hru); soil input files (.sol); basin files (.bsn); groundwater files (.gw) and channel input files (.rte).
Parameters were changed by a value within the specified range during (v), as a percentage of their default (r), or manually adjusted (*)

### 2.4.5 Evaluating Model Performance

In addition to visual inspection of observed and simulated time series values at the watershed outlets, model performance was also evaluated using KGE, Nash-Sutcliffe efficiency (NSE; Nash and Sutcliffe, 1970) (Equation 2.15), coefficient of determination ($R^2$) (Equation 2.14) and percent bias ($P_{BIAS}$) (Equation 2.16). The $R^2$ value is an indicator of the strength of the linear relationship between the observed and simulated values. The NSE simulation coefficient indicates how well the plot of observed versus simulated values fits the 1:1 line, and can range from -∞ to +1, with +1 being perfect agreement between the model and observed data (Santhi et al., 2001). The limitation with $R^2$ and NSE is that they are both sensitive to high flows, and therefore $P_{BIAS}$ was used to measure the average tendency of the simulated data to be larger or smaller than the measured data. The optimum $P_{BIAS}$ value is zero, where low magnitude values indicate better simulations. Positive values indicate model underestimation and negative values indicate model over estimation. The equations are as follows:

$$R^2 = \frac{[\sum_i (Q_{m,j} - \overline{Q}_m)(Q_{s,j} - \overline{Q}_s)]^2}{\sum_i (Q_{m,j} - \overline{Q}_m)^2 \sum_i (Q_{s,j} - \overline{Q}_s)^2} \quad (2.14)$$

$$NSE = 1 - \frac{\sum_i (Q_m - Q_s)_i^2}{\sum_i (Q_{m,j} - \overline{Q}_m)^2} \quad (2.15)$$

$$P_{BIAS} = 100 * \frac{\sum_{i=1}^{n} (Q_m - Q_s)_i}{\sum_{i=1}^{n} Q_{m,j}} \quad (2.16)$$

where $\bar{Q}_m$ is the average measured values during the simulation period, $\bar{Q}_s$is the average of the simulated value during the simulation period, $Q_m$ is the measured data on day i, $Q_s$ is the simulated output on day i, and j represents the rank.

Based on model evaluation performance-ratings adopted from Moriasi et al. (2007) and (Larose et al., 2007; Van Liew and Garbrecht, 2003), streamflow simulations were considered reasonable if NSE > 0.50, $R^2$ > 0.50, and $P_{BIAS}$ was within ±25 percent, while nitrogen and simulations were considered reasonable if NSE > 0.36, $R^2$ > 0.50 and $P_{BIAS}$ was within ±70 percent.

## 2.5 Results

SWAT was successfully calibrated for monthly streamflow at the outlets of four watersheds located in northeastern Indiana (Figures 2.2a through 2.2d). All four watersheds were calibrated for the period January 2006 to December 2009 and validated for the period January 2010 to December 2013. SWAT calibration and validation results of monthly streamflow, soluble N, total N, soluble P and total P are presented in Tables 2.10 through 2.14 for all four-watershed configurations. The initial SWAT simulation results before calibration are also included in the respective tables for comparison purposes.

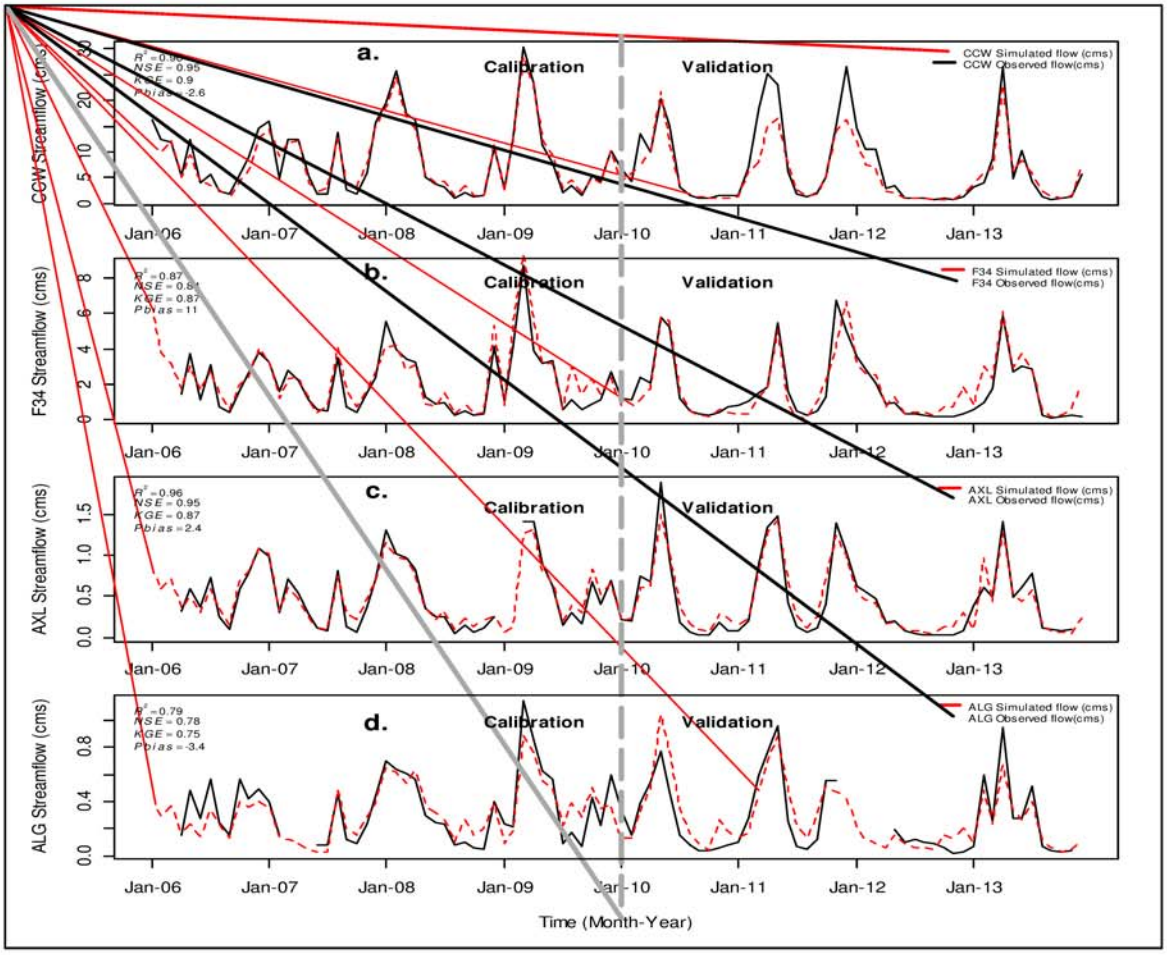


Figure 2.2. Monthly time series of simulated and observed streamflow for CCW, F34, AXL and ALG.

### 2.5.1 Streamflow Calibration and Validation

For the calibration period, WHAT estimated 58%, 61%, 56% and 59% of measured streamflows at the outlets of CCW, F34, AXL and ALG, respectively, were baseflows. In comparison, SWAT-simulated streamflow estimated 52%, 53%, 51% and 51% as baseflows at the respective watershed outlets (Table 2.9). The long-term water balance simulated by the model was similar to that simulated for the Cedar Creek Watershed in

prior studies (Kumar and Merwade, 2009; Larose et al., 2007). Thus, the long-term water balances simulated by the SWAT configurations were considered to generate acceptable predictions representative of the study areas (Table 2.9).

Table 2.9. Baseflow index (BFI) and average annual water balance components during the calibration/validation period (2006 to 2013).

| Water Balance | Calibration Scales | | | |
|---|---|---|---|---|
| | CCW | F34 | AXL | ALG |
| Measured BFI (using WHAT) | 0.58 | 0.61 | 0.56 | 0.59 |
| Simulated BFI (SWAT) | 0.52 | 0.53 | 0.50 | 0.51 |
| Precipitation (mm) | 946.8 | 944.9 | 957.5 | 952.1 |
| Surface runoff (mm) | 128.0 | 96.1 | 138.4 | 132.4 |
| Lateral flow (mm) | 32.6 | 22.9 | 28.0 | 32.5 |
| Tile flow (mm) | 131.8 | 191.7 | 177.4 | 179.0 |
| Return flow (mm) | 105.7 | 73.0 | 66.1 | 74.4 |
| Deep aquifer recharge (mm) | 5.5 | 7.1 | 3.9 | 4.7 |
| Water yield (mm) | 403.5 | 393.7 | 406.4 | 409.2 |
| Evapotranspiration (mm) | 524.9 | 489.9 | 518.8 | 500.6 |

Measured monthly streamflow data for the Cedar Creek watershed (USGS Gauge #04180000) and the ARS CEAP study watersheds (F34, AXL and ALG outlets) were compared with monthly SWAT simulated streamflow for the calibration period. Plots of simulated versus observed monthly streamflow at the different calibration scales are presented in Figures 2.3a through 2.3d. As depicted in Figure 2.3, SWAT was able to predict monthly streamflow well at all four watershed sizes, with a majority of the data points falling along the 1:1 line. Regression lines drawn through the data points indicated that streamflow was best predicted at the CCW, F34 and AXL outlets but slightly underestimated at the ALG outlet (the smallest of the watersheds). In general, modeled

streamflow at the respective watershed outlets produced similar results despite the size of the watershed at which the model was calibrated (Figure 2.3).

A summary of the statistical analyses of monthly streamflow for calibration, validation, and non-calibrated modes are presented in Table 2.10. Before calibration, there were acceptable KGE, NSE, $R^2$, and PBIAS values for SWAT simulations at all four watersheds; however, calibration improved the performance metrics at all four-watershed outlets, especially in terms of KGE and PBIAS. When SWAT was calibrated at the CCW scale (KGE = 0.90, NSE = 0.95, $R^2$ = 0.96 and PBIAS = -2.6%), NSE, $R^2$ and PBIAS values were within the acceptable ranges (NSE > 0.50, $R^2$ > 0.50 and $P_{BIAS}$ ±25%) when its optimized parameter values were implemented at the F34, AXL and ALG watershed scales. During the validation period, all four watersheds also produced acceptable results.

When SWAT was calibrated at the F34 scale (KGE = 0.87, NSE = 0.84, $R^2$ = 0.87, and PBIAS = 11.0%) and its optimized parameters implemented at the CCW, AXL and ALG watershed scales, NSE, $R^2$ and PBIAS values were all within acceptable ranges. During the validation period, all four-watershed simulations also produced acceptable KGE, NSE, $R^2$ and PBIAS values.

When SWAT was calibrated at the AXL scale (KGE = 0.88, NSE = 0.95, $R^2$ = 0.96 and PBIAS = 3.0%) and its optimized parameters implemented in CCW, F34 and ALG watershed simulations, the NSE, $R^2$ and PBIAS values were all within acceptable ranges.

During the validation period, all four SWAT watershed simulations also produced acceptable KGE, NSE, $R^2$ and PBIAS values.

When calibration was performed at ALG (NSE = 0.65, $R^2$ = 0.68 and PBIAS = 16.20%) and the optimized parameters implemented in CCW, F34 and AXL watershed simulations, the NSE, $R^2$ and PBIAS values for all cases were acceptable (NSE > 0.50, $R^2$ > 0.50 and $P_{BIAS}$ is ±25%). During the validation period, all four-watershed simulations produced acceptable KGE, NSE, $R^2$ and PBIAS values.

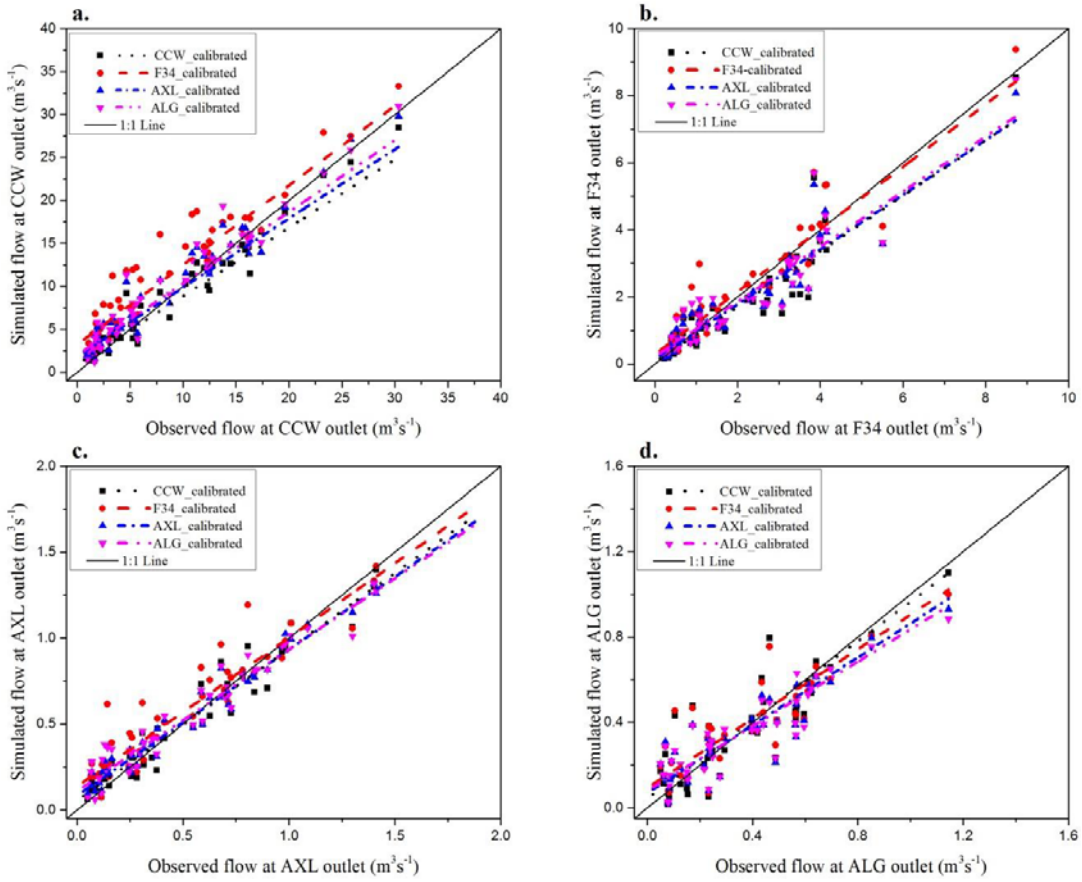


Figure 2.3. One to one plots of SWAT simulated vs. observed monthly streamflow (1/2006 to 12/2009) at the CCW, F34, AXL and ALG watershed outlets.

Table 2.10. Streamflow calibration and validation statistical metrics for SWAT performance at CCW, F34, AXL and ALG watersheds.

| | CCW Outlet | | | | F34 Outlet | | | | AXL Outlet | | | | ALG Outlet | | | |
|---|---|---|---|---|---|---|---|---|---|---|---|---|---|---|---|---|
| | KGE | NSE | $R^2$ | PBIAS | KGE | NSE | $R^2$ | PBIAS | KGE | NSE | $R^2$ | PBIAS | KGE | NSE | $R^2$ | PBIAS |
| Non-Calibrated Mode (01/2006 to 12/2013) | | | | | | | | | | | | | | | | |
| | 0.68 | 0.77 | 0.90 | 27.8 | 0.83 | 0.83 | 0.85 | -13.2 | 0.81 | 0.90 | 0.95 | 15.9 | 0.82 | 0.76 | 0.77 | 4.5 |
| Calibration WS | Streamflow Calibration (01/2006 to 12/2009) | | | | | | | | | | | | | | | |
| CCW | 0.90 | 0.95 | 0.96 | -2.6 | 0.85 | 0.84 | 0.86 | 11.3 | 0.94 | 0.94 | 0.94 | 0.3 | 0.86 | 0.73 | 0.74 | 0.5 |
| F34 | 0.63 | 0.70 | 0.90 | 36.3 | 0.87 | 0.84 | 0.87 | 11.0 | 0.81 | 0.84 | 0.89 | 16.8 | 0.81 | 0.74 | 0.75 | 5.8 |
| AXL | 0.86 | 0.92 | 0.95 | 11.6 | 0.84 | 0.86 | 0.87 | -8.0 | 0.88 | 0.95 | 0.96 | 3.0 | 0.78 | 0.78 | 0.79 | -3.4 |
| ALG | 0.84 | 0.91 | 0.94 | 14.1 | 0.87 | 0.85 | 0.85 | -5.4 | 0.85 | 0.92 | 0.94 | 7.4 | 0.75 | 0.77 | 0.78 | -3.4 |
| Streamflow Validation (01/2010 to 12/2013) | | | | | | | | | | | | | | | | |
| CCW | 0.69 | 0.82 | 0.88 | -16.6 | 0.77 | 0.83 | 0.85 | -15.5 | 0.90 | 0.91 | 0.91 | 0.6 | 0.78 | 0.72 | 0.80 | 14.9 |
| F34 | 0.68 | 0.74 | 0.83 | 30.3 | 0.88 | 0.81 | 0.82 | 7.0 | 0.82 | 0.86 | 0.88 | 15.2 | 0.76 | 0.71 | 0.76 | 20.1 |
| AXL | 0.73 | 0.80 | 0.83 | -6.1 | 0.79 | 0.85 | 0.87 | -13.0 | 0.87 | 0.91 | 0.92 | 3.1 | 0.86 | 0.79 | 0.80 | 9.7 |
| ALG | 0.78 | 0.85 | 0.88 | 2.4 | 0.82 | 0.78 | 0.78 | -6.9 | 0.85 | 0.89 | 0.90 | 5.4 | 0.84 | 0.78 | 0.79 | 8.0 |

### 2.5.2 Nitrogen Loss Calibration and Validation

Measured monthly nitrogen loads in the form of nitrate+nitrite (referred to as soluble N) and total nitrogen (referred to as total N) for the Cedar Creek watershed (USGS Gauge #04180000) and the ARS CEAP study watersheds (F34, AXL and ALG outlets) were compared with SWAT simulated monthly soluble N and total N loads. Results showed that SWAT was successfully calibrated at all four watershed scales for monthly soluble N load and at F34, AXL and ALG for monthly total N load. No data were available for total N at the CCW scale, and soluble N data at CCW were only available from 2008 to 2013. Performance evaluation metrics for calibration, validation and non-calibrated model results are presented in Tables 2.11 and 2.12 for soluble N and total N, respectively. Plots of simulated versus observed monthly soluble N loads at the different watershed sizes are presented in Figures 2.4a through 2.4d, with total N presented in Figures 2.5a through 2.5c. Here, SWAT was able to predict monthly soluble N and total N loads well at the different watershed sizes, with a majority of the data points occurring close to the 1:1 line.

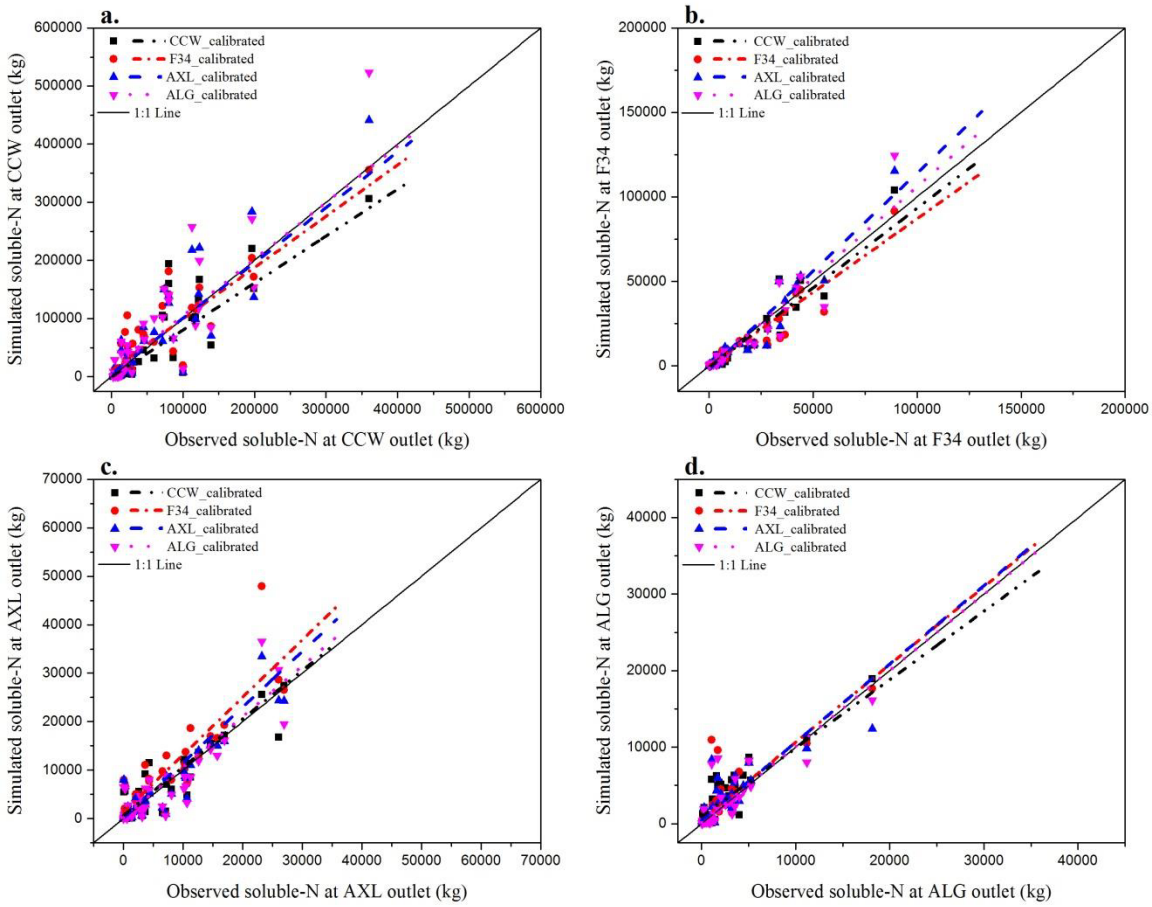


Figure 2.4. One to one plot of SWAT simulated vs. observed monthly $NO_3$+$NO_2$ (soluble N) (1/2006 to 12/2009) at the CCW, F34, AXL and ALG watershed outlets.

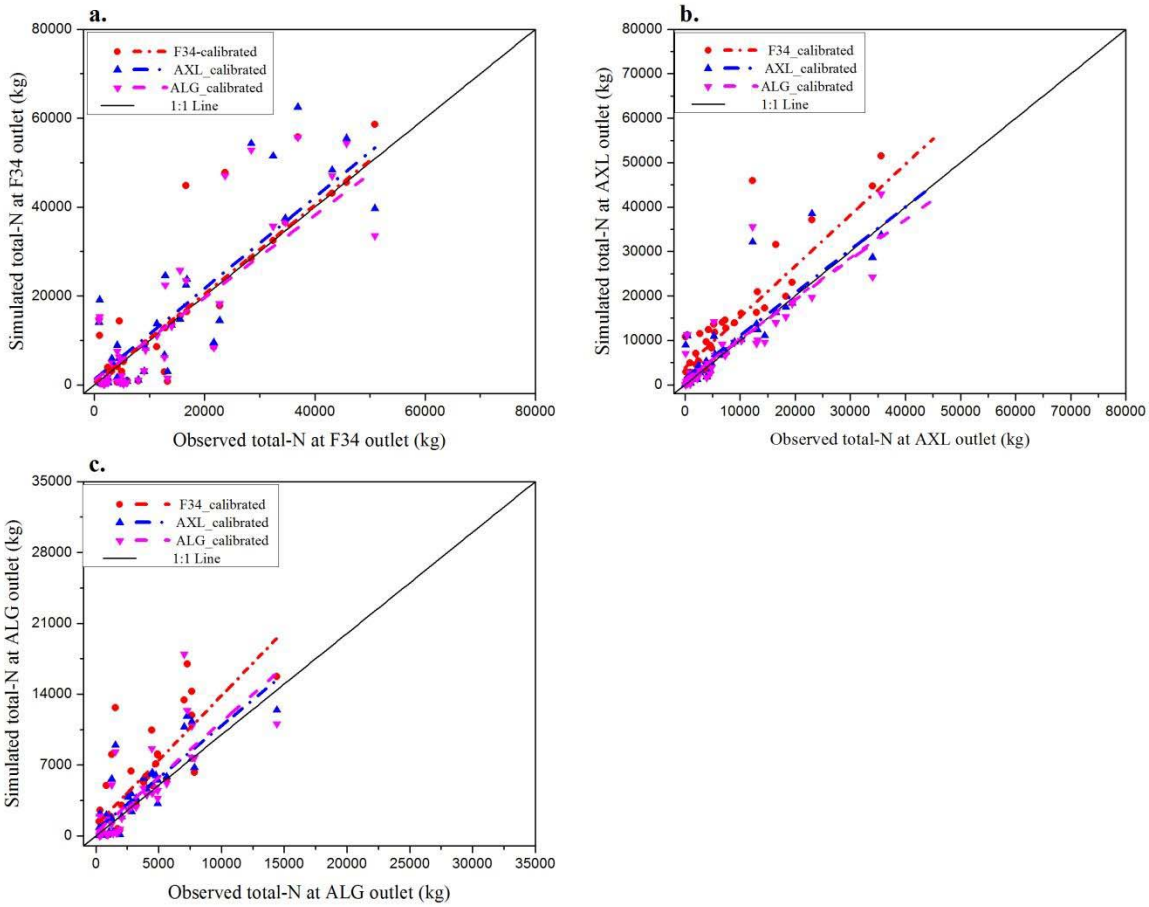


Figure 2.5. One to one plots of SWAT simulated vs. observed monthly total nitrogen (1/2006 to 12/2009) at the F34, AXL and ALG watershed outlets.

For soluble N, when SWAT was calibrated at the CCW scale (KGE = 0.86, NSE = 0.75, $R^2$ = 0.78 and PBIAS = -7.7%), NSE, $R^2$ and PBIAS values were all within acceptable ranges when its optimized parameter values were used in F34, AXL and ALG watershed simulations. During the validation period, all four watersheds also produced acceptable KGE, NSE, $R^2$ and PBIAS values. Despite $R^2$ values above 0.50 and PBIAS lower than 70%, when SWAT was calibrated at the F34 scale (KGE = 0.76, NSE = 0.87, $R^2$ = 0.90, and PBIAS = -21.3%) and its optimized parameters implemented at the CCW, AXL and

ALG watershed scales, both the KGE and NSE values were below the acceptable limits in the CCW (KGE = 0.38, NSE = 0.30), AXL (KGE = 0.34, NSE = 0.34), and ALG (KGE = 0.47, NSE = 0.31) simulations. During the validation period, only F34 and ALG produced acceptable results. When SWAT was calibrated at the AXL watershed outlet (KGE = 0.91, NSE = 0.83, $R^2$ = 0.85 and PBIAS = -0.1%) and its optimized parameters implemented at the CCW, F34 and ALG watersheds sizes, NSE, $R^2$ and PBIAS values were all within acceptable ranges. During the validation period, all four-watershed simulations also produced acceptable KGE, NSE, $R^2$ and PBIAS values. When calibration was performed at the ALG watershed outlet (KGE = 0.80, NSE = 0.65, $R^2$ = 0.69 and PBIAS = 9.8%) and the optimized parameters implemented at the CCW, F34 and AXL watershed sizes, NSE, $R^2$ and PBIAS values were also all within the acceptable ranges. During the validation period, all four-watershed simulations also produced acceptable KGE, NSE, $R^2$ and PBIAS values.

For total N, despite reasonable $R^2$ values and a PBIAS of 59.4 at the ALG outlet, when SWAT was calibrated at the F34 watershed outlet (KGE = 0.87, NSE = 0.84, $R^2$ = 0.87 and PBIAS = 3.9%) and its optimized parameters used in AXL and ALG watershed simulations, the resulting model performance was unacceptable. KGE and NSE values were below the acceptable limits for the AXL (KGE = 0.27, NSE = 0.30), and ALG (KGE = 0.29, NSE = 0.32) simulations. During the validation period, both F34 and ALG produced acceptable results, whereas AXL produces unacceptable results with KGE = 0.06, NSE = -0.15 and $P_{BIAS}$ = 72.6%. When SWAT was calibrated at the AXL watershed

outlet (KGE = 0.83, NSE = 0.77, $R^2$ = 0.81 and PBIAS = 12.7%) and its optimized parameters used in the CCW, F34 and ALG watershed simulations, the NSE, $R^2$ and PBIAS values were all within the acceptable range. During the validation period, all four-watershed simulations had acceptable KGE, NSE, $R^2$ and PBIAS values. When calibration was performed at the ALG watershed outlet (KGE = 0.83, NSE = 0.70, $R^2$ = 0.72 and PBIAS = 8.9%) and the optimized parameters applied in CCW, F34 and AXL watershed simulations, NSE, $R^2$ and PBIAS values were all within the acceptable ranges. During the validation period, all four-watershed simulations also produced acceptable KGE, NSE, $R^2$ and PBIAS values.

Table 2.11. Soluble N calibration and validation statistical metrics for SWAT model performance at CCW, F34, AXL and ALG watersheds.

| | CCW | | | | F34 | | | | AXL | | | | ALG | | | |
|---|---|---|---|---|---|---|---|---|---|---|---|---|---|---|---|---|
| | KGE | NSE | $R^2$ | PBIAS | KGE | NSE | $R^2$ | PBIAS | KGE | NSE | $R^2$ | PBIAS | KGE | NSE | $R^2$ | PBIAS |
| | Non-Calibrated Mode (01/2006 to 12/2013) | | | | | | | | | | | | | | | |
| | 0.61 | 0.58 | 0.61 | -23.1 | -0.92 | -3.74 | 0.47 | 104.9 | 0.43 | 0.28 | 0.73 | 24.0 | 0.41 | 0.29 | 0.70 | 39.3 |
| Calibration WS | Soluble N Calibration (01/2006 to 12/2009) | | | | | | | | | | | | | | | |
| CCW | 0.86 | 0.75 | 0.78 | -7.7 | 0.86 | 0.89 | 0.92 | -10.9 | 0.90 | 0.82 | 0.83 | 1.4 | 0.58 | 0.68 | 0.81 | 37.8 |
| F34 | 0.38 | 0.30 | 0.51 | 50.8 | 0.76 | 0.87 | 0.90 | -21.3 | 0.34 | 0.34 | 0.81 | 46.6 | 0.47 | 0.31 | 0.62 | 41.0 |
| AXL | 0.52 | 0.43 | 0.73 | 27.9 | 0.80 | 0.87 | 0.93 | 0.0 | 0.91 | 0.83 | 0.85 | -0.1 | 0.72 | 0.62 | 0.65 | 20.1 |
| ALG | 0.37 | 0.26 | 0.74 | 37.4 | 0.78 | 0.81 | 0.89 | -2.0 | 0.85 | 0.75 | 0.79 | -3.4 | 0.80 | 0.65 | 0.69 | 9.8 |
| | Soluble N Validation (01/2010 to 12/2013) | | | | | | | | | | | | | | | |
| CCW | 0.68 | 0.59 | 0.78 | -24.1 | 0.84 | 0.92 | 0.92 | -12.5 | 0.65 | 0.64 | 0.83 | 24.30 | 0.81 | 0.88 | 0.81 | 17.0 |
| F34 | 0.24 | -0.68 | 0.51 | 21.0 | 0.91 | 0.89 | 0.90 | -3.8 | 0.04 | -0.10 | 0.81 | 70.00 | 0.60 | 0.87 | 0.62 | 26.2 |
| AXL | 0.59 | 0.68 | 0.73 | 8.6 | 0.77 | 0.86 | 0.93 | 4.8 | 0.60 | 0.83 | 0.85 | 35.80 | 0.73 | 0.93 | 0.65 | 23.0 |
| ALG | 0.56 | 0.52 | 0.74 | 13.6 | 0.89 | 0.90 | 0.89 | -5.4 | 0.62 | 0.56 | 0.79 | 22.90 | 0.91 | 0.97 | 0.69 | 5.9 |

Table 2.12. Total N calibration and validation statistical metrics for SWAT model performance at CCW, F34, AXL and ALG watersheds.

| | F34 | | | | AXL | | | | ALG | | | |
|---|---|---|---|---|---|---|---|---|---|---|---|---|
| | KGE | NSE | $R^2$ | PBIAS | KGE | NSE | $R^2$ | PBIAS | KGE | NSE | $R^2$ | PBIAS |
| | Non-Calibrated Mode (01/2006 to 12/2013) | | | | | | | | | | | |
| | -3.79 | -24.66 | 0.15 | 268.6 | -0.97 | -3.92 | 0.53 | 109.2 | 0.56 | 0.46 | 0.71 | 30.9 |
| Calibration WS | Total N Calibration (01/2006 to 12/2009) | | | | | | | | | | | |
| F34 | 0.87 | 0.84 | 0.87 | 3.9 | 0.27 | 0.30 | 0.82 | 79.0 | 0.29 | 0.30 | 0.66 | 59.4 |
| AXL | 0.76 | 0.73 | 0.82 | 13.9 | 0.83 | 0.77 | 0.81 | 12.7 | 0.75 | 0.63 | 0.68 | 18.2 |
| ALG | 0.82 | 0.82 | 0.87 | 7.3 | 0.77 | 0.64 | 0.73 | 10.9 | 0.83 | 0.70 | 0.72 | 8.9 |
| | Total N Validation (01/2010 to 12/2013) | | | | | | | | | | | |
| F34 | 0.76 | 0.60 | 0.87 | 15.1 | 0.06 | -0.15 | 0.82 | 72.6 | 0.76 | 0.71 | 0.76 | 20.1 |
| AXL | 0.80 | 0.66 | 0.82 | 10.8 | 0.51 | 0.49 | 0.81 | 30.4 | 0.86 | 0.79 | 0.80 | 9.7 |
| ALG | 0.78 | 0.68 | 0.87 | -2.1 | 0.74 | 0.76 | 0.73 | 16.4 | 0.84 | 0.78 | 0.79 | 8.0 |

### 2.5.3 Phosphorus Loss Calibration and Validation

Measured monthly phosphorus loads in the form of orthophosphate (referred to as soluble P) and total phosphorus (referred to as total P) for the Cedar Creek watershed (USGS Gauge #04180000) and the ARS CEAP study watersheds (F34, AXL and ALG outlets) were compared with SWAT simulated monthly soluble P and total P loads. Results indicate that SWAT was successfully calibrated at F34, AXL and ALG for monthly soluble P loads and at all four watersheds for monthly total P loads from January 2006 to December 2009, and validated for the period January 2010 to December 2013. No data were available for soluble P for CCW. A summary of the performance evaluation metrics for calibration, validation and non-calibrated model results are presented in Tables 2.13 and 2.14 for monthly soluble P and total P losses, respectively. Here SWAT predicted monthly soluble P and total P loads well, with a majority of the data points occurring close to the 1:1 line (Figures 2.6 and 2.7).

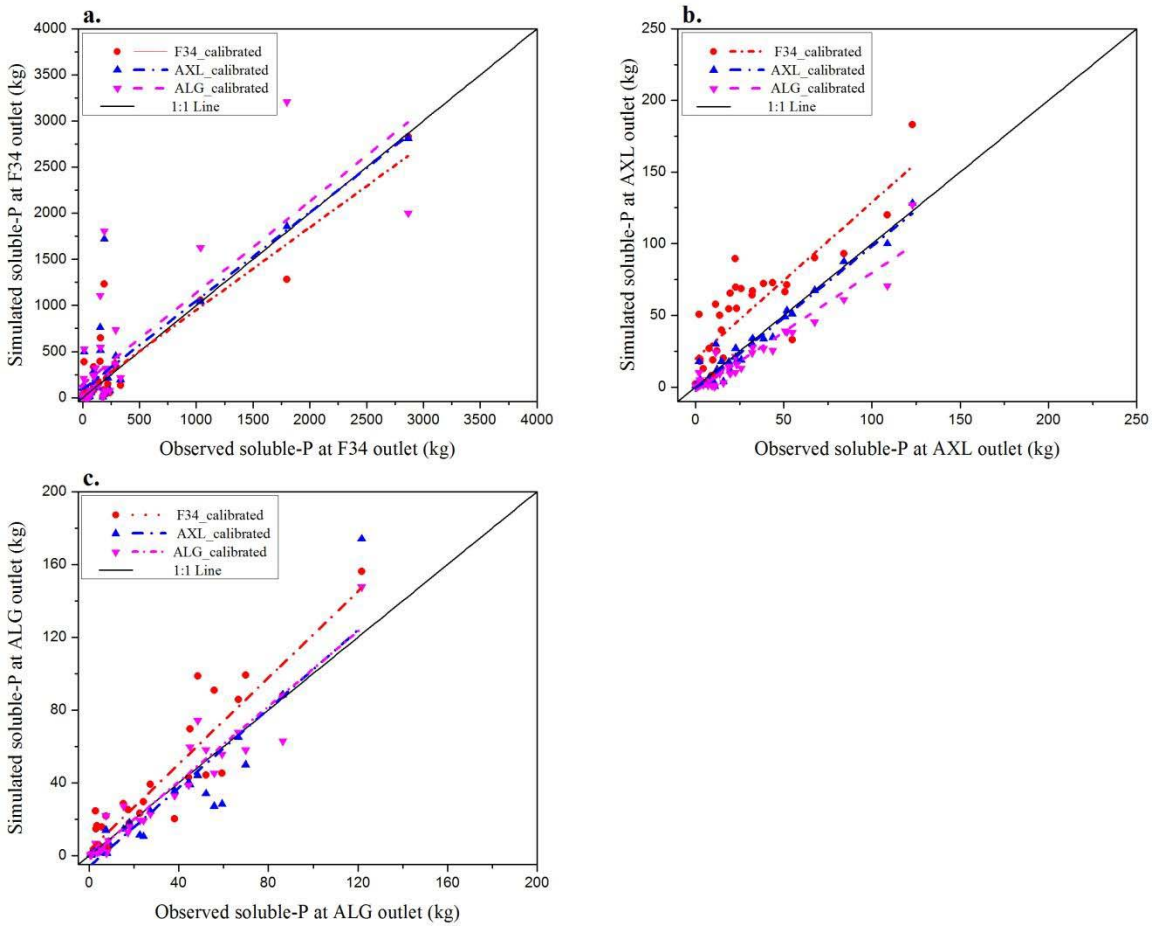


Figure 2.6. One to one plot of SWAT simulated vs. observed monthly soluble P (1/2006 to 12/2009) at the F34, AXL and ALG watershed outlets.

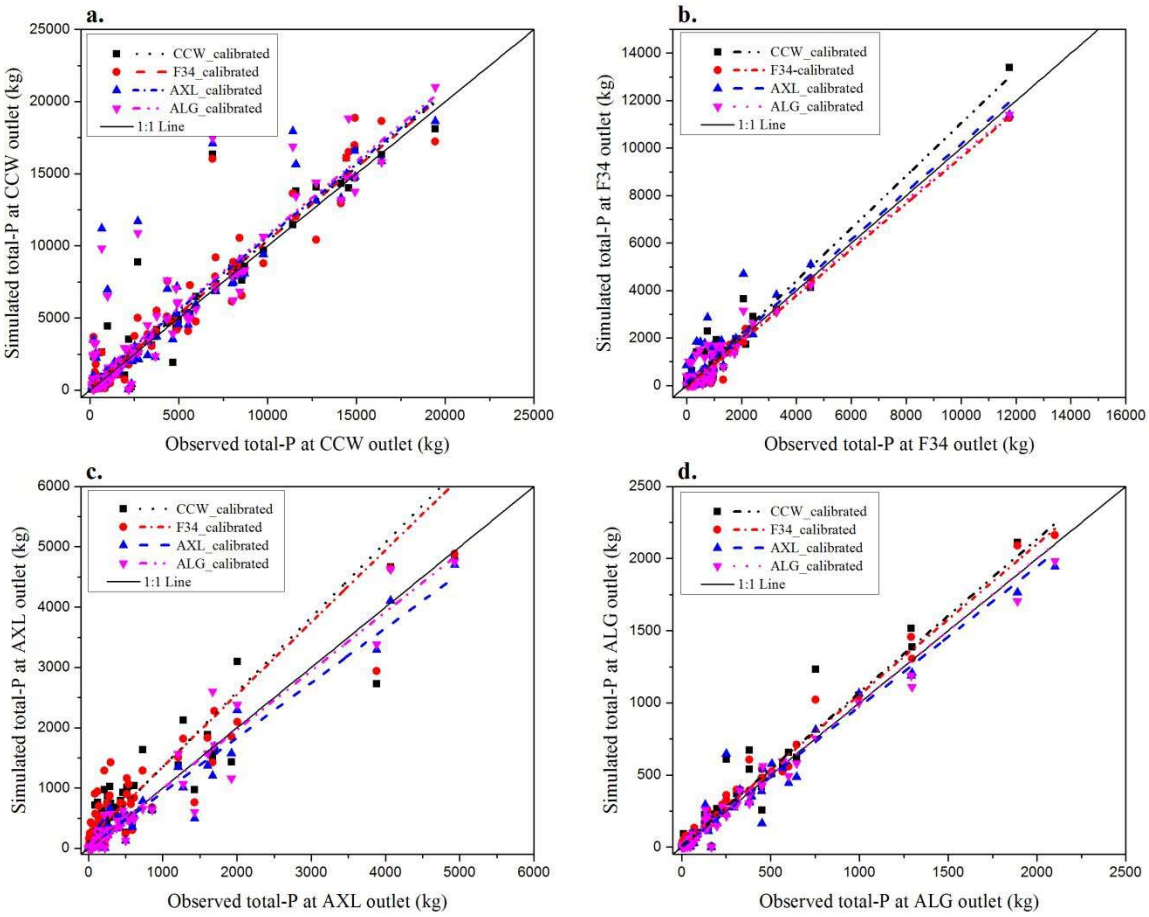


Figure 2.7. One to -one plot of SWAT simulated vs. observed monthly total P (1/2006 to 12/2009) at the CCW, F34, AXL and ALG watershed outlets.

Modeled soluble P load at the F34 watershed outlet (Figure 2.6a), AXL watershed outlet (Figure 2.6b), and ALG watershed outlet (Figure 2.6c) produced similar results despite the watershed size at which the model was calibrated, with a few exceptions. When calibration was performed at the F34 watershed outlet (KGE = 0.85, NSE = 0.81, $R^2$ = 0.82, PBIAS = 11.2%) and its optimized parameters applied to the AXL watershed, the KGE, NSE and PBIAS values were outside the acceptable ranges (KGE = -1.55, NSE = -5.66, PBIAS = 171.4%). However, when the F34-optimized parameters were applied in

the ALG watershed simulations, they produced acceptable results (KGE = 0.76, NSE = 0.74, $R^2$ = 0.79 and PBIAS = 21.1%). During the validation period, only F34 and ALG produced acceptable results.

When calibration was performed at the AXL watershed outlet (KGE = 0.94, NSE = 0.95, $R^2$ = 0.95, PBIAS = -5.5%), NSE, $R^2$ and PBIAS values for predictions of monthly soluble P losses were all acceptable at F34 and ALG. Model results were also within acceptable range during the validation period for all three-watershed simulations.

When calibration was performed at the ALG watershed (KGE = 0.94, NSE = 0.93, $R^2$ = 0.93, PBIAS = -3.0%) and the optimized parameters applied in the F34 and AXL watershed simulations, the performance metrics were unacceptable at F34 where KGE = 0.35 and NSE = 0.31. However, during the validation period, all three-watershed simulations produced acceptable KGE, NSE, $R^2$ and PBIAS values.

For total P, SWAT was able to predict monthly loads well at all four watershed scales, with a majority of the data points occurring close to the 1:1 line (Figure 2.7). Modeled total P load at the CCW (Figure 2.7a), F34 (Figure 2.7b), AXL (Figure 2.7c), and ALG (Figure 2.7d) watershed outlets produced similar results despite the scale at which the model was calibrated, with only a few exceptions.

When SWAT was calibrated at the CCW outlet (KGE = 0.86, NSE = 0.84, $R^2$ = 0.87, PBIAS = 9.6%), the NSE, $R^2$ and PBIAS values were all within the acceptable ranges when its optimized parameter values were applied to the four watershed simulations. During the validation period, the NSE, $R^2$ and PBIAS values were also all acceptable.

When SWAT was calibrated at the F34 watershed outlet (KGE = 0.80, NSE = 0.98, $R^2$ = 0.99, PBIAS = -19.4%) and its optimized parameters applied in the CCW, AXL and ALG watershed simulations, the resulting model performance was acceptable, except at AXL where KGE = 0.35. During the validation period, all four watersheds produced results within the acceptable range. When calibration was performed at the AXL watershed outlet (KGE = 0.91, NSE = 0.97, $R^2$ = 0.97, PBIAS = -6.9%), and at the ALG watershed outlet (KGE = 0.97, NSE = 0.96, $R^2$ = 0.96, PBIAS = -2.0%), the KGE, NSE, $R^2$ and PBIAS values were all within the acceptable range for CCW, F34, AXL and ALG watershed simulations. During the validation period, all four watershed scales also produced acceptable KGE, NSE, $R^2$ and PBIAS values. During the validation period, all model evaluation statistics were also acceptable.

Table 2.13. Soluble P loss calibration and validation statistical metrics for SWAT performance at CCW, F34, AXL and ALG watersheds.

| | F34 | | | | AXL | | | | ALG | | | |
|---|---|---|---|---|---|---|---|---|---|---|---|---|
| | KGE | NSE | $R^2$ | PBIAS | KGE | NSE | $R^2$ | PBIAS | KGE | NSE | $R^2$ | PBIAS |
| Non-Calibrated Mode (01/2006 to 12/2013) | | | | | | | | | | | | |
| | -12.66 | -128.14 | 0.22 | 94.8 | -2.80 | -15.01 | 0.68 | 91.2 | 0.23 | 0.41 | 0.86 | -53.5 |
| Calibration WS | Soluble P Calibration (01/2006 to 12/2009) | | | | | | | | | | | |
| F34 | 0.85 | 0.81 | 0.82 | 11.2 | -1.55 | -5.66 | 0.90 | 171.4 | 0.76 | 0.74 | 0.79 | 21.1 |
| AXL | 0.65 | 0.69 | 0.77 | 31.1 | 0.94 | 0.95 | 0.95 | -5.5 | 0.69 | 0.78 | 0.85 | -30.2 |
| ALG | 0.65 | 0.61 | 0.61 | 55.6 | 0.69 | 0.83 | 0.91 | -27.0 | 0.94 | 0.93 | 0.93 | -3.0 |
| Soluble P Validation (01/2010 to 12/2013) | | | | | | | | | | | | |
| F34 | 0.85 | 0.92 | 0.82 | -13.3 | 0.19 | 0.39 | 0.90 | 71.5 | 0.76 | 0.81 | 0.79 | 21.9 |
| AXL | 0.90 | 0.93 | 0.77 | -7.4 | 0.87 | 0.96 | 0.95 | -12.9 | 0.87 | 0.85 | 0.85 | -10.4 |
| ALG | 0.74 | 0.84 | 0.61 | 13.2 | 0.75 | 0.90 | 0.91 | -24.0 | 0.86 | 0.87 | 0.93 | 10.6 |

Table 2.14. Total phosphorus (total P) loss calibration and validation statistical metrics for SWAT performance at CCW, F34, AXL and ALG watersheds.

| | CCW | | | | F34 | | | | AXL | | | | ALG | | | |
|---|---|---|---|---|---|---|---|---|---|---|---|---|---|---|---|---|
| | KGE | NSE | $R^2$ | PBIAS | KGE | NSE | $R^2$ | PBIAS | KGE | NSE | $R^2$ | PBIAS | KGE | NSE | $R^2$ | PBIAS |
| Non-Calibrated Mode (01/2006 to 12/2013) | | | | | | | | | | | | | | | | |
| | -29.10 | -17.50 | 0.45 | 76.5 | -1.80 | -7.59 | 0.36 | 87.9 | -0.69 | -3.12 | 0.46 | 64.7 | 0.87 | 0.93 | 0.94 | -8.5 |
| Calibration WS | Total P Calibration (01/2006 to 12/2009) | | | | | | | | | | | | | | | |
| CCW | 0.86 | 0.84 | 0.87 | 9.6 | 0.78 | 0.91 | 0.95 | 15.8 | 0.60 | 0.69 | 0.87 | 56.1 | 0.85 | 0.94 | 0.96 | 11.6 |
| F34 | 0.85 | 0.84 | 0.88 | 8.7 | 0.80 | 0.98 | 0.99 | -19.4 | 0.35 | 0.66 | 0.86 | 62.1 | 0.92 | 0.96 | 0.96 | 7.3 |
| AXL | 0.68 | 0.57 | 0.74 | 20.5 | 0.69 | 0.86 | 0.89 | 30.3 | 0.91 | 0.97 | 0.97 | -6.9 | 0.95 | 0.95 | 0.95 | -2.6 |
| ALG | 0.65 | 0.61 | 0.78 | 23.0 | 0.88 | 0.95 | 0.95 | 11.5 | 0.91 | 0.93 | 0.94 | -6.8 | 0.97 | 0.96 | 0.96 | -2.0 |
| Total P Validation (01/2010 to 12/2013) | | | | | | | | | | | | | | | | |
| CCW | 0.94 | 0.96 | 0.87 | 4.1 | 0.92 | 0.89 | 0.95 | -1.8 | 0.41 | 0.55 | 0.87 | 41.8 | 0.86 | 0.92 | 0.96 | 10.8 |
| F34 | 0.88 | 0.92 | 0.88 | 7.4 | 0.89 | 0.94 | 0.99 | -10.4 | 0.41 | 0.56 | 0.86 | 44.6 | 0.88 | 0.98 | 0.96 | 11.2 |
| AXL | 0.91 | 0.92 | 0.74 | 8.3 | 0.92 | 0.91 | 0.89 | 1.3 | 0.91 | 0.93 | 0.97 | -3.9 | 0.97 | 0.96 | 0.95 | -2.2 |
| ALG | 0.88 | 0.91 | 0.78 | 11.7 | 0.91 | 0.93 | 0.95 | -8.3 | 0.93 | 0.91 | 0.94 | 5.7 | 0.98 | 0.99 | 0.96 | -1.1 |

## 2.6 Discussion

Calibration processes play an important role in model performance. The use of autocalibration may generate parameter sets that will result in model outputs displaying good agreement with observed data but may misrepresent other important processes. As a result, applying these parameter sets to other areas may yield unsatisfactory results. Therefore, when considering autocalibration, special care must be taken to select parameter ranges that are representative of the study areas. Choosing the appropriate objective function is also another important step to consider during autocalibration. The use of multi-objective functions that improve multiple aspects of the hydrograph simultaneously is often recommended when considering autocalibration (White and Chaubey, 2005; Zhang et al., 2008, 2009). However, most existing autocalibration tools associated with SWAT do not facilitate the use of multi-objective functions (simultaneously) and as such, the use of manual calibration to adjust the results of autocalibration may be useful in obtaining results that are more realistic.

Previous studies (White and Chaubey, 2005; Zhang et al., 2008) have shown that simultaneous multi-site calibrations of SWAT produced better parameter estimates than those obtained by optimization at a single monitoring site. However, in most instances where monitoring data are limited, model calibrations are confined to a single monitoring site. Moreover, it has been suggested by White and Chaubey (2005) that non-nested or mutually independent watersheds provide a better format for multi-site calibration than

nested data sites, such as those used in this study (due to data availability and the study objective).

The effects of watershed size on SWAT model calibration for streamflow, nitrogen and phosphorus were evaluated at four watersheds of varying size. The four watersheds included the Cedar Creek watershed (CCW) located in northeastern Indiana, F34 (approximately 27% of CCW), AXL (approximately 6% of CCW), and ALG (approximately 3% of CCW). Based on the results presented here, SWAT satisfactorily simulated streamflow, soluble N, total N, soluble P and total P at the four watershed scales with slight differences between the scales at which the calibrations were performed.

Model efficiency evaluations show that streamflow calibration at the smaller AXL and ALG watershed sizes produced similar KGE, NSE, $R^2$ and PBIAS values when compared to calibrations performed at the larger watershed sizes. While there are very few studies examining the effects of calibration scale on SWAT model performance, the results presented agree with Heathman et al. (2007) and Thampi et al. (2010) findings that SWAT performed adequately despite the size at which calibration was performed. The notable similarities in both of these studies are that the study watersheds are nested within each other and have similar physiographic features (such as slope, land use distribution, soil type) that may result in similar parameterization of the model. Because the CN method, which was used to estimate surface runoff, is not very sensitive to the size of the

watershed, the impact of surface runoff contributions to streamflow will not be influenced significantly by watershed size (Jha et al., 2004).

In terms of nitrogen and phosphorus simulations, results show that calibration does have a large impact on SWAT model predictions. Despite much improved results at all watershed sizes due to calibration, when SWAT was calibrated at the larger CCW watershed, its optimized parameters produced improved soluble N and total P simulations when applied at the smaller watershed sizes. Optimizing SWAT parameters at the AXL watershed resulted in much improved predictions of soluble N and total N losses when applied at the smaller ALG watershed. This was due to the closeness in their average slope, land use distribution, management practices and other physiographic properties that resulted in similar values for the calibration parameters. Similarly, calibrating SWAT at the smaller ALG and AXL watersheds produced improved NSE, $R^2$ and PBIAS values for soluble P and total P when applied to the larger watersheds. The calibrated parameters for CCW, AXL and ALG were similar in terms of final values (or percent change) and level of sensitivity (Table 2.8), which is the underlying reason for the different watershed configurations producing satisfactory results regardless of the optimization scale.

In general, SWAT predictions at the respective watershed outlets produced similar results despite the scale at which the model was calibrated, with one notable exception. Although calibration at the F34 outlet was satisfactory for each constituent, when the SWAT parameters optimized for F34 were applied to the other watershed configurations, the results were not always satisfactory. This is most likely due to inconsistencies in the F34

observed dataset used for SWAT calibrations. There were a larger proportion of high flow events for F34 in comparison to the other three watersheds, and because nitrogen and phosphorus loads were calculated as a function of streamflow, they too are affected by any adjustments made during the calibration process. During autocalibration, SWAT parameters were adjusted to accommodate the higher events (as demonstrated by the large difference in final calibration values, Table 2.8), which would then overestimate the various processes when applied to the different watershed configurations. These results indicate there is greater uncertainty in SWAT calibrations at F34, which may be due to the characteristics of farmed closed depressions (potholes) within F34, compared to the other watersheds. The average depth of farmed closed depressions in F34 was much smaller than that of CCW, AXL and ALG, which would affect the maximum volume of ponded water in the watershed. These potholes hydrologically modify the landscape and undermine the assumption of similar physiographic features. The inclusion of potholes adds to the complexities of SWAT and the model calibration process. Consequently, optimizing SWAT model parameters at the F34 scale often resulted in over-prediction of streamflow, nitrogen and phosphorus loss when applied to the CCW, AXL and ALG watersheds.

The nitrogen and phosphorus loads calculated for the F34 outlet were affected by the observed flow data, which indirectly influenced the calibration parameters. This was evident in the parameter sensitivity rankings (Table 2.8) where the most sensitive nitrogen and phosphorus parameters for F34 were the nitrogen uptake distribution factor

(N_UPDIS) and the phosphorus soil-partition coefficient (PHOSKD), respectively. While the most sensitive parameters for CCW were the nitrogen percolation coefficient (NPERCO) and phosphorus uptake distribution (P_UPDIS), at both the AXL and ALG watersheds the most sensitive nitrogen and phosphorus parameters were the Denitrification exponential rate constant (CDN) and P_UPDIS. These differences in sensitivity between F34 and the other watersheds mean that small changes in a non-sensitive parameter at F34 may result in big differences when applied at the other scales. For example, the least sensitive parameter in the simulation of nitrogen at F34 was humus mineralization of active organic nitrogen (CMN), which was the second most sensitive at AXL and ALG. The final calibrated CMN value at F34 was twice that of AXL and ALG, which means that, applying the F34 CMN at AXL and ALG will result in more nitrogen mineralization and over prediction of soluble N ($NO_3$+$NO_2$).

Additionally, it is worthy to note that a major disadvantage with the NSE and $R^2$ evaluation is that differences between the observed and simulated values are calculated as squared values, which makes them biased towards high flows. As a result, larger values in the calibration time series strongly influenced the calibration outcome whereas lower values were neglected (Legates and McCabe, 1999). As seen in Figures 2.3 through 2.7, there were more occurrences of higher monthly values in the F34 dataset above the 1:1 line, which could explain the poor statistics for nitrogen calibration at the F34 scale, despite satisfactory results over the calibration period.

## 2.7 Summary and Conclusions

There are several issues to consider in the application of watershed scale hydrologic modeling, one of which is the influence of watershed size on model calibration parameters. This is especially true when using the model as an environmental assessment tool or as a decision-support system for soil and water resource management. The objective of this study was to investigate the influence that watershed size has on SWAT calibration for streamflow, nitrogen and phosphorus estimates in agricultural watersheds.

Based on the results presented here, calibrating the model at one watershed size and applying the optimized parameters at different sizes may produce satisfactory results. These results are possible in SWAT model simulations because the study watersheds are nested within each other and have similar physiographic features that resulted in similar parameterization of SWAT. However, as shown in the optimization performed at F34, when SWAT parameters vary in sensitivity between watersheds, they are likely to produce lower KGE and NSE values when applied at different watershed sizes.

Based on the results of this study and the constraint of similar physiographic properties, the size of the watershed for which SWAT is calibrated tends to have a greater impact on nitrogen and phosphorus simulations than on streamflow predictions. Calibrating SWAT at the smaller watershed sizes was successful in reducing the bias between measured data and SWAT model simulations while maintaining model efficiency. In some instances, the goodness-of-fit measures used to evaluate model efficiency were improved when the

model was calibrated at the smaller ALG (20 $km^2$) watershed then applied at the larger CCW (679 $km^2$) watershed.

The inclusion of pothole simulation in SWAT has added more complexity to the calibration process. More study is needed that will help to streamline the pothole representation in SWAT and to identify the proportion of tile flow that is directly attributed to tile inlets versus contributions from the water table, and direct interception of infiltrate. This study has demonstrated that with proper calibration of SWAT, it is possible to transfer optimized parameters from one watershed size to another, however, more research is need to determine under what condition (or sets of conditions) this will be applicable.

# CHAPTER 3. QUANTIFYING THE EFFECTS OF FUTURE CLIMATE CONDITIONS ON RUNOFF, SEDIMENT AND CHEMICAL LOSSES AT DIFFERENT WATERSHED SIZES

## 3.1 Synopsis

Assessing the sensitivity of agricultural watersheds to possible changes in future climate is imperative when developing appropriate management practices. Agricultural management practices are often assessed at the watershed scale and therefore, understanding the influence of climate change at different watershed sizes will provide insight into the effectiveness of watershed management strategies under future climate conditions, especially in highly agricultural watersheds with modified hydrologic landscapes. In this study, the Soil and Water Assessment Tool (SWAT) and downscaled weather data generated using the MarkSim weather file generator were used to evaluate the potential impact of climate change on surface flow, tile flow, sediment and chemical losses in the hydrologically modified Cedar Creek, F34, AXL and ALG watersheds located in northeastern Indiana.

There was no clear evidence to suggest watershed size will have an impact on the simulation of climate change effects. Results of this study indicate that surface flow will decrease significantly towards the end of this century (ranging from 9% in CCW to 22% in ALG), while subsurface tile flow will increase significantly (ranging from 20% in

CCW to 26% in AXL). The percentage increases in predicted sediment loss at the CCW, AXL and ALG watersheds were significant at $\alpha = 0.05$, though the magnitudes of overall sediment loss were low, especially in the CEAP monitored watersheds (F34, AXL and ALG) in which several best management practices are implemented. Differences in predicted atrazine, soluble N, total N, and total P losses between the baseline period and the end of the century were not significant for any of the watersheds, while increased soluble P losses were only significant for the larger CCW and F34 watersheds.

## 3.2 Introduction

Changes in future climate conditions are expected to have important effects on national and regional hydrologic conditions and subsequently affect runoff volume and chemical losses at the watershed scale (Jeppesen et al., 2009; Pfister et al., 2004; Sun et al., 2000). Increasing greenhouse gas concentrations in the atmosphere are expected to influence the pattern and amounts of precipitation, increase Earth's average temperature and reduce ice and snow cover (USEPA, 2014). The rate at which greenhouse gas concentrations continue to increase, as well as the degree to which climate features (e.g., precipitation, temperature) respond to these increases will determine the rate and magnitude of future climate change impacts.

The Intergovernmental Panel on Climate Change (IPCC) assesses future climate change and publishes a series of comprehensive 'Assessment Reports' based on different emission scenarios that describe possible future population growth and socio-economic developments and are backed by relevant scientific and technical information (IPCC,

2014). These emission scenarios are considerably different in terms of projected changes in precipitation and temperature for different regions (Jones and Thornton, 2013).

In the 2014 IPCC assessment report (Fifth Assessment Report), possible future socioeconomic pathways, climate change and its risks, and the SRES scenarios were assessed and a special report published on four possible representative concentration pathways (RCPs). These scenarios (RCP2.6, RCP4.5, RCP6.0 and RCP8.5) represent the radiative forcing values of 2.6 - 8.5 $W/m^2$ for the period extending to the year 2100 (Moss et al. 2010; Taylor et al. 2012). RCP2.6 refers to a peak in radiative forcing at 2.6 $W/m^2$ before 2100 followed by a gradual decline. RCP4.5 represents stabilization without an overshoot pathway to 4.5 $W/m^2$, with stabilization occurring after 2100. RCP6.0 represents a stabilization (without overshoot) pathway to 6.0 $W/m^2$ after 2100, while RCP8.5 represents a rising radiative forcing pathway leading to 8.5 $W/m^2$ in 2100 (IPCC, 2014).

Several stochastic weather file generating tools (e.g. MarkSim and LARS-WG) have been developed and used to produce downscaled climate information from general circulation models (GCM) results for use in climate change studies. These climate projections are usually based on one or more representative concentration pathways. Climate files generated by MarkSim have been applied successfully in several climate change studies on agricultural watersheds, globally (Bharati et al., 2014; Lobell and Burke, 2010; Rao et al., 2015; Thornton et al., 2010).

Researchers have simulated the impacts of climate change scenarios on streamflow in parts of the United States and India, using the Soil and Watershed Assessment Tool (SWAT) (Ficklin et al., 2009; Gosain et al., 2006; Narsimlu et al., 2013), and concluded that there will be significant changes in annual average streamflow for both wet and dry seasons. Changes in precipitation and temperature may also have significant effects on water yield, evapotranspiration, irrigation water use, as well as plant growth patterns (Ficklin et al., 2009). While climate change may have some positive effects in the Midwest United States such as increased water supply in certain areas and longer growing season (Southworth et al., 2002); the negative impacts of future climate change are expected to outweigh the positive impacts (USEPA, 2014). The implications on future water quality may be severe; therefore, a more in-depth assessment is required, especially in specific agricultural watersheds of interest, such as those in the Lake Erie Basin.

Lake Erie is smallest of the five Great Lakes (by volume) located in North America, and is the most heavily polluted from agricultural activities. Significant algae growth during the early 1970s led to poor water quality conditions in Lake Erie. The overabundance of algae, which was primarily due to excess loading of nutrients, such as phosphorus, into the lake, resulted in anoxic conditions that subsequently lead to large fish kills. The Great Lakes Water Quality Agreement (GLWQA) of 1972 established guidelines for pollutants using the best available technology and knowledge, which provides the impetus for reducing phosphorus levels in Lake Erie. Limits were set to reduce the amount of phosphorus entering the lake gradually (P concentration limit of 1.0 mg $L^{-1}$). To achieve

these limits, the Great Lakes states passed a ban against detergents that use phosphorus, while program guidelines were developed to improve the treatment of human sewage. As point sources of phosphorus entering the lake reduced from more than 15 000 Mg P $yr^{-1}$ in 1972 to less than 3000 Mg P $yr^{-1}$ in 1982 (Dolan, 1993), water quality improved. However, nonpoint sources of  (and other nutrients) from fertilizer application continue to enter the lake and dominate total loading to Lake Erie (approximately 2000 Mg $yr^{-1}$ above the GLWQA limit) by the early 1980s (Baker and Richards, 2002). A non-point source reduction (mainly through agriculture loading) of 1700 Mg P $yr^{-1}$ was assigned to the United States (USEPA, 2014), of which 1390 Mg P $yr^{-1}$ was subsequently assigned to Ohio.

Conservation practices such as conservation tillage and integrated crop management operations have been shown to reduce phosphorus loading to the lake during the 1980s. Approximately 75 to 80% of total  loading was particulate P associated with total suspended sediment (TSS) transport therefore, plans for reducing nonpoint sources of P focused exclusively on reductions associated with various erosion control programs (Baker and Richards, 2002). However, P fertilizer application was also reduced substantially during the 1980's (Richards et al., 2002). Results of the annual monitoring program carried out by the USEPA's Great Lakes National Program Office found that an upward trend in total P began in the 1990s continued to the present day. The ongoing effects of excessive nutrient loading include seasonal depleted oxygen conditions intensifying in the central basin; Blue-green algal blooms are occurring regularly in the

western basin. Fouling of nearshore areas of the eastern basin; and loading of soluble reactive phosphorus is increasing in the Sandusky and Maumee rivers and may be increasing in other Lake Erie tributaries as well (Lake Erie LAMPs. 2011).

This study seeks to examine the effects of future climate conditions on runoff, sediment, pesticide, and nutrient losses from four watersheds within the Lake Erie Basin to determine whether climate change will cause the problems occurring in Lake Erie to become better or worse. SWAT was the tool of choice for undertaking such an extensive evaluation because it is a comprehensive model that provides the capability to simulate watershed hydrology, plant growth, surface and subsurface water quality as well as climate change impacts (Arnold et al., 1998). Future climate data used to parameterize SWAT were projected using the MarkSim DSSAT weather file generator (the web application version) (Jones and Thornton, 2000, 2013).

### 3.2.1 SWAT Model Description

The Agricultural Research Service (ARS) developed SWAT (Arnold et al., 1998) as an operational model that incorporates processes simulated by several different computer programs into one comprehensive system to assist water resource managers in assessing water supplies and nonpoint source pollution in large river basins (Arnold and Fohrer, 2005). The impact of land management on water, sediment, nutrients, and pesticides leaving the edge of a field is simulated using algorithms from the Chemicals, Runoff and Erosion from Agricultural Management Systems (CREAMS) model (Knisel, 1980). The

CREAMS model was modified to include pesticide groundwater loadings (GLEAMS) (Leonard et al., 1987), and to simulate the impact of erosion on crop production (EPIC) (Williams et al., 1983). The development of several other hydrologic models in the mid to late 1980s influenced the capabilities of SWAT to simulate hydrology and water quality of complex watersheds with varying soils, land use and management (Arnold and Fohrer, 2005). One of the primary considerations in SWAT development was its ability to simulate climate and land management impacts on water quality. It is computationally efficient; allows considerable spatial detail; requires readily available inputs; operates on a continuous time step; is capable of simulating land-management scenarios; and can capture management effects on large river basins through long-term simulations (Arnold and Fohrer, 2005).

The climatic conditions of a watershed (rainfall, maximum and minimum temperature, relative humidity, solar radiation and wind speed) provide information needed to control the water balance that drives the different components of the hydrologic cycle, which is the driving force behind all other processes simulated by SWAT. SWAT is equipped with a weather generator capable of generating climate data for each, however, climate data may also be input from records of measured or predicted values. SWAT is capable of simulating hydrologic and subsequent processes for the entire period of input daily climate, which provides the capability to perform simulations for both historic and future climate conditions.

For this study, SWAT model configurations were developed and calibrated specifically to simulate surface flow, tile flow, sediment, atrazine, soluble N, total N, soluble P and total P losses in the CCW, F34, AXL and ALG watersheds under a baseline and multiple future climate conditions.

### 3.2.2 MarkSim Weather File Generator Description

Due to the uncertainty of future climatic conditions, the choice of general circulation models (GCM) and RCP scenarios can influence the projected weather data. In addition to differences between emissions scenarios used to drive the climate models, the GCMs themselves vary greatly in consistency for regional climate projections (IPCC, 2007). Therefore, the MarkSim Decision Support System for Agrotechnology Transfer (DSSAT), a web-based version of the MarkSim application (Jones and Thornton, 2000), operating on a Google Earth platform was designed to downscale results from multiple climate models to generate global averages of surface warming (relative to 1980-1999) for the four RCP scenarios. MarkSim DSSAT allows selection of one of the four RCP scenarios, and one of 17 climate models, or their average for climate downscaling (Jones, 2014).

During data processing, results from the GCMs were obtained for five time slices (i.e. 1991-2010, 2021-2040, 2041-2060, 2061-2080 and 2081-2100) for average daily precipitation, daily maximum and minimum air temperatures and solar radiation that were projected from their original resolution to $0.5^{o}$ latitude-longitude. The absolute

changes (anomalies) in daily rainfall, mean daily maximum and minimum temperature were calculated for each time slice relative to the model calibration period (1961-1990). These anomalies were then downscaled to a higher resolution and used to generate daily weather data that are characteristic of future climatology, using a stochastic weather generator (Jones and Thornton, 1993).

Though MarkSim does not explicitly account for uncertainties in projected climate data, it was calibrated using data from 10,000 stations worldwide (WorldClim), with most stations having 15-20 years of historical daily data and some having up to 100 years of historical data. During calibration, 20$^{th}$ century climate outputs from the GCMs were used to fit WorldClim data through Markov Chain regression (Jones and Thornton, 2013). The regression equations developed were then applied to 21$^{st}$ century output from GCMs to create downscaled future climate data. Evaluations of the MarkSim weather file generator by a few researchers have produced mixed results. MarkSim outputs are said to have high inter-annual variability and long chains of wet days (Hartkamp et al., 2003; Mavromatis and Hansen, 2001), however, due to its reduced data requirement and certain theoretical assumptions, the MarkSim weather file generator is suitable for application in developing countries (Hartkamp et al., 2003). The noted advantages of MarkSim include its global applicability, its minimal input requirements and its applicability in locations that often have no available observed climate data (Jones and Thornton, 2000; Thornton et al., 2010; Trotochaud et al., 2016).

## 3.3 Objective

This study seeks to examine the effects of future climate conditions on runoff, sediment, pesticide, and nutrient losses from four watersheds within the St. Joseph River Watershed (SJRW). SWAT was selected for undertaking such an extensive evaluation because it is a comprehensive model that provides the capability to simulate watershed hydrology, plant growth, surface and subsurface water quality as well as climate change impacts (Arnold et al., 1998). Future climate data used to parameterize SWAT were projected using the MarkSim DSSAT weather file generator (the web application version).

## 3.4 Methodology

### 3.4.1 Study Area Description

Lake Erie is having critical problems with algal blooms resulting from nitrogen and phosphorus loadings to the lake. For this reason, the Cedar Creek Watershed (CCW), F34, AXL and ALG watersheds, which are part of the Lake Erie Basin, were chosen to evaluate whether climate change will have a significant impact on future nitrogen and phosphorus loadings to Lake Erie. CCW is a 679 $km^2$ catchment that intersects Allen, DeKalb and Noble Counties in northeastern Indiana (85°19'28.101" to 84°54'12.364"W and 41°11'47.494" to 41°32'8.776"N) (Figure 3.1). Cedar Creek is the largest tributary to the St. Joseph River, which joins the St. Mary's River near Ft. Wayne, Indiana to form the Maumee River. The Maumee River flows into the Maumee Bay of Lake Erie in Toledo, Ohio. CCW is predominantly an agricultural watershed (68%) with approximately 15%

forest and 10% urban (Figure 3.1). The majority of soils in the watershed are comprised of the Eel-Martinsville-Genesee (deep, moderately well drained and medium to moderately fine-textured soils) and Morley-Blount associations (moderately to poorly drained soils with nearly level to deep medium-textured soils). Tile drainage systems are used to drain water from many of these soils into managed drainage ditches, which resulted in alteration of the watershed hydrology and the transport of pesticide and nutrients across the landscape (Pappas and Smith, 2007; Smith et al., 2008).

CCW is the largest of four watersheds analyzed in this study. The three remaining watersheds (F34 = 182.5 $km^2$, AXL = 41.5 $km^2$ and ALG =19.7 $km^2$) are nested within the upper Cedar Creek and share similar physiographic features to that of Cedar Creek. Average annual precipitation in the watersheds is approximately 950 mm. The average annual minimum and maximum temperatures in the watersheds are approximately 4$^oC$ and 16$^oC$ respectively.

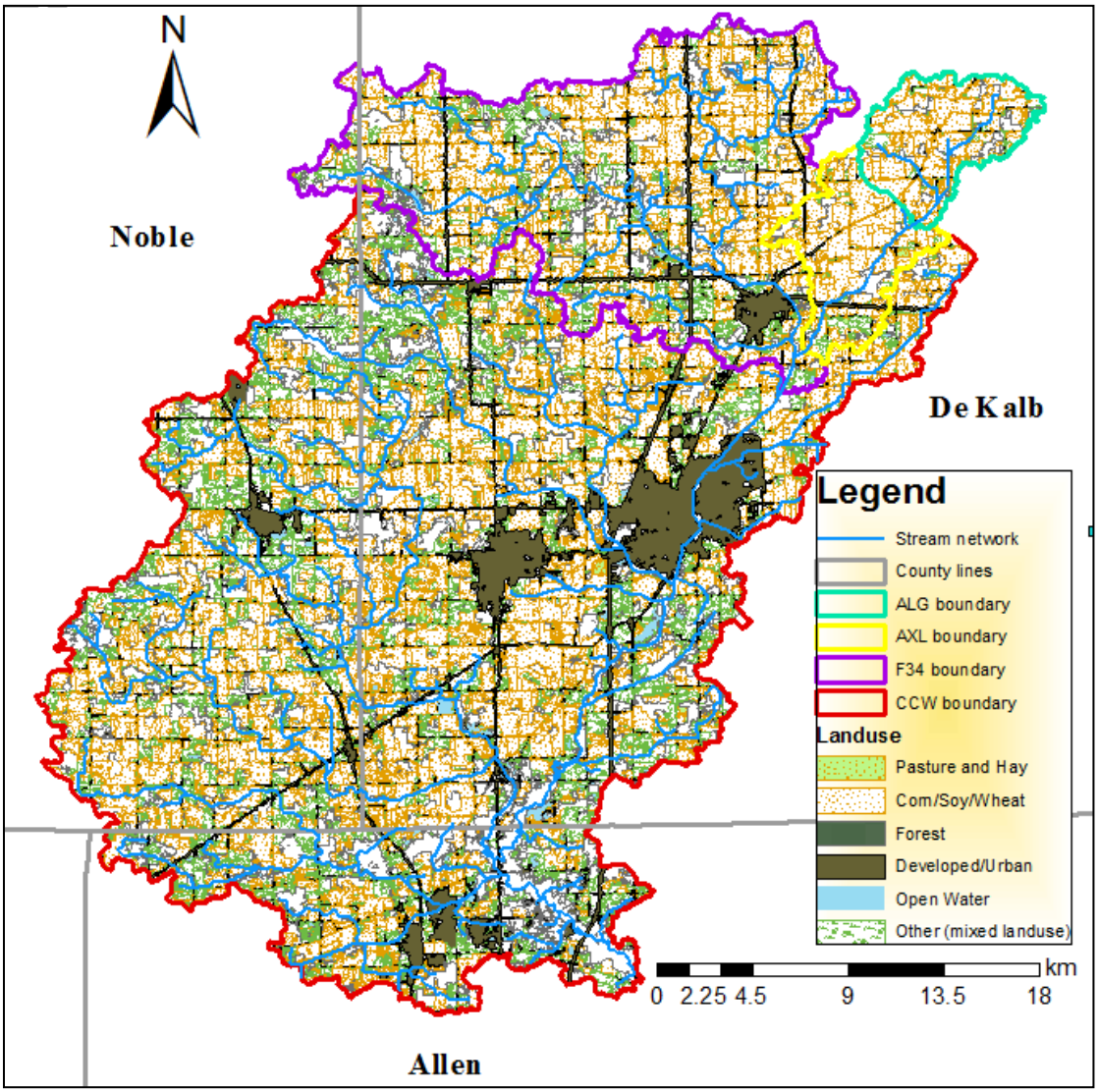


Figure 3.1. Location map of the study areas (CCW, F34, AXL and ALG).

### 3.4.2 Projecting Future Climate Conditions using MarkSim

For this study, the MarkSim DSSAT weather file generator was used to create and download downscaled climate projections from the IPCC Fifth Assessment Report (rainfall, maximum and minimum temperature, and solar radiation) at the Garrett weather

station (within the Cedar Creek watershed) for the period 2020 to 2099. These climate projections represent an ensemble mean of the 17 General Circulation Models (GCM) from the Coupled Model Intercomparison Project Phase 5 (CMIP5) simulated under the RCP 6.0 scenario (intermediate when compared to RCP 2.6, RCP 4.5 and RCP 8.5 pathways).

Ninety-nine (99) replicates of climate data were generated for each decade centered at the fifth year in each decade (i.e. 99 possibilities for 2020-2030, centered at 2025), and for the WorldClim baseline period (1961-1990) centered at 1975. The raw output from MarkSim, in the form of daily data, was strung together, end to end, to create a 99-year dataset representing each decade, using a Microsoft Excel macro (Trotochaud et al., 2016). The macro was used to reformat MarkSim outputs into a format compatible for ArcSWAT (version 2012_10.5a). Baseline data used in the projections are from 1961–1990, while simulation of future climate is from the 2020s through the 2090s, the time horizons for which water management decisions have to be made.

### 3.4.3 SWAT model setup

The ArcSWAT version 2012.10.5a interface was used to develop independent SWAT model configurations for each of the four watersheds (CCW, F34, AXL and ALG) and to expedite SWAT model input and output display. Descriptions of the data used during the model setup, calibration and validation periods are presented in Table 3.1. To obtain suitable flowpaths, stream delineation from the National Hydrograph Dataset (NHD) was used to burn in the location of the streams in a 10-m Digital Elevation Model (DEM)

obtained from USGS at a map scale of 1:24,000. In the watershed delineation process, a catchment outlet and a critical source area (CSA) were specified. The outlet point is used to determine the extent of the watershed area. The CSA (a percentage of the total watershed area) is used to specify the minimum upstream drainage area for a channel to occur, hence, determining the total number of subbasins that will be generated.

Table 3.1. Model input data information.

| Data Type | Source | Description |
|---|---|---|
| DEM | viewer.nationalmap.gov/viewer | 10-m Resolution, Digital Elevation Model (USGS 2011) |
| Soils | soildatamart.nrcs.usda.gov/ | Soil Survey Geographic Database (SSURGO) (USDA-NRCS 2011) |
| Land use | nassgeodata.gmu.edu/CropScape | National Agricultural Statistics Service (USDA-NASS 2011) |
| Hydrographic | nhd.usgs.gov/data.html | National Hydrograph Dataset (NHD) (USGS 2011) |
| Weather | ARS CEAP Water Quality Assessment Program | Daily precipitation, max and min daily temperature, solar radiation, wind, relative humidity |
| Weather | NOAA-NCDC: ncdc.noaa.gov/data-access/ | Daily precipitation, max and min daily temperature |
| Crop Management | ARS CEAP watershed survey, DeKalb and Allen County SWCDs | Tillage operations, fertilizer and herbicide applications, time of planting and time of harvesting |
| Water Quality | St. Joseph River Watershed Initiative | Streamflow, bi-weekly pesticide and nutrient concentration (TP, TN, NO2+NO3) |
| Water Quality | ARS CEAP Water Quality Assessment Program | Streamflow, daily pesticide and nutrient concentration (TP, PO4, TN, NO2+NO3) |

The Soil Survey Geographic Database (SSURGO) spatial data at a map scale of 1:12,000 and the USDA National Agricultural Statistics Service (USDA-NASS, 2009) Indiana Cropland Layer were used to create SWAT hydrologic response units (HRUs). HRUs are the smallest modeling units of SWAT, and are created for each overlapping unique combination of land use and soil type for each subbasin fixed threshold value. For this

study, a CSA of 5% was used to delineate subbasins for all four watersheds. A threshold area of 0% was used to capture every possible land use and soil type combination. The disadvantage of using a 0% threshold area is that it increases simulation time significantly, but it was necessary in order to facilitate the inclusion of closed depressions scattered through the watersheds. Closed depressions (potholes) occur throughout much of the Midwest because of glaciation and can range from a few square meters to several square kilometers. These potholes are often drained through surface tile inlets to increase productivity in croplands, therefore modifying the watershed hydrology. Subsurface tiles were assumed for 100 percent of cropped area with 20-meter spacing at a depth of one meter.

SWAT management files were created for F34, AXL and ALG based on area-specific land management data collected by the ARS-NSERL through the CEAP program. Management files for CCW and portions of F34 were created using land management data from the DeKalb and Allen County Soil and Water Conservation Districts (SWCDs), and represented countywide averages of current management practices occurring in the watersheds. Conservation tillage has been widely adopted in all of AXL and ALG, and much of CCW and F34 watersheds. In DeKalb County, 34% of all corn and 77% of all soybeans planted in 2012 were under a no-till system or mulch-till system (DeKalb SWCD, 2014); therefore, both no-till and conventional tillage were used as input in the SWAT management file. In cropland classified as corn or soybeans, a two-year rotation system was setup in the management file (corn/soybean or soybean/corn), but in areas

where wheat is grown, the management files were constructed with a three-year crop rotation (corn/soybeans/wheat). The management scheme includes yearly tillage and nutrient application rate, pesticide application rate, and planting and harvesting dates (Tables 3.2 and 3.3).

Downscaled climate data used in this study (precipitation, temperature and solar radiation) were generated using the web-based MarkSim DSSAT weather file generator as described above. Water quality and streamflow data for Cedar Creek were obtained from the USGS National Water Quality Assessment Program (NAWQA) water quality/streamflow gauge station located near Cedarville, Allen County. Water quality and streamflow data at the F34, AXL and ALG outlets were obtained from the Agricultural Research Service (ARS) National Soil Erosion Research Laboratory (NSERL), which has been monitoring the various sites from as early as 2002.

Table 3.2. Management operations for land in corn/soybeans rotation.

| Crop | Date | Management Operation | Rate |
|---|---|---|---|
| Corn | 22-Apr | Nitrogen Application (as Anhydrous Ammonia) | 176.0 kg/ha |
| | 22-Apr | ($P_2O_5$) Application (as DAP/MAP) | 54.0 kg/ha |
| | 22-Apr | Pesticide Application (as Atrazine) | 2.2 kg/ha |
| | 6-May | Tillage, Offset disk (60% mixing) | |
| | 6-May | Planting - row planter, double disk openers | |
| | 10-Oct | Harvest | |
| Soybeans | 10-May | ($P_2O_5$) Application (as DAP/MAP) | 40.0 kg/ha |
| | 24-May | No-Tillage planting- Drill | |
| | 7-Oct | Harvest | |
| | 20-Oct | Tillage, chisel (30% mixing) | |

Table 3.3. Management operations for land in winter wheat production (following corn/soybeans rotation in Table 3.2).

| Crop | Date | Management Operation | Rate |
|---|---|---|---|
| Wheat | 23-Oct | ($P_2O_5$) Application (as DAP) | 45.0 kg/ha |
| | 25-Oct | Tillage, disk (60% mixing) | |
| | 25-Oct | Planting – Drill, double disk openers | |
| | 1-Mar | Nitrogen Application (as Urea) | 75.0 kg/ha |
| | 1-Jul | Harvest | |

### 3.4.4 SWAT model calibration and validation

Each of the four SWAT model configurations was calibrated and validated independently on a monthly time step for streamflow, $NO_3$+$NO_2$ (referred to as soluble N from here on), total nitrogen (total N), orthophosphate (soluble P), and total  (total P) losses. The model calibration period was from January 2006 to December 2009, and validation from January 2010 to December 2013. Calibration was necessary to develop better parameters sets for the model based on physically observed conditions in the watersheds, hence minimizing prediction uncertainty.

Climate data such as daily precipitation, maximum and minimum air temperatures, solar radiation, relative humidity, and wind speed that were used for the SWAT calibration and validation period were obtained from eight CEAP weather stations located in the upper Cedar Creek region for the period 2001 to 2013. Daily precipitation and maximum and minimum air temperatures were also obtained from the National Climate Data Center (Diamond et al., 2013) for the Garrett and Waterloo stations located within CCW, with records from 1989 to 2013.

Model parameters for all four-watershed configurations were calibrated using the SWAT-CUP autocalibration tool. Manual calibration was also used to improve the results of autocalibration based on best professional judgment (Arnold et al., 2012). During manual calibration, adjustments were made only to the most sensitive parameters while ensuring that the parameter values remained within an acceptable range. Examples of monthly observed and simulated time series for streamflow, soluble N, total N, soluble P and total P are presented in Figure 3.2. In addition to visual inspection, when comparing observed and simulated values at the watershed outlets, the Kling-Gupta efficiency (KGE), Nash-Sutcliffe efficiency (NSE), coefficient of determination ($R^2$) and percent bias (PBIAS) were also used to evaluate model performance. The values calculated for the calibration and validation periods were all within the acceptable range (KGE > 0.5, NSE > 0.50, $R^2$ > 0.50, PBIAS ±25%) (Larose et al., 2007; Moriasi et al., 2007; Van Liew and Garbrecht, 2003).

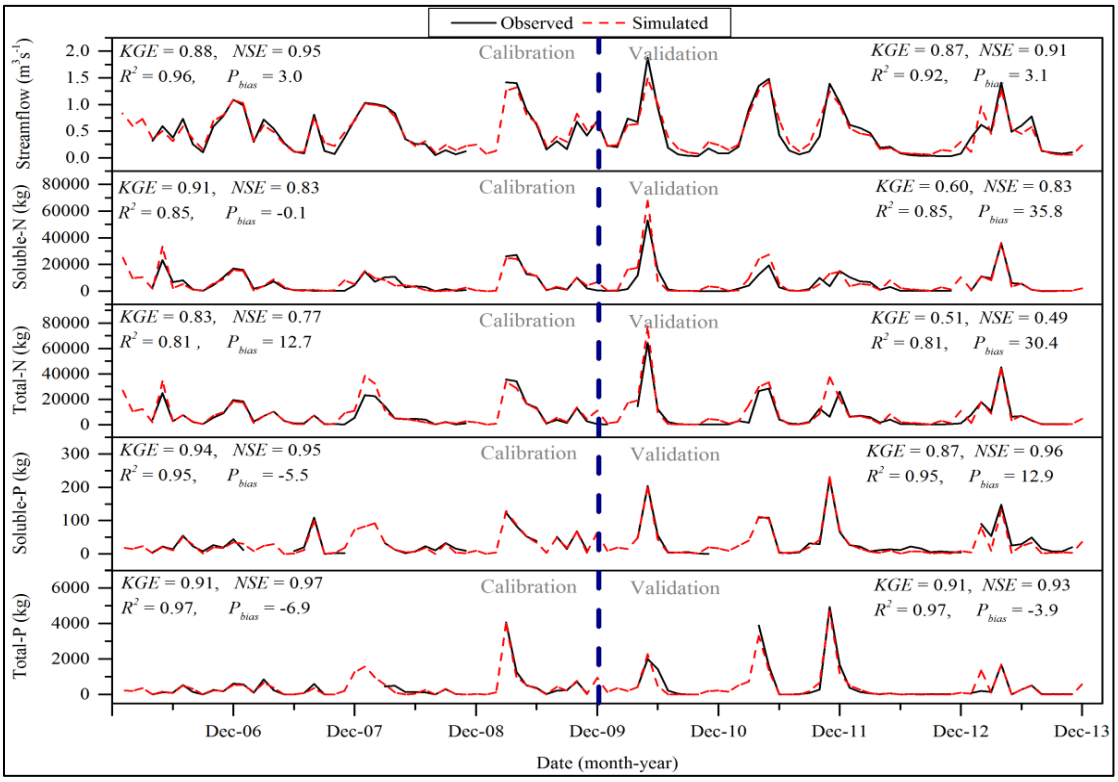


Figure 3.2. Observed and simulated monthly flow, soluble N, total N, soluble P and total P at AXL including the $R^2$, NSE, KGE and PBIAS values for the calibration/validation period.

Following satisfactory model calibration and validation, SWAT was run with climate data from the MarkSim weather generator for 1961-1990 (baseline), 2020-2029, 2030-2039, 3040-2049, 2050-2059, 2060-2069, 2070-2079, 2089-2089, and 2090-2099. The impact of climate change on runoff, sediment, atrazine, nitrogen, and phosphorus losses was assessed at four watershed sizes by comparing the baseline with the projected outputs.

## 3.5 Results

### 3.5.1 Characteristics of the baseline and future climate

Average monthly mean precipitation, maximum and minimum temperature for the baseline climate (1961-90) and future climate projections were compared to measured data obtained from a nearby weather station (GHCND:USC00120334) in Auburn, Indiana for the period 1961-90 to determine whether MarkSim was predicting climate representative of the region. Except for the months of June and July, the monthly mean precipitation for the MarkSim baseline and the observed precipitation were not significantly different, with p-value = 0.6043 at $\alpha$ =0.05. The average observed precipitation for June is approximately 10 mm larger than the baseline precipitation while the average observed precipitation for July is approximately 10 mm less than the MarkSim baseline precipitation.

The average monthly maximum and minimum temperatures for the MarkSim baseline were also not significantly different from the observed monthly average maximum and minimum temperatures (p-value = 0.1288 and 0.1729, respectively). Figure 3.3 shows the monthly variations in precipitation, maximum and minimum temperature for observed, baseline and projected future climate. Most precipitation occurs in the watershed from April to June, and the dry season extends from November to February. Bias correction is often encouraged when working with projected future climate due to the uncertainties in General Circulation Models (GCM). However, because this study focused on average annual outputs from SWAT and there was no significant difference between the MarkSim

simulated baseline climate and the observed climate data (for the 10 months excluding June and July), a bias correction was not performed.

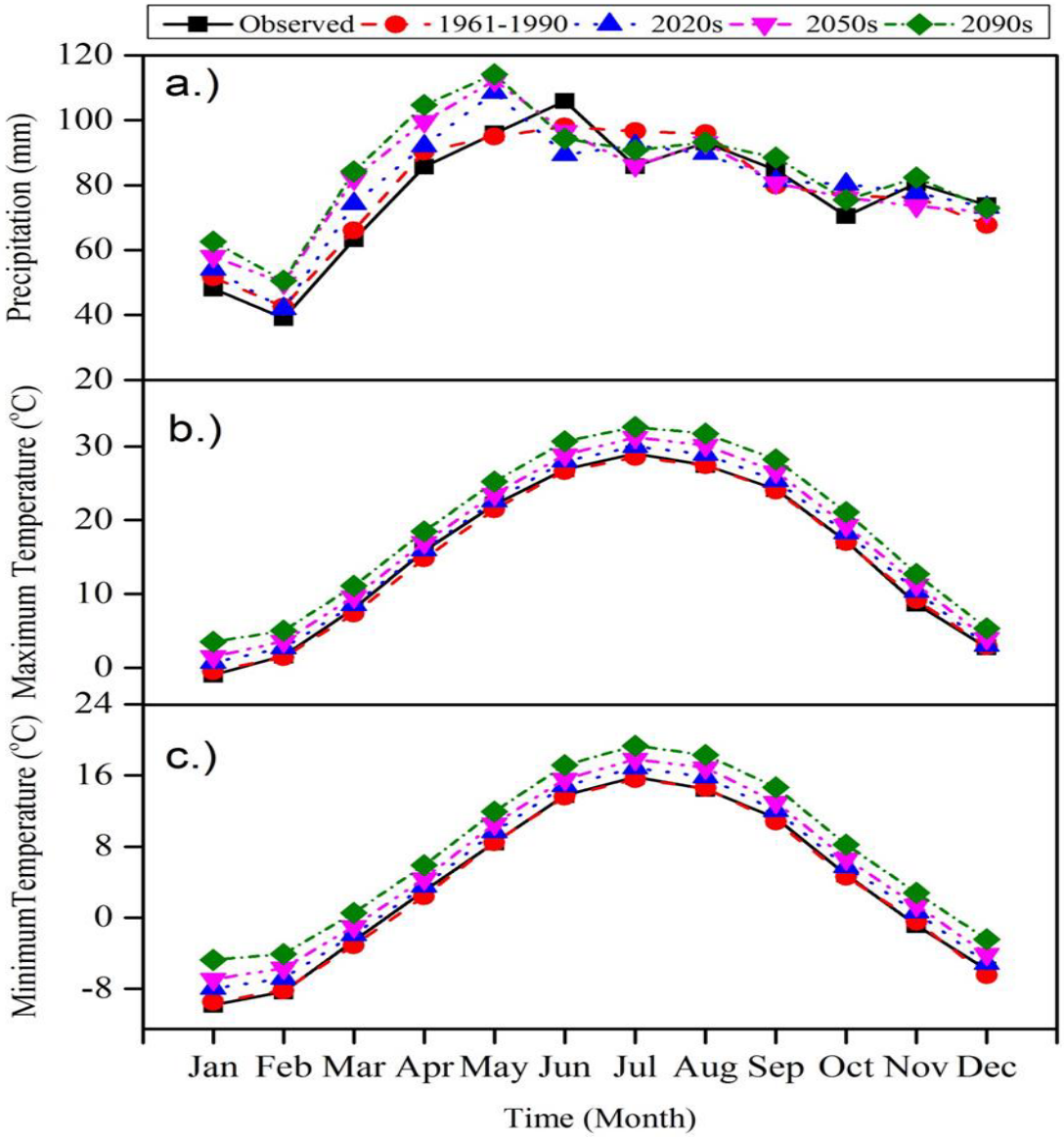


Figure 3.3. Meteorological data measured at the Auburn weather station, Indiana (1961-90) compared to meteorological data projected using the MarkSim weather file generator (1961-90, 1920s, 1950s and 1990s); mean monthly (a) precipitation, (b) maximum temperature and c) minimum temperature.

The simulated average daily solar radiation was projected to increase by approximately 2.4%, with respect to baseline climate. The simulated average annual minimum and maximum daily temperature for the baseline period were 3.6 °C and 15.0 °C, respectively, which are approximately 0.5 and 0.2 °C less than the average annual lows and highs, respectively, measured at the Auburn weather station. Based on the SWAT simulation design, model simulations under baseline climate were expected to predict reasonable hydrological results representative of the period 1961-90. Average annual maximum and minimum daily temperature were projected to increase 3.9 and 4.0 °C, respectively, to the end of the century. Other studies (Wuebbles and Hayhoe, 2004; USGCRP, 2009; Winkler et al., 2012; Pryor et al., 2014) of future climate change in the Midwest suggest that temperature during winter will increase 3 to 7 °C while summer temperatures will increase 4 to 11 °C over the Great Lakes area by the end of this century.

Average annual precipitation generated by MarkSim during the baseline 30-year period (relative to the location of the Auburn weather station) was 937 mm, approximately 13 mm less than the observed precipitation measured at the Auburn weather station. With respect to future climate, average annual precipitation was projected to increase gradually from 937 mm in the baseline period to approximately 1016 mm (8.5%) by the end of this century. Similar to other climate change studies in the Midwest (Pryor et al., 2014), spring and summer precipitation are expected to increase by approximately 9% and 8%, respectively. Based on previous studies (USGCRP, 2009; Winkler et al., 2012; Pryor et al., 2014), projected precipitation in the Midwest is likely to fall more frequently in heavy

downpours with longer dry periods between each heavy rainfall event. Climate projections obtained using the MarkSim weather file generator suggest, however, that the majority of precipitation will occur in smaller storm events, which could potentially lessen the impact of changes in precipitation to soil erosion and surface runoff. Figure 3.4 shows the distribution for precipitation as projected by MarkSim for three individual GCMs (MIROC5, IPSL_CM5A_MR and HadGEM2_EM) and the ensemble mean of 17 GCMs from the CMIP5 model outputs. As presented in Figure 3.4, most precipitation occurs in the range 5.0 to 10.0 mm. The IPSL_CM5A_MR, HadGEM2_EM and the ensemble mean show precipitation in the range 0.01 to 30.0 mm is increasing while precipitation in the range 40.0 to 200.0 mm is decreasing from the 2020s to the end of the century. The MIROC5, however, showed greater increase during the mid-century period for the 0.01 to 30.0 mm range. MIROC5 also shows that precipitation in the range 40.0 to 200.0 mm will increase between the mid-century period and the end of the century. Figure 3.4 shows that the choice of GCM will have implications on projected precipitation and consequently surface runoff, erosion and sediment loss. Therefore, caution is required when comparing results from climate change studies.

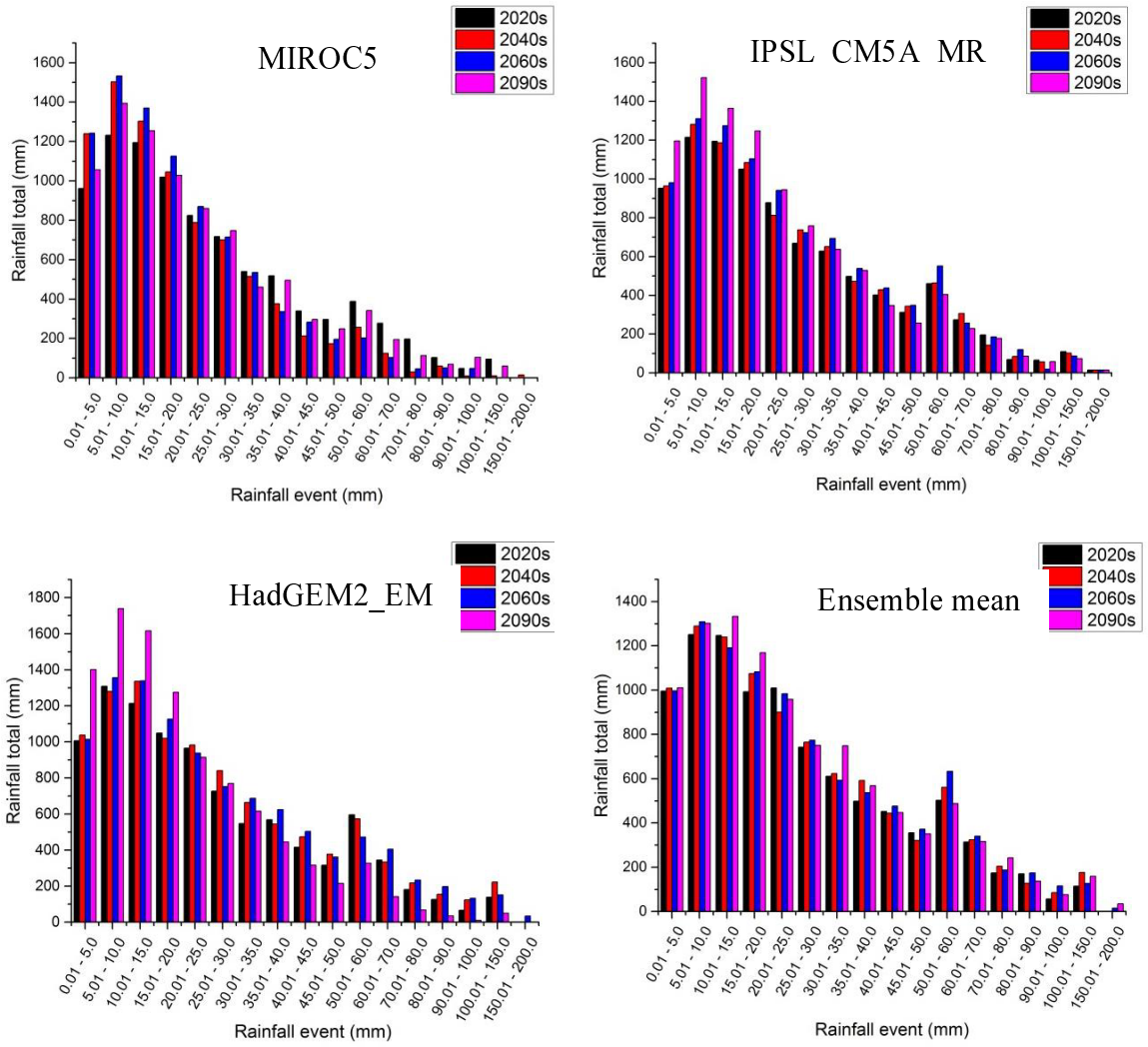


Figure 3.4. Distribution of rainfall based on MarkSim climate projections (2020s, 2040s, 2060s and 2090s).

Another factor affecting the outcome of climate change studies is the downscaling approach. Climate projections obtained from GCMs are often at coarse resolutions and require downscaling to a finer resolution in order to capture the changes at the regional scale (Wuebbles and Hayhoe, 2004). A common downscaling approach used in climate

change studies in the Midwest uses an empirical statistical technique that maps the probability density functions for modeled monthly and daily precipitation and temperature for the climatological period (1961– 1990) onto those of gridded historical observed data, so the mean and variability of both monthly and daily observations are reproduced by the climate model outputs. In a study of climate change in the Midwest (Wuebbles and Hayhoe, 2004), monthly GCM temperature and precipitation fields (at 2.0 to 2.5 degrees) were statistically downscaled to daily values across the entire Midwest region with a resolution of 1/8 degrees. The resulting projections of future precipitation indicate that heavy downpours are likely to occur, primarily in winter and spring months, which may lead to increased runoff and erosion (USEPA, 2014).

Instead of statistical downscaling, MarkSim uses a combination of stochastic downscaling and weather typing on top of a simple interpolation method (Jones and Thornton, 2013). MarkSim first interpolates the results of each GCM spatially using bicubic interpolation of the 16 points closest on a 1-degree grid. It then performs stochastic downscaling by fitting a third order Markov model to the GCM output and uses it to generate weather data for the site indicated. The coefficients for the third order Markov rainfall generator is calculated from predetermined clusters (720 classes) of weather, worldwide (weather typing). Each weather class defines a set of regression equations that MarkSim uses to determine the coefficients for the modelling process. When a climate changes, such that it no longer applies to the original class, the whole regression structure changes so that changing climate will be modelled by the one most

like it in the real world (Jones and Thornton, 2013). This downscaling approach coupled with the RCP 6.0 scenario, as used in this study, produced climate projections suggesting that more precipitation will likely occur in smaller storm events.

The effect of changes in atmospheric carbon dioxide ($CO_2$) concentrations on SWAT model simulations should be small (Wang et al., 2016) and therefore, was not accounted for in this study. Hence, all changes in watershed responses were due to changes in precipitation, temperature and solar radiation. Changes in average annual climate to the end of this century affect watershed hydrology and consequently affect runoff, sediment and nutrient losses in the four highly agricultural watersheds evaluated in this study. The average annual metrics (rainfall, surface flow, tile flow, sediment, atrazine, soluble N, total N, and soluble P and total P losses) for the CCW, F34, AXL and ALG simulations are summarized in Table 3.4 and depicted in Figure 3.5 and Figure 3.6.

Table 3.4. Average annual metrics (rainfall, surface flow, tile flow, sediment, atrazine, soluble N, total N, and soluble P and total P losses) under baseline and future climate.

| | | Base | 2020s | 2030s | 2040s | 2050s | 2060s | 2070s | 2080s | 2090s | p-value |
|---|---|---|---|---|---|---|---|---|---|---|---|
| Precipitation (mm $yr^{-1}$) | | 937 | 955 | 963 | 980 | 978 | 998 | 1013 | 1006 | 1016 | 0.002 |
| Surface flow (mm $yr^{-1}$) | CCW | 80.7 | 78.6 | 78.7 | 79.8 | 78.5 | 77.8 | 77.2 | 75.0 | 73.5 | 0.037 |
| | F34 | 78.1 | 75.8 | 73.0 | 74.0 | 72.3 | 72.6 | 69.7 | 66.4 | 64.2 | 0.000 |
| | AXL | 68.0 | 64.1 | 64.0 | 64.5 | 63.5 | 63.2 | 63.2 | 60.3 | 58.8 | 0.005 |
| | ALG | 41.0 | 35.4 | 35.3 | 35.6 | 35.0 | 34.8 | 34.3 | 32.2 | 31.8 | 0.005 |
| Tile flow (mm $yr^{-1}$) | CCW | 67.7 | 69.9 | 71.0 | 74.0 | 72.7 | 77.2 | 80.1 | 78.6 | 81.3 | 0.004 |
| | F34 | 99.0 | 108.0 | 106.9 | 110.6 | 110.2 | 120.3 | 120.9 | 121.1 | 124.6 | 0.003 |
| | AXL | 81.8 | 86.4 | 88.1 | 91.3 | 90.9 | 96.6 | 100.1 | 99.4 | 102.7 | 0.002 |
| | ALG | 95.2 | 99.9 | 101.5 | 104.7 | 104.6 | 110.8 | 115.6 | 115.4 | 118.4 | 0.005 |
| Sediment loss ( t $ha^{-1}yr^{-1}$) | CCW | 5.39 | 5.54 | 5.56 | 6.08 | 6.17 | 6.41 | 6.38 | 6.27 | 6.12 | 0.000 |
| | F34 | 5.24 | 5.14 | 5.19 | 5.70 | 5.75 | 5.89 | 5.99 | 5.83 | 5.54 | 0.441* |
| | AXL | 0.71 | 0.71 | 0.72 | 0.83 | 0.92 | 1.10 | 1.42 | 1.48 | 1.44 | 0.000 |
| | ALG | 0.41 | 0.33 | 0.35 | 0.45 | 0.54 | 0.75 | 0.98 | 0.97 | 0.98 | 0.000 |
| Atrazine loss (g $ha^{-1}$ $yr^{-1}$) | CCW | 2.45 | 2.73 | 2.76 | 3.00 | 2.95 | 2.79 | 2.99 | 2.94 | 2.65 | 0.575* |
| | F34 | 2.27 | 2.55 | 2.57 | 3.04 | 2.94 | 2.80 | 3.00 | 3.07 | 2.55 | 0.559* |
| | AXL | 1.55 | 1.76 | 1.80 | 2.17 | 2.09 | 1.96 | 2.13 | 2.28 | 1.96 | 0.590* |
| | ALG | 0.95 | 1.01 | 1.01 | 1.29 | 1.23 | 1.08 | 1.19 | 1.11 | 0.94 | 0.143* |
| Soluble N loss (kg $ha^{-1}$ $yr^{-1}$) | CCW | 9.2 | 9.3 | 9.4 | 9.8 | 9.6 | 9.6 | 9.9 | 10.5 | 10.3 | 0.169* |
| | F34 | 14.9 | 15.1 | 15.1 | 15.5 | 15.5 | 15.8 | 15.8 | 15.4 | 15.4 | 0.346* |
| | AXL | 10.1 | 10.5 | 10.6 | 11.0 | 10.9 | 11.2 | 11.4 | 11.8 | 11.5 | 0.427* |
| | ALG | 11.9 | 11.5 | 11.6 | 11.9 | 11.7 | 12.0 | 12.3 | 12.5 | 12.5 | 0.405* |
| Total N loss (kg $ha^{-1}$ $yr^{-1}$) | CCW | 10.0 | 9.8 | 10.0 | 10.4 | 10.1 | 10.1 | 10.4 | 11.0 | 10.7 | 0.345* |
| | F34 | 15.5 | 15.5 | 15.5 | 15.9 | 15.9 | 16.2 | 16.2 | 16.7 | 16.3 | 0.673* |
| | AXL | 12.8 | 13.0 | 13.2 | 13.8 | 13.8 | 14.5 | 15.0 | 15.4 | 15.0 | 0.008* |
| | ALG | 13.0 | 12.3 | 12.4 | 12.9 | 12.9 | 13.4 | 13.9 | 14.0 | 14.0 | 0.223* |
| Soluble P loss (kg $ha^{-1}$ $yr^{-1}$) | CCW | 0.21 | 0.20 | 0.20 | 0.21 | 0.21 | 0.22 | 0.21 | 0.19 | 0.19 | 0.031 |
| | F34 | 0.11 | 0.10 | 0.10 | 0.10 | 0.10 | 0.10 | 0.10 | 0.09 | 0.09 | 0.001 |
| | AXL | 0.05 | 0.05 | 0.05 | 0.05 | 0.05 | 0.05 | 0.05 | 0.05 | 0.04 | 0.164* |
| | ALG | 0.05 | 0.04 | 0.04 | 0.05 | 0.05 | 0.05 | 0.06 | 0.05 | 0.05 | 0.450* |
| Total P loss (kg $ha^{-1}$ $yr^{-1}$) | CCW | 1.39 | 1.32 | 1.32 | 1.39 | 1.44 | 1.45 | 1.45 | 1.37 | 1.36 | 0.989* |
| | F34 | 1.29 | 1.19 | 1.18 | 1.22 | 1.21 | 1.19 | 1.20 | 1.14 | 1.12 | 0.051* |
| | AXL | 0.60 | 0.55 | 0.55 | 0.59 | 0.61 | 0.66 | 0.72 | 0.70 | 0.68 | 0.161* |
| | ALG | 0.26 | 0.19 | 0.19 | 0.22 | 0.24 | 0.28 | 0.32 | 0.28 | 0.29 | 0.426* |

Note: * indicates that the percentage change in pollutant losses were not significant at $\alpha = 0.05$

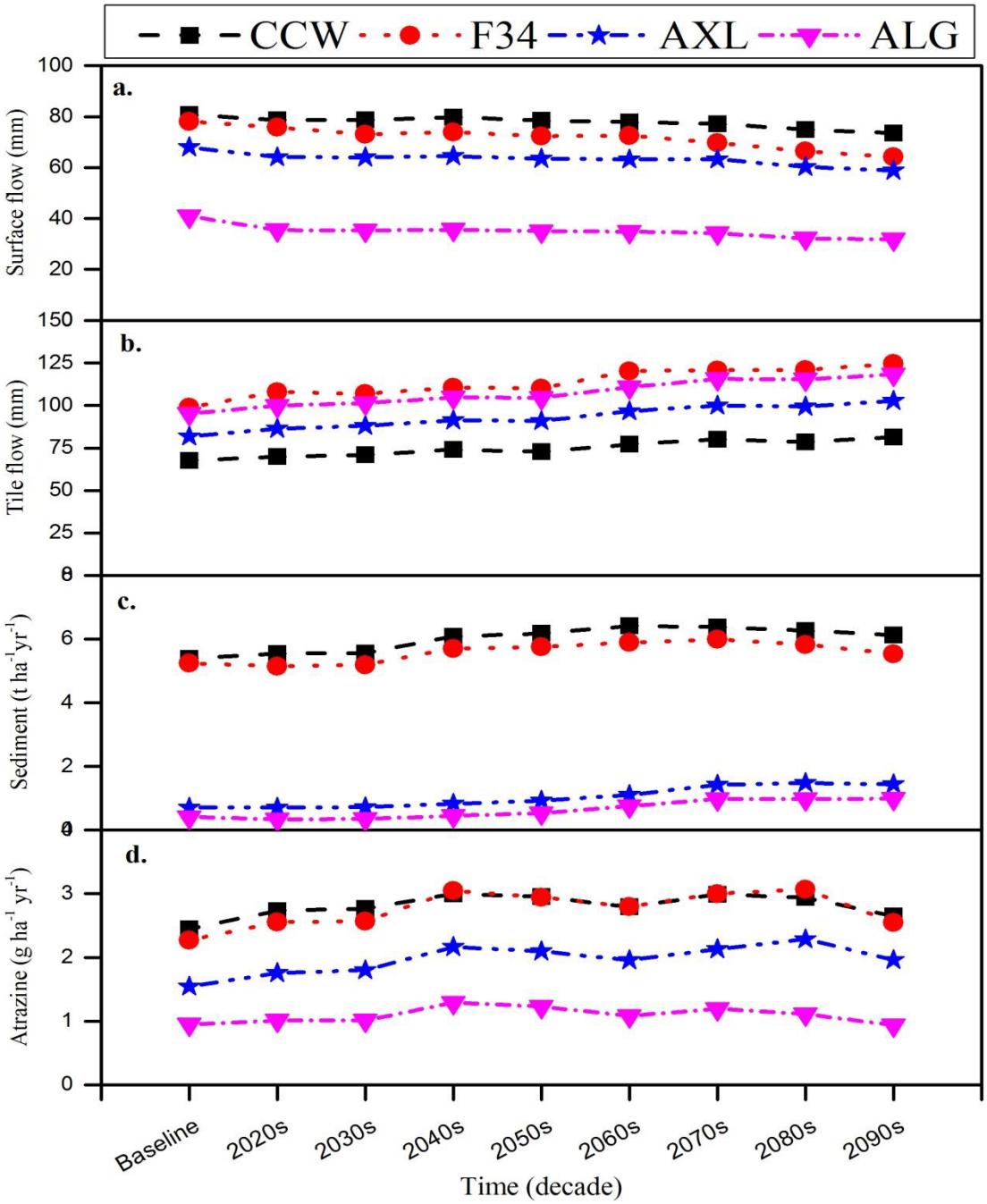


Figure 3.5. Average annual surface flow, tile flow, sediment, and atrazine losses under baseline and future climate conditions.

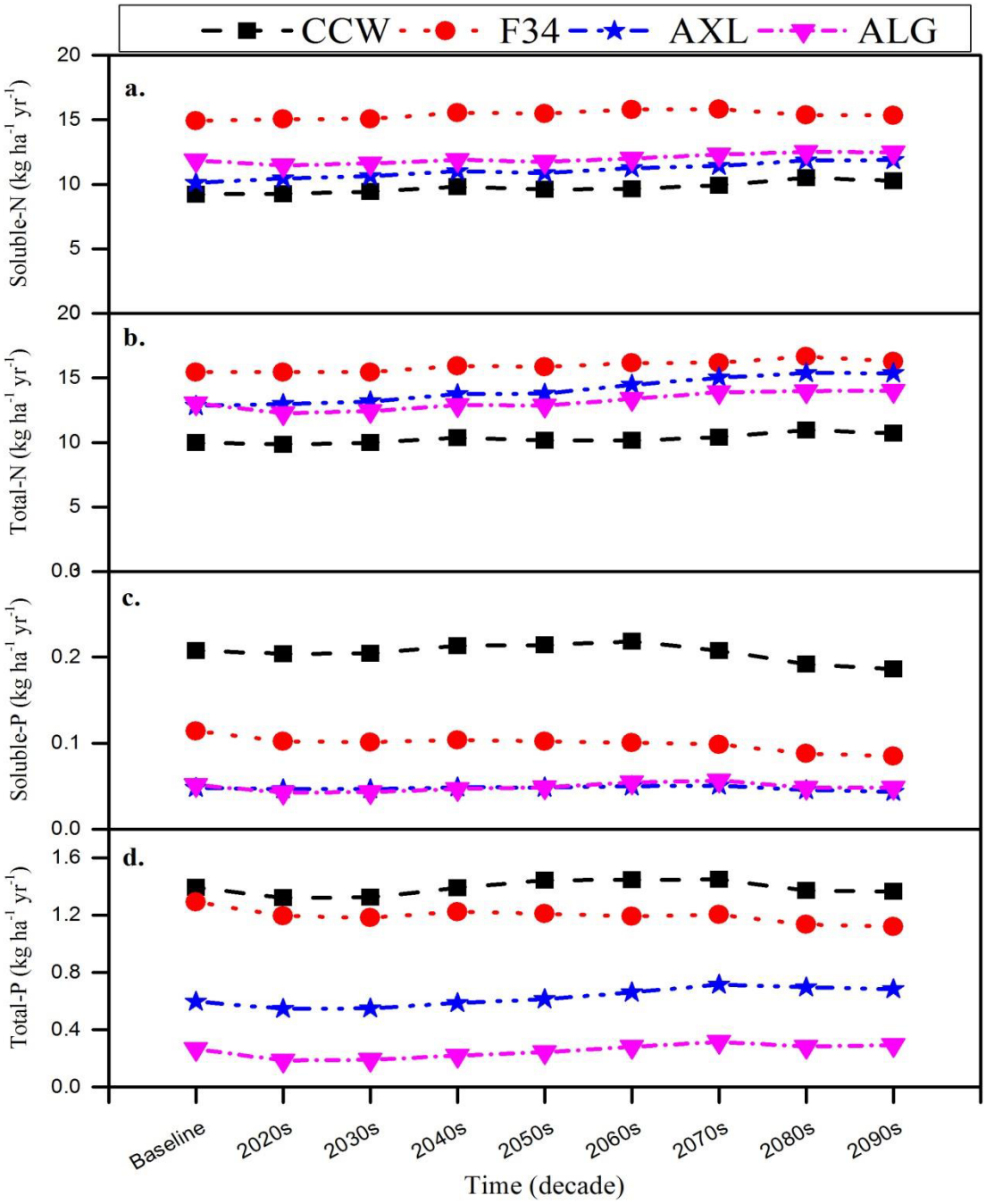


Figure 3.6. Average annual soluble N, total N, soluble P, and total P losses under baseline and future climate conditions.

### 3.5.2 Climate change impact on surface flow and tile flow

As shown in Table 3.4, all four watersheds had a gradual decrease in surface flow and a gradual increase in tile flow toward the end of the century despite a steady increase in rainfall volume (Figure 3.5a-b). In CCW, surface flow decreased from 80.7 mm/yr in the baseline period to 73.5 mm/yr by 2099 (approximately 9%). Tile flow increased gradually from 67.7 mm/yr to 81.3 mm/yr (approximately 20%). In F34 surface flow decreased from 78.1 mm/yr in the baseline period to 64.2 mm/yr by 2099 (18%). Tile flow in F34 increased gradually from 99.0 mm/yr to 124 mm/yr (25%). In AXL surface flow decreased from 68.0 mm/yr in the baseline period to 58.8 mm/yr by 2099 (13.5%), while tile flow increased gradually from 81.8 mm/yr to 102.7 mm/yr (25.5%). In ALG surface flow decreased from 41.0 mm/yr in baseline period to 31.8 mm/yr by 2099 (22%), while tile flow increased gradually from 95.2 mm/yr to 118.4 mm/yr (24%).

Changes in surface flow between the baseline period and end of the century were significant at $\alpha = 0.05$ with $p = 0.0372$, 0.0000, 0.0046 and 0.0048 for CCW, F34, AXL, and ALG watersheds, respectively. Similarly, changes in tile flow were also significant at $\alpha = 0.05$ with $p = 0.0044$, 0.0030, 0.0017 and 0.0049 for the CCW, F34, AXL, and ALG watersheds, respectively.

The shift observed between surface flow and tile flow was most likely due to a combination of rising water table (from increased precipitation) and increasing temperatures during the winter months that resulted in less storage of water until the spring melt. The U.S. Global Change Research Program (USGCRP, 2009) predicts that

precipitation in the Midwest is likely to fall more frequently in heavy downpours. This seem counter-intuitive to the MarkSim generated precipitation that showed a noticeable shift in precipitation to smaller events, which would subsequently result in more infiltration and higher water tables. Higher water table increases the amount of water available for tile flow (Du et al., 2005). The dynamic water table routine used in SWAT to estimate tile drainage, forces more water to enter the subsurface tiles whenever the water table rises to a certain height (above subsurface tiles) (Du et al., 2005; Du et al., 2006).

Soil temperature affects the movement of water through the soil profile (Running and Reid, 1980; Yang et al., 1996). In SWAT, soil layer temperature is a function of average annual air temperature and soil surface temperature (Neitsch, 2002), and if soil temperature is $0^{o}C$ or below, no redistribution of water is allowed. As winter temperature increases towards the end of the century, greater soil-water movement will occur, which will increase the rate at which downward flow, percolation or tile flow occurs. As depicted in Figure 3.7, significant increases in tile flow volume occurred during the winter season (December/January/February) between the baseline period and the end of the century. During winter, tile flow increased approximately 129% in CCW, 160% in F34, 179% in AXL and 183% in ALG, while surface flow decreased by approximately 15%, 21%, 29% and 30% in CCW, F34, AXL, and ALG, respectively, between the baseline period and the end of this century.

Additionally, because the CN method was used to estimate the amount of water available for surface flow in SWAT, the influence of initial abstraction ($I_a$) on surface flow becomes greater (as demonstrated in Equation. 3.1) if the factors driving $I_a$ increased.

$$Q_{surf} = \frac{(R_{day} - I_a)^2}{(R_{day} - I_a + S)} \quad (3.1)$$

where $Q_{surf}$ is the amount of water available for overland flow (mm), $R_{day}$ is the amount of rainfall for a given day (mm) and $S$ is the surface detention (mm) parameter. $I_a$ is the amount of water before surface flow can occur such as evaporation, infiltration and interception. Evapotranspiration (ET) is a major component of the water balance accounting for approximately 55% of precipitation; therefore, increasing ET will likely reduce the amount of water available for runoff to occur (Mishra et al., 2005; Mishra et al., 2004). Figure 3.8 and Figure 3.9 show the change in average monthly ET in all four watersheds. Except for the months of August, September, and October, ET increased significantly with greater percentage changes occurring in the winter months. Increasing ET resulted from increasing precipitation and temperatures. However, despite increasing temperatures, decreasing precipitation in the summer months (June through August) resulted in decreased ET for the months of August through October.

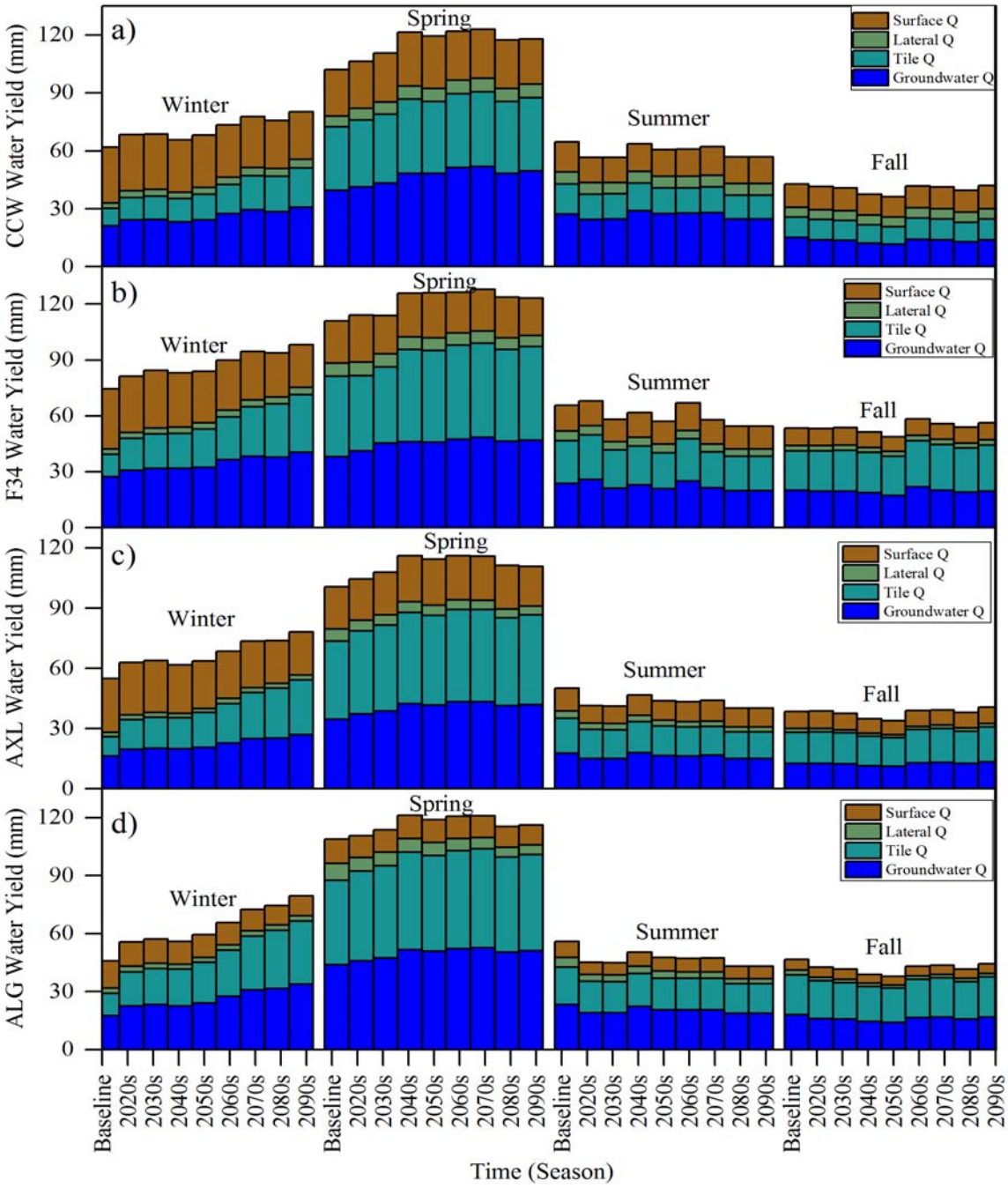


Figure 3.7. Major components of the water balance, displaying seasonal variation in surface flow, lateral flow, tile flow and groundwater flow at a) CCW, b) F34, c) AXL and d) ALG watersheds. Seasons include winter (Dec/Jan/Feb), spring (Mar/Apr/May), summer (Jun/Jul/Aug) and fall (Sep/Oct/Nov).

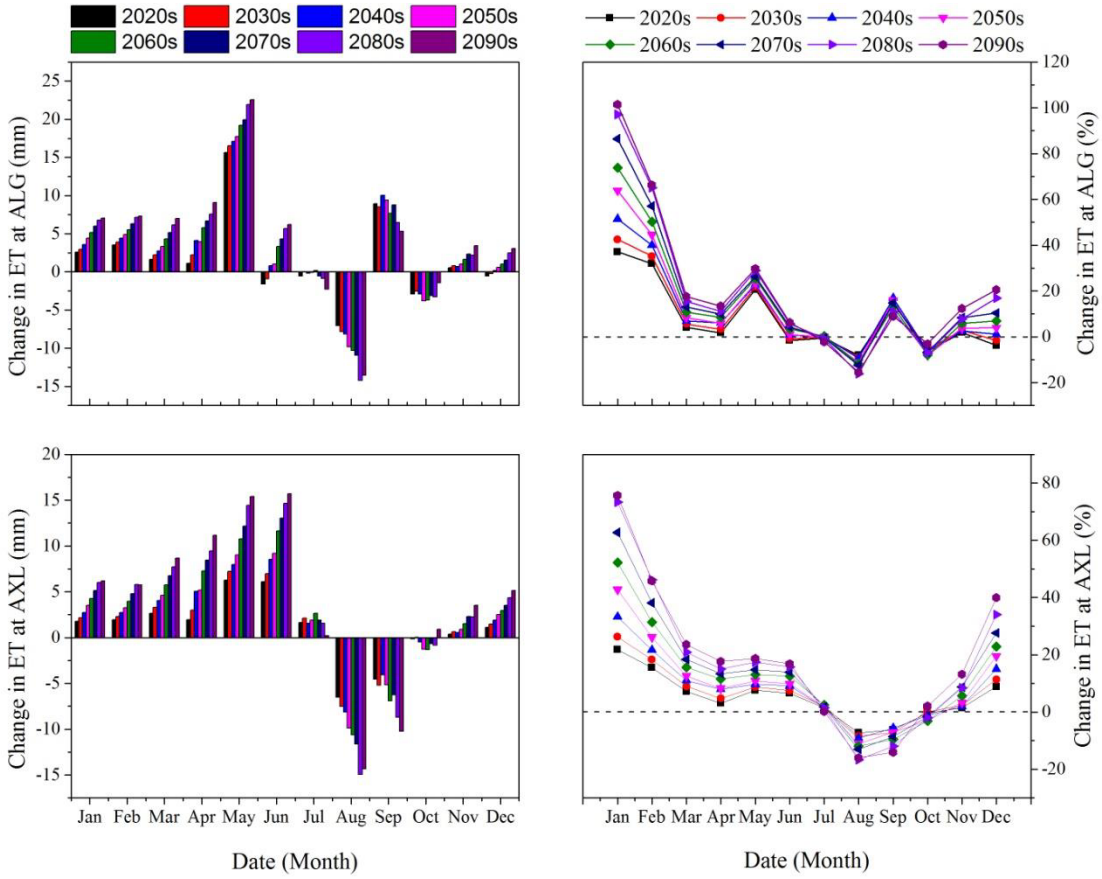


Figure 3.8. Percent change in monthly ET with respect to the baseline climate for ALG and AXL watersheds.

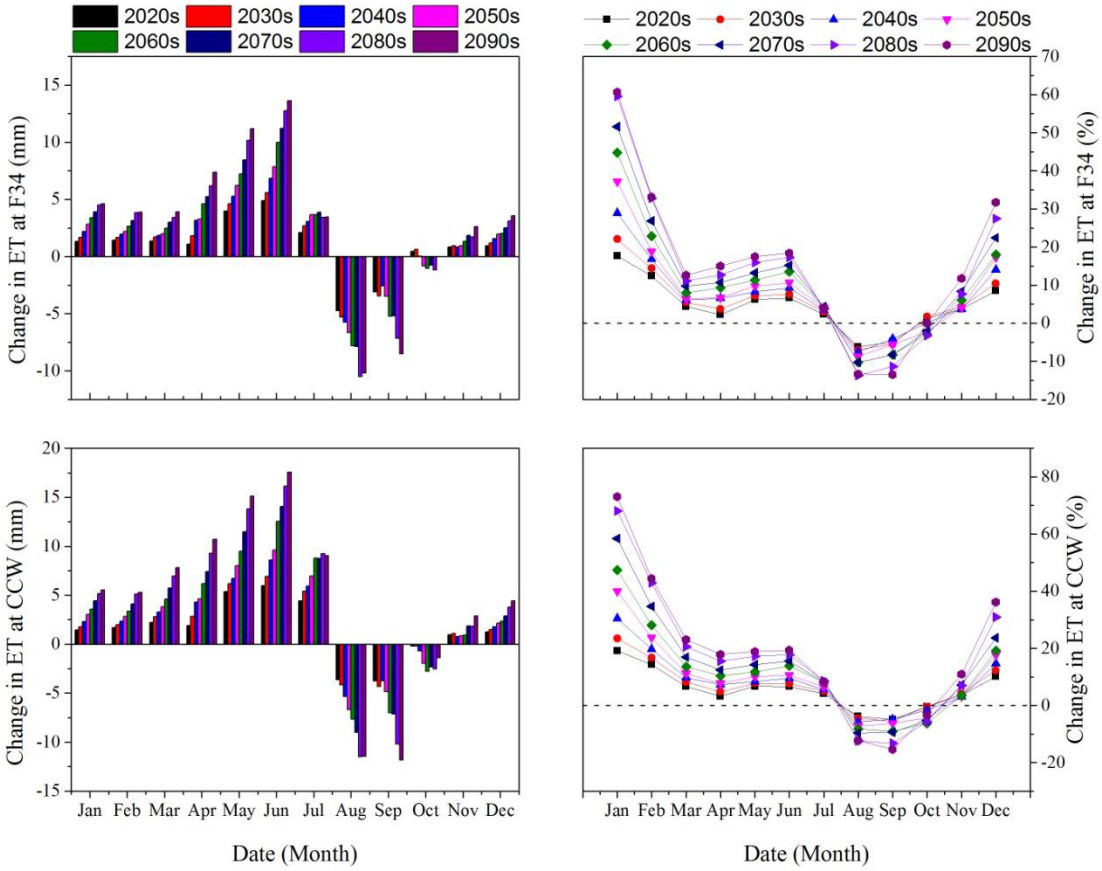


Figure 3.9. Percent change in monthly ET with respect to the baseline climate for F34 and CCW watersheds.

### 3.5.3 Climate change impact on sediment loss

At the larger CCW and F34 watersheds, there were slight increases in sediment loss from the baseline period to the end of the century (Figure 3.5c). There was little change in sediment loss for the smaller AXL and ALG watersheds until after the 2050s when the number of days with rainfall above 20 mm increased from 14 to 16 and the number of days with rainfall greater than 30 mm increased from seven to eight.

The results presented in Table 3.5 indicate that in CCW, sediment loss increased significantly by approximately 0.75 t $ha^{-1}yr^{-1}$ (13.5%) between the baseline period and the end of the century, with $p = 0$ at $\alpha = 0.05$. There was no significant increase in sediment loss in F34, with $p = 0.373$ at $\alpha = 0.05$. In AXL sediment loss increased from 0.71 t $ha^{-1}yr^{-1}$ in the baseline period to 0.92 t $ha^{-1}yr^{-1}$ (29.5%) in the 2050s and then to 1.44 t $ha^{-1}yr^{-1}$ by 2099 (103.6%). In ALG, sediment loss increased from 0.41 t $ha^{-1}yr^{-1}$ in the baseline period to 0.50 t $ha^{-1}yr^{-1}$ (31.7%) in the 2050s, then to 0.98 t $ha^{-1}yr^{-1}$ by 2099 (139%).

Though the statistical analysis implies significant percentage increase in sediment loss at $\alpha = 0.05$ with p = zero, the large percentage increase in AXL and ALG should not be too alarming considering the magnitude of sediment loss is small. There has been extensive BMPs implementation in the ALG, AXL and large sections of F34 primarily to reduce soil loss. Approximately 77% of soybeans and 20% of corn areas have been cultivated under a no-tillage system, which was represented in SWAT during the model set-up and calibration process.

The proportion of sediment loss in CCW and F34 was much greater than that of AXL and ALG mainly due to the effects of the calibration process. There was no sediment data available for calibration of sediment in any of the four watersheds; however, each watershed was calibrated separately for nitrogen and phosphorus, which included optimization of the sediment transport coefficient (SPCON) and an exponent (SPEXP) used in the sediment transport equation (Table 3.5). These parameters are necessary to estimate the proportion of nitrogen and phosphorus being transported with sediment. A

large SPEXP value means a greater maximum concentration of sediment that can be transported by water, and a large SPCON value suggests a larger sediment transport capacity. While there were little differences in SPEXP values for the four watersheds, the SPCON value for CCW and F34 was approximate twice that of AXL and ALG, which resulted in the sediment transport capacity of CCW and F34 being much greater than that of AXL and ALG. This was not surprising considering sediment delivery is very sensitive to changes in SPCON and SPEXP parameters especially when using the simplified Bagnold equation (Almendinger and Ulrich, 2010).

Table 3.5. The final SPCON and SPEXP values for CCW, F34, AXL and ALG watersheds after calibration.

| | CCW | F34 | AXL | ALG |
|---|---|---|---|---|
| SPCON | 0.0067 | 0.0057 | 0.0035 | .0030 |
| SPEXP | 1.37 | 1.44 | 1.28 | 1.22 |

Additionally, the subsurface tile drains with open-surface tile inlets provide a direct pathway for sediment transfer to drainage ditches. Landscape in the study area was formed on young glacial till plains and contains many closed depressions (potholes) that are often drained using surface tile inlets (tile risers). These closed depressions were implemented in SWAT setup for all four watersheds (see Figure 3.10 for an example of closed depressions identified in ALG). SWAT assumes sediment entering a pothole is instantaneously distributed throughout the pothole water volume (Neitsch, 2002). Therefore, if a tile inlet is installed in that pothole sediment is allowed to enter the subsurface drainage system directly and are like to be deposited into the nearest stream

segment, which suggests that the more potholes, and consequently the more tile inlets there are, the greater the potential for sediment to be transported directly to streams.

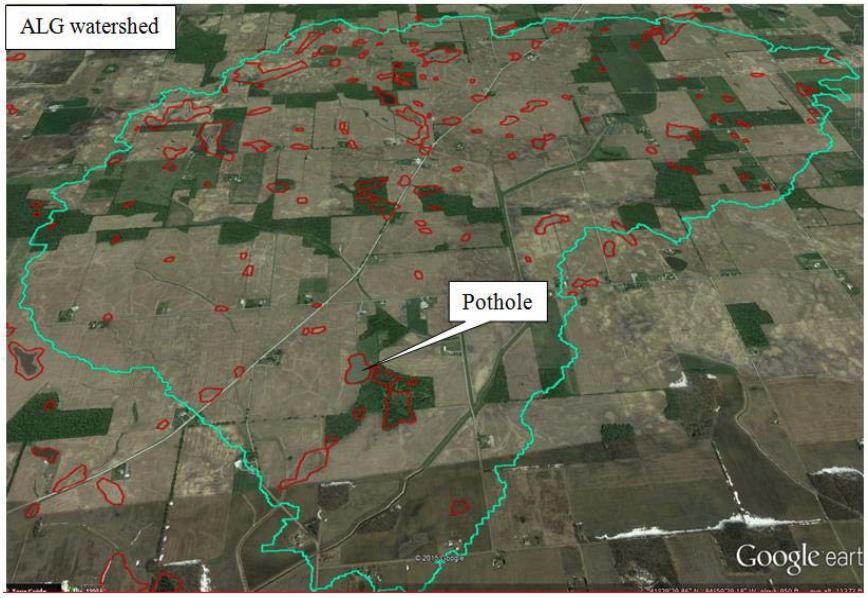


Figure 3.10. Google Earth imagery of ALG with the closed depressions identified.

### 3.5.4 Climate change impact on atrazine loss

As summarized in Table 3.4 and Figure 3.5d, there were no significant change in average annual atrazine loss at $\alpha = 0.05$ with $p = 0.5746, 0.5595, 0.5901, 0.1432$ for CCW, F34, AXL and ALG, respectively. These results indicate that projected future climate change to the end of this century will have little impact on average annual atrazine loss. A primary pathway for atrazine to streams is through surface runoff, and as demonstrated earlier, surface runoff had a decreasing trend toward the end of the century. The inclusion of surface inlets to drain depressional areas, as well as increased lateral flow, however, may accelerate atrazine loss. Atrazine loss through lateral flow had the largest percentage

increase among the contributing sources, with 21% increase in CCW, 8% in F34, 23% in AXL, and 4% in ALG, respectively. Further assessments are required to understand how atrazine half-life used in the pesticide degradation equation in SWAT is affected over an extended period with increasing temperatures and changes in rainfall seasonality.

### 3.5.5 Climate change impact on soluble N and total N losses

As shown in Figures 3.6a-b, all four watersheds showed signs of increasing soluble N loss and total N loss toward the end of the century, with most of the nitrogen loss moving with tile flow. In the results summarized in Table 3.4, soluble N loss in CCW went from 9.2 kg $ha^{-1}yr^{-1}$ in the baseline period to 10.3 kg $ha^{-1}yr^{-1}$ by 2099 (11.3%). Total N loss went from 10.0 kg $ha^{-1}yr^{-1}$ to 10.7 kg $ha^{-1}yr^{-1}$ (7.3%).

In F34, soluble N loss went from 14.9 kg $ha^{-1}yr^{-1}$ in the baseline period to 15.4 kg $ha^{-1}yr^{-1}$ by 2099 (2.8%). Total N loss in F34 went from 15.5 kg $ha^{-1}yr^{-1}$ to 16.3 kg $ha^{-1}yr^{-1}$ (5.5%). In AXL, soluble N loss went from 10.1 kg $ha^{-1}yr^{-1}$ in the baseline period to 11.5 kg $ha^{-1}yr^{-1}$ by 2099 (17.5%), while total N loss increased gradually from 12.8 kg $ha^{-1}yr^{-1}$ to 15.0 kg $ha^{-1}yr^{-1}$ (19.8%). In ALG, soluble N loss went from 11.9 kg $ha^{-1}yr^{-1}$ in the baseline period to 12.5 kg $ha^{-1}yr^{-1}$ by 2099 (5.4%), while total N loss went from 13.0 kg $ha^{-1}yr^{-1}$ to 14.0 kg $ha^{-1}yr^{-1}$ (7.5%).

In general, changes in soluble N loss between the baseline period and end of the century were not significant at $\alpha = 0.05$ with $p = 0.1694$, 0.3460, 0.4270 and 0.4050 for the CCW, F34, AXL, and ALG watersheds, respectively. Similarly, changes in total N were also not

significant at $\alpha = 0.05$, except for AXL ($p = 0.0081$), with p-values of 0.3453, 0.3727, and 0.2228 for CCW, F34 and ALG, respectively.

In agricultural watersheds, nitrate in drainage water is the primary source of nitrogen loss from the soil, especially under high flow conditions (Hoang et al., 2014). The results presented here indicate that the nitrogen processes in the soil and shallow aquifer were strongly influenced by the high amount of water infiltrating into the soil profile and shallow aquifer. The increasing tile flow volume from rising water table depth supports this.

### 3.5.6 Climate change impact on soluble P and total P losses

As shown in Figure 3.6c, all four watersheds experienced a slight decrease in soluble P loss toward the end of the century. For CCW and F34, soluble P loss decreased by approximately 10.3% and 25.5%, respectively. These reductions were found to be significant at $\alpha = 0.05$ with $p = 0.0308$ and 0.0007 for CCW and F34, respectively. Changes in soluble P loss at AXL and ALG were not significant, with $p = 0.1640$ and 0.4499, respectively.

As depicted in Figure 3.6d, total P loss showed a slight decreasing trend in CCW and F34 and a slight decreasing trend in AXL and ALG. However, the percentage change in average annual total P loss were not significant at $\alpha = 0.05$, with p-values of 0.9892, 0.0511, 0.1610, and 0.4261 for CCW, F34 AXL and ALG, respectively.

Despite the slight changes in total P between the baseline period and end of the century, a close look at Figures 3.5c and 3.6d shows that the trend in total P through to the end of the century closely matched that of sediment loss.  attached to soil particles (organic-P and mineral-P) are typically transported to the stream channel by surface runoff. Therefore, changes in sediment loss are likely to affect these forms of  (Neitsch, 2002). Higher temperatures also increase mineralization and release of phosphorus. In recent studies, the simulation of future climate change effects on phosphorus losses at the watershed scale produced similar results to those in this study. Jeppesen et al. (2009) predicted that by the end of this century, climate change would result in a 3.3 to 16.5% increase in total P loss to the lowland streams of Denmark. Bouraoui et al. (2004) predicted an average increase in total P loss of approximately 2% in the Vantaanjoki watershed (Finland) due to climate change.

## 3.6 Summary and Conclusions

This study examined the effect of climate change on surface flow, tile flow, sediment, atrazine, and nutrient losses in four agricultural watersheds of different sizes. Climate information (baseline and future projections) were obtained using the MarkSim weather file generator. Projections of future climate were based on an ensemble mean of 17 GCMs simulated under the RCP 6.0 scenario. With respect to the baseline climate, average annual maximum and minimum temperatures will increase by approximately 4°C by the end of this century. Average annual rainfall volume will increase by approximately 8.5% between the baseline period (1961-90) and the end of this century with most of the

precipitation occurring in smaller storm events. The climate change scenarios and their effects on surface flow, tile flow, sediment, atrazine, and nutrient losses were simulated for the CCW, F34, AXL and ALG watersheds located in Northeastern Indiana using SWAT.

The results indicate that higher rainfall volume does not always lead to increased surface flow. In fact, despite increasing rainfall volume, surface flow decreased while tile flow increased between the baseline periods (1961-90) to the end of the century for all four watersheds. These changes were found to be significant at the 95% confidence level. There were significant increases in sediment loss for all four watersheds. However, changes in atrazine, soluble N, total N and total P losses were not significant at the 95% confidence level. Changes in average annual soluble P loss were significant at the larger CCW and F34 watersheds, but insignificant at AXL and ALG.

As it relates to watershed size, there was no clear evidence to suggest changes in watershed size will have an impact on the simulation of climate change effects. The changes observed were mainly due to watershed characteristics and SWAT model configuration. SWAT was configured, calibrated and validated independently for all four watersheds, and therefore, as expected, the magnitude of changes differed despite similar trends in climate change effects.

The representation of potholes in SWAT could also be improved. Currently, pothole parameters have to be determined by the user and added to an HRU for SWAT to recognize that HRU as being a pothole, which makes simulations susceptible to user

input error. A more automated method is need, preferably during the watershed delineation process.

Using the MarkSim weather file generator to obtain climate files seems to produce outputs comparable to observed climate. However, there may be concerns regarding the MarkSim downscaling method that tends to project future precipitation dissimilar to other climate change studies in the Midwest. MarkSim tends to smooth outputs obtained from the various GCMs and thus result in more precipitation being in small events. To explore whether the MarkSim downscaling method resulted in a larger proportion of rainfall occurring in small events for future climate compared to baseline climate, future studies could compare projected future climate obtained by MarkSim with climate projections obtained using different downscaling techniques. Additionally, individual climate model results should be compared with the ensemble mean of multiple climate model results.

# CHAPTER 4. QUANTIFYING THE EFFECT OF CONSERVATION PRACTICE IMPLEMENTATION ON PREDICTED RUNOFF AND CHEMICAL LOSSES

## 4.1 Synopsis

A major water quality concern in agricultural watersheds stems from surface runoff and tile flow that transports sediment, pesticides, and nutrients to surface water bodies. Conservation practices are often implemented to mitigate water quality concerns. These conservation practices are available through conservation programs (such as cost sharing, tax breaks, and storm water utility charges) that provide incentives for the implementation of Best Management Practices (BMPs) in areas of the watershed contributing to pollutant loading. As part of the Conservation Effects Assessment Project (CEAP), evaluation of these conservation practices is required to provide insight on how their implementation is benefiting the environment.

In this study, the Soil and Water Assessment Tool (SWAT) with downscaled weather data generated using the MarkSim weather file generator was used to evaluate the impact of long-term conservation practice implementation on runoff, sediment, atrazine, soluble N, total N, soluble P, and total P losses in the Matson Ditch (AXL) Watershed located in Northeastern Indiana. The results indicate that individual conservation practices were effective in reducing a particular pollutant load, but combined practices were more

effective in reducing multiple pollutant loadings simultaneously. Of the individual BMPs assessed, no-till was the most effective in reducing multiple pollutant loads (reduced surface runoff by an average of 25%, sediment by 46%, atrazine by 46%, total N by 9%, soluble P by 16%, and total P by 29%). When individual BMPs were combined, pollutant load reductions were increased significantly (at $\alpha = 0.05$) for all pollutants, both under baseline and future climate scenarios. The percent change for each decade of future climate ranged from 15% to 25% for surface runoff, 32% to 68% for sediment loss, 37% to 60% for atrazine loss, 5% to 13% for soluble N loss, 12% to 35% for total N loss, 9% to 41% for soluble P loss, and 33% to 60% for total P loss.

## 4.2 Introduction

Nonpoint sources of pollution such as agricultural runoff and atmospheric deposition are often considered when developing water quality protection plans. Pollutants from agricultural runoff, such as sediment, pesticides and nutrients, may detrimentally affect off-site water bodies. The St. Joseph River Watershed Initiative (SJRWI) assessed the water quality in the St. Joseph River, Indiana, USA, and identified pesticide and nutrient runoff from agricultural lands as primary stressors of surface and subsurface water quality (SJRWI, 2005).

The St. Joseph River transports agricultural runoff from northeastern Indiana to the Maumee River that eventually drains into Lake Erie (SJRWI, 2005). The presence of pesticides and nutrients in open waters above the EPA's allowable limits threatens aquatic

life by killing small species of animals, disrupting plant growth, and eventually causing aquatic life use impairments (USEPA, 2002).

An overabundance of algae, which was primarily due to excess loading of nutrients such as phosphorus into Lake Erie, resulted in anoxic conditions that subsequently led to large fish kills during the 1970s (Baker and Richards, 2002; Rawls et al., 1980; Rawls and Richardson, 1983). Despite large-scale efforts to mitigate nutrient loadings to Lake Erie, the ongoing effects of excessive nutrient loading are still causes for concern. Seasonal depleted oxygen conditions continue to intensify in the central basin, blue-green algal blooms are occurring regularly in the western basin, as well as fouling of near-shore areas of the eastern basin (Lake Erie LAMPs, 2011). As recent as August 2014, high levels of microcystin above the standard for consumption, most likely from algae in Lake Erie, resulted in a ban on regional water supply to over 500, 000 residents of the City of Toledo, Ohio (Fitzsimmons, 2014).

Agricultural conservation practices, also referred to as Best Management Practices (BMP), are often implemented in watersheds to reduce nonpoint source pollution caused by agricultural runoff and improve surface water quality. Monitoring the effectiveness of alternative BMPs is time consuming, expensive and uncertain. The use of computer models such as the Soil and Watershed Assessment Tool (SWAT) provide a timely and cost-effective means of evaluating the impact of alternative conservation practices on reducing pollutant loading and improving water quality.

Several studies conducted using computer models show that agricultural BMPs can reduce pollutant loading and improve water quality ( Bracmort et al., 2004; Lee et al., 2010; Dechmi and Skhiri, 2013). Despite protecting millions of hectares, the environmental benefits of BMPs have not been quantified to the extent that they can be reported at the national scale (Mausbach and Dedrick, 2004).

In 2003, USDA's Natural Resources Conservation Service (NRCS) and the ARS initiated a nationwide Conservation Effects Assessment Project (CEAP) to quantify the environmental benefits of BMPs and to provide a measure of accountability for how the money being spent is meeting the goals of the 2002 Farm Bill (Mausbach and Dedrick, 2004). According to the 2002 Farm Security and Rural Investment Act (Farm Bill Act, 2002), there has been an 80 percent increase in funding for conservation programs throughout the United States, above the level set under the 1996 Farm Bill (Mausbach and Dedrick, 2004). Subsequently, the Farm Bill Act of 2014 consolidated 23 overlapping conservation programs into 13, tightened eligibility rules for funding of these programs, and streamlined means tests to make farm programs more accountable.

CEAP has two main areas of focus: one is a national and regional assessment for which it provides modeled estimates of conservation benefits for annual reporting, and the other is an assessment component which establishes scientific understanding of the effects and environmental benefits of specific BMPs at the watershed scale (Mausbach and Dedrick, 2004). CEAP uses a mix of research, data collection, model development, and model application in estimating the effects and benefits of BMPs. The program also provides

research and assessment on how to best use BMPs in managing agricultural landscapes to protect and enhance environmental quality.

The impact of climate change on agricultural runoff and nutrient loading to surface water bodies has been assessed in numerous studies using different watershed models coupled with climate models (Gosain et al., 2006; Zhang et al., 2007; Raneesh and Santosh, 2011; Khoi and Suetsugi, 2012; Haddad et al., 2013; Kim et al., 2013; Park et al., 2013; Zahabiyoun et al., 2013). However, few studies have examined the combined effects of future climate change and BMP implementation on agricultural runoff, sediment and chemical losses.

Understanding the influence of climate change on BMP performance is important for water resources management, and the development of future best management scenarios to mitigate nonpoint source pollution. Woznicki and Nejadhashemi (2014) quantified the performance of seven individual BMPs under future climate change scenarios in the Tuttle Creek Lake watershed, located in eastern Kansas and Nebraska, and emphasized the fact that uncertainties associated with conservation practices performance are compounded by changes in future climate. However, since conservation programs often recommend the use of combined BMP implementation in mitigating water quality concerns, additional assessments are needed to ascertain the significance of climate change impact on both individual and combined BMP implementation. In a recent study, Chiang et al. (2012) evaluated 171 management practice combinations with future

climate conditions in a pasture-dominated watershed and emphasized the importance of different BMP combinations in reducing nonpoint pollution.

This study assesses the impact of long-term BMP implementation using the Soil Watershed Assessment Tool (SWAT) coupled with future climate data downscaled with the MarkSim weather file generator. SWAT is a physically based model used to simulate watershed scale hydrology, water quality and plant growth (Arnold et. al., 1998). It is computationally efficient, allows considerable spatial detail, requires readily available inputs, operates on a continuous time step, is capable of simulating land-management scenarios, and captures management effects at the watershed scale. SWAT has been used to simulate the effects of conservation practices in order to determine which set of practices are needed to achieve desired reductions in pollutant loads (Vache et al., 2002).

### 4.2.1 Conservation Practices Implemented to Reduce Sediment, Pesticide and Nutrient Runoff in Agricultural Watersheds

In an effort to protect the nation's waters and restore water quality standards for impaired water bodies, the United States Department of Agriculture (USDA) through the Farm Services Agency (FSA) provides significant financial incentives for the implementation of conservation practices in agricultural watersheds such as AXL. The NRCS's natural resources conservation programs helps stakeholders reduce soil erosion, enhance water supplies, improve water quality, increase wildlife habitat, and reduce damages caused by floods and other natural disasters (USDA NRCS, 2014).

The Source Water Protection Initiative Project (SWPI), which was a collaborative effort between America's Clean Water Foundation (ACWF), the Agricultural Research Service (ARS) and its National Soil Erosion Research Laboratory (NSERL) in West Lafayette, Indiana, focused on identifying BMPs for reducing the effects of agriculture on drinking water supplies. The SWPI project designed and implemented BMPs, and measured their ability to remove or reduce sediment, pesticides and nutrients from field runoff at the watershed scale. Implementation of environmentally safe and economically viable conservation practices at the watershed scale is critical not only to agricultural lands, but also to the consumers that use the water resources for drinking and recreation. The conservation practices discussed here include BMPs commonly implemented by the ARS SWPI project and CEAP in the AXL watershed (i.e. no-tillage, vegetative filter strips, grassed waterways, blind inlets and nutrient management).

#### 4.2.1.1 No-Tillage

No-Tillage (NRCS practice #329) is a form of conservation tillage practice where seeds are planted directly into the soil with no other tillage operations, thereby minimizing soil disturbance, and sediment and nutrient transport to surface waters. This practice further seeks to reduce sheet, rill and wind erosion, maintain or increase soil quality and organic matter content, reduce energy use in crop production, increase water use and precipitation storage efficiency and provide food and escape cover for wildlife (USDA NRCS, 2014).

Over the last two decades, significant emphasis has been placed on trying to encourage farmers to utilize no-tillage when planting crops (Smith et al., 2008). In Northeastern

Indiana, the primary conservation practice on agricultural lands is to use the no-tillage approach for planting soybeans following corn. In 2012, 34% of corn and 77% of soybeans were planted using no-tillage in DeKalb County, Indiana (DeKalb SWCD, 2014), where the AXL watershed is located. No-till was selected for this study because it is a common practice in the study area and easily implementable in SWAT. Additionally, no-till conservation agriculture avoids tillage; therefore, it is less time-consuming and can be more cost-effective than conventional farming methods.

#### 4.2.1.2 Vegetative Barriers

Vegetative Barrier (NRCS practice #601), also known as vegetative filter strips (VFS), are regions of dense vegetation established along the general contour of slopes or across concentrated flow areas (USDA NRCS, 2014). Vegetative filter strips (VFS) act as natural barriers during fertilizer and pesticide applications (Smith et al., 2008) and are intended to remove nonpoint source pollutants such as sediment and associated contaminants from overland flow (USDA NRCS, 2014). Commonly located along open waterways, VFS seek to intercept runoff before reaching ditches and streams. VFS have been implemented along more than 60% of the agricultural drainage ditches in Northeastern Indiana (Smith et al., 2008).

#### 4.2.1.3 Grassed Waterways

Grassed waterways (NRCS practice #412) are vegetated channels created to carry concentrated surface runoff at low (non-erosive) velocities to a stable outlet with the

purpose of preventing erosion and associated nonpoint source pollution (USDA NRCS, 2014). Additionally, grassed waterways reduce gully erosion and protect water quality. In an assessment of BMPs used to reduce nonpoint source pollution, grassed waterways were found to have minimal impact on TP and TN loads, but were able to significantly reduce sediment loads (Zhang et al., 2013). However, combining grassed waterways with other conservation practices (e.g. conservation tillage, vegetative filter strips, and a simple nutrient reduction strategy) could result in sediment reduction in the range of six to 65 percent, nitrate reduction in the range of six to 20 percent and total reduction in the range of 28 to 59 percent (Secchi et al., 2007).

#### 4.2.1.4 Blind Inlets

Blind inlets are a novel approach that is being studied as a possible replacement for the surface tile inlets in watersheds where subsurface tiles are used to drain closed depressions. Closed depressions are usually found in landscapes formed from glaciation. These closed depressions, also known as prairie potholes, form natural detention ponds for surface runoff, and restrict cultivation in agricultural lands. As a result, closed depressions pose significant challenges in large parts of the Midwestern United States where most of the productive soils are formed on glacial till landscapes. Surface tile inlets are often used to alleviate the problem caused by closed depressions/potholes in the Midwestern United States. These surface tile inlets are pipes (generally with 2–6 cm inlet holes) that connect to the subsurface tile drainage network, and are used to convey surface runoff water that collects in the lowest point of the closed depressions directly to

the subsurface tile drainage network, which drains into the off-site stream network. Tile inlets in closed depressions are potential contributors to water quality problems in the AXL watershed because there is little filtration or processing of the surface runoff water before it reaches the stream network (Smith and Livingston, 2013). Pollutants (such as sediment and agricultural chemicals) suspended in the ponded-water enter the subsurface tiles and are transported directly to the stream network.

Discharge from surface tile inlets was identified as a major contributor to water quality degradation, transporting sediment and nutrients (nitrogen and phosphorus) from the field directly to rivers or streams (Ginting et al., 2000; Smith et al., 2008; Tomer et al., 2010). Therefore, in order to provide an alternative that will improve the quality of water drained from closed depressions, ARS-NSERL developed blind inlets, which are implemented by removing surface tile inlets and constructing a filter bed at the lowest point of a closed depression (Smith and Livingston, 2013). The filter bed consists of coarse limestone gravel, geotextile fabric and coarse-textured soil material to facilitate infiltration. Smith and Livingston (2013) found that blind inlets reduced sediment loss from potholes by 48% to 85%; soluble P loss by 34% to 94%; total P loss by 26% to 88%; soluble N loss by 1% to 78%; and total N loss by approximately 20% to 81%, when compared to the surface tile inlets. Additional field-scale studies by Feyereisen et al. (2015), in which paired comparisons between surface tile inlets and blind inlets were performed on a storm event basis in Indiana and Minnesota, found that blind inlets

reduced total suspended sediment loads by approximately 64 percent and soluble and total by approximately 55 percent.

#### 4.2.1.5 Nutrient Management

Nutrient Management (NRCS practice #590) is the practice of managing plant nutrient application rates, source, application method and timing wisely for optimum economic benefit, while minimizing impact on the environment (USDA NRCS, 2014). Plants nutrients (especially nitrogen, phosphorus, and potassium) are used to achieve optimum crop yields, and when applied correctly, are essential for crop production. Improper application of nutrients may cause water quality problems both locally and downstream.

Soluble phosphorus in particular has been identified as a major problem for Lake Erie over the years, with massive algal blooms and deteriorating water quality (Lake Erie LaMP, 2011). The drainage area to Lake Erie (containing the AXL watershed) is largely agricultural, with a significant amount of phosphorus loading attributed to runoff from agricultural land, particularly from row cropping operations (Baker and Richards, 2002). Therefore, a nutrient management approach should be adopted to limit the amount of available for transport. The Natural Resources Conservation Services (USDA NRCS, 2014) established nutrient management standards that should be used on all lands where plant nutrients and soil amendments are applied. Before each crop is planted and fertilizer applied, the soil should be tested to determine its nutrient content, and applications made based on recommendations from experts such as Tri-State Fertilizer Recommendations (Vitosh et al., 1995) and the Agronomic Handbook (Jones Jr., 2002) that have studied

nutrient requirements and uptake by various crops, and thereby eliminating excessive application.

## 4.3 Objective

This study seeks to quantify the impact of long-term implementation of individual and combined BMPs on runoff and chemical losses from an agricultural watershed dominated by row crop cultivation, using the Soil and Watershed Assessment Tool (SWAT) coupled with future climate data downscaled with the MarkSim weather file generator. Results of this study will provide insight into the long-term effectiveness of agricultural conservation practices and their response to climate change.

## 4.4 Methodology

### 4.4.1 Study Area Description

The AXL watershed located in DeKalb County, Northeastern Indiana (85°1'39.102"W to 84°54'5.48"W and 41°24'32.205"N to 41°30'21.884"N) is a small 42 $km^2$ catchment (HUC_12 = 041000030603) in the St. Joseph River basin (Figure 4.1). AXL is predominantly an agricultural watershed having approximately 71.3% row crops (mainly corn and soybean), 12.8% pasture/hay, 10.1% forest, and 5.8% urban (based on NASS 2010-2013 data).

The majority of soils in the watershed are comprised of Blount silt loam (very deep, somewhat poorly drained soils), Pewamo silty clay (very deep, very poorly drained soils), Glynwood loam (very deep, moderately well drained soils), Rawson sandy loam (very

deep, moderately well drained soils), Rensselaer loam (very deep, poorly drained or very poorly drained soils), and Sebewa sandy loam (very deep, poorly drained or very poorly drained soils) (USDA, 2014). Many of these soils are drained into managed drainage ditches using subsurface tile drainage systems, which results in alteration of the watershed hydrology and the transport of pesticide and nutrients across the landscape (Pappas and Smith, 2007; Smith et al., 2008).

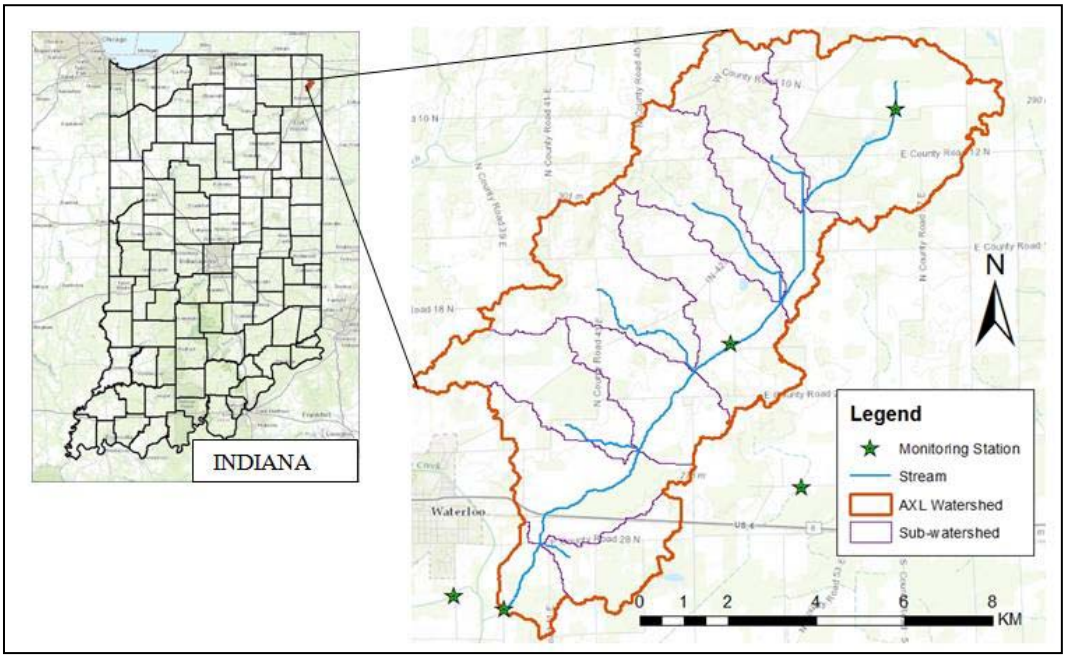


Figure 4.1. Location map of the AXL watershed within northeastern Indiana.

### 4.4.2 Watershed Monitoring and Data Availability

AXL is one of the watersheds benchmarked by the USDA Agricultural Research Service (USDA-ARS) as part of its Conservation Effects Assessment Project (CEAP). CEAP conducts research, data collection, and model application in order to quantify the effects

of conservation practices on water quality and other environmental parameters. The USDA-ARS has monitored climate, streamflow and water quality at multiple locations through the AXL watershed since 2002 (Smith et al., 2008). However, complete datasets are only available from April 2004 through November 2013 via the USDA-ARS National Soil Erosion Research Laboratory (NSERL) CEAP website. Flow velocity sensors were replaced in 2006 (Smith et al., 2008) and therefore, only data from 2006 forward were used in model calibration and validation. A description of the data obtained for AXL is presented in Table 4.1. Climate data such as daily precipitation, maximum and minimum air temperatures, solar radiation and wind speed were obtained for the CEAP weather stations located near the AXL outlet and for two upstream locations (ALG and AME indicated in Figure 4.1). These were used to create SWAT weather input files during model warm-up/calibration/validation.

Continuous water quality measurements at the AXL outlet are available each year from mid-March to mid-November with grab samples collected during the winter months. For this study, streamflow and concentrations of atrazine and nutrients measured at the AXL outlet were obtained from the ARS-NSERL for the period April 2004 to November 2013. Nutrient data obtained included Kjeldahl nitrogen, ammonium ($NH_4$-N), $NO_3$+$NO_2$, total phosphorus, and orthophosphate concentrations. Using the streamflow data, all concentration values for water quality were converted to average daily loads by applying simple arithmetic. Average daily loads were further amalgamated into average monthly loads for calibration/validation of SWAT.

Table 4.1. Input data used in SWAT setup and simulations.

| Data Type | Date | Source | Description |
|---|---|---|---|
| DEM | 2011 | USGS: viewer.nationalmap.gov /viewer/ | 10-m Resolution, Digital Elevation Model |
| Soils | 2011 | USDA-NRCS: soildatamart.nrcs.usda.gov/ | Soil Survey Geographic Database (SSURGO) |
| Land use | 2010-2013 | USDA-NASS: nassgeodata.gmu.edu/CropScape/ | National Agricultural Statistics Service data layer |
| Hydrographic | 2011 | USGS: nhd.usgs.gov/data.html | National Hydrograph Dataset (NHD) |
| Weather | 2004- 2013 | ARS CEAP Water Quality Assessment Program | Daily precipitation, maximum and minimum daily temperature, solar radiation, wind speed, relative humidity at AXL, ALG & AME |
| Crop Management | 2009- 2012 | ARS CEAP watershed survey, DeKalb County SWCDs | Tillage operations, fertilizer and herbicide applications, crop rotation, time of planting and time of harvesting |
| Streamflow | 2004- 2013 | ARS CEAP | Daily flow measured at AXL outlet |
| Water Quality | 2004- 2013 | ARS CEAP | Daily pesticide and nutrient concentration (TP, PO4, TN, NO2+NO3) at the AXL outlet |

### 4.4.3 SWAT Model Set-up

The ArcSWAT version 2012.10_1.15 interface was used to expedite SWAT model input and output display. Data used in SWAT model set-up/calibration/validation are presented in Table 4.1. To obtain suitable flowpaths, the stream delineation from the National Hydrograph Dataset (NHD) was used to burn in the location of the streams in a 10-m resolution Digital Elevation Model (DEM) obtained from USGS National Elevation Dataset (NED, USDA, 2011b). Using a minimum stream threshold value of 200 ha (5% of watershed area), 11 sub-basins were delineated in the AXL watershed (42 $km^2$). The USDA-ARS NSERL water quality/streamflow gauge station (latitude 41.413 and longitude -85.005) was used to specify the location of the AXL outlet (Figure 4.1).

In SWAT, hydrologic response units (HRUs) are determined by the unique combination of land use and soils within each sub-basin, whereby, the model establishes management practices. The Soil Survey Geographic Database (SSURGO, USDA, 2014) spatial data at a map scale of 1:12,000 and the USDA National Agricultural Statistics Service (NASS, USDA, 2011) Indiana Cropland Layer were used to determine HRUs with the following thresholds: 0% land, 0% soil, and 0% slope. Selecting threshold values of zero allows SWAT to model all possible unique combination of land cover/soil types; totaling 806 HRUs (average size of 5.37 ha).

Management input files were set-up to simulate corn/soybeans and soybeans/corn rotations on all lands classified as corn and soybeans respectively in the land use layer file (Table 4.2). When land use was classified as wheat, a wheat/corn/soybean rotation was used (Tables 4.2 and 4.3). Management inputs include yearly planting and harvesting dates, tillage operations, and pesticide and nutrient application.

Table 4.2. Management operations for land in corn/soybeans rotation.

| Crop | Date | Management Operation | Rate |
|---|---|---|---|
| Corn | 22-Apr | Nitrogen application (as Anhydrous Ammonia) | 176.0 kg/ha |
| | 22-Apr | ($P_2O_5$) Application (as DAP/MAP) | 54.0 kg/ha |
| | 22-Apr | Pesticide Application (as Atrazine) | 2.2 kg/ha |
| | 6-May | Tillage, Offset disk on 70% of corn area (60% mixing) | |
| | 6-May | No-Tillage on 30% of corn area | |
| | 6-May | Planting | |
| | 10-Oct | Harvest | |
| Soybeans | 10-May | ($P_2O_5$) application (as DAP/MAP) | 40.0 kg/ha |
| | 24-May | No-Tillage on 77% of soybeans area | |
| | 24-May | Tillage, disk chisel on 23% of soybeans area | |
| | 24-May | Planting | |
| | 7-Oct | Harvest | |

Table 4.3. Management operations for land in winter wheat production (following corn/soybeans rotation in Table 4.2).

| Crop | Date | Management Operation | Rate |
|---|---|---|---|
| Wheat | 23-Oct | ($P_2O_5$) application (as DAP) | 45.0 kg/ha |
| | 25-Oct | Tillage, Tandem disk (60% mixing) | |
| | 25-Oct | Planting | |
| | 1-Mar | Nitrogen application (as Urea) | 75.0 kg/ha |
| | 1-Jul | Harvest | |

SWAT was initially set up to run on a daily time step for the period 2001 to 2013 with a warm-up period of five years (01/2001 to 12/2005) for the model to initialize and approach reasonable starting values for model variables (Tolson and Shoemaker, 2007). SWAT was then calibrated for streamflow, soluble N, total N, soluble P and total P using observed data at the AXL outlet for 01/2006 to 12/2009, and validated for the period 01/2010 to 12/2013.

Climate data obtained from the CEAP weather stations located in AXL, ALG and AME (upstream of the AXL outlet) were used to create SWAT weather input files during model warm-up/calibration/validation. Baseline (1961 to 1990) and future (2020 to 2099) climate files were obtained using the MarkSim weather file generator at a location central to the AXL watershed in order to assess the effect of future climate change on sediment, atrazine, nitrogen, and  losses. Twentieth century outputs from MarkSim (1961 to 1990) represented the current baseline climate, and future climate was assessed for 2020 to 2099.

### 4.4.4 SWAT Model Calibration and Validation

SWAT was calibrated on a monthly time step for streamflow, nitrate + nitrite (referred to as soluble N from here on), total nitrogen (total N), mineral phosphorus (soluble P), and total phosphorus (total P) using the streamflow records from the CEAP monitoring station at the AXL watershed outlet. The model calibration period was from January 2006 to December 2009, and validation from January 2010 to December 2013. During calibration, baseflow contribution to streamflow was analyzed using the Web-based Hydrograph Analysis Tool (WHAT) developed by Purdue University (Lim et al., 2005) based on the (Arnold and Allen, 1999) base flow filter program. Model calibration was performed using the SWAT-CUP autocalibration tool. Manual calibration was also used to improve the results of autocalibration based on best professional judgment (Arnold et al., 2012). In addition to visual inspection of observed and simulated time series values at the watershed outlet, model performance was also evaluated using the Kling-Gupta efficiency (KGE), Nash-Sutcliffe efficiency (NSE), coefficient of determination ($R^2$) and percent bias (PBIAS). Based on Moriasi et al. (2007) and Van Liew and Garbrecht (2003), SWAT calibration and validation results were acceptable for KGE > 0.5, NSE > 0.50, $R^2$ > 0.50, PBIAS ±25% (Figure 4.2).

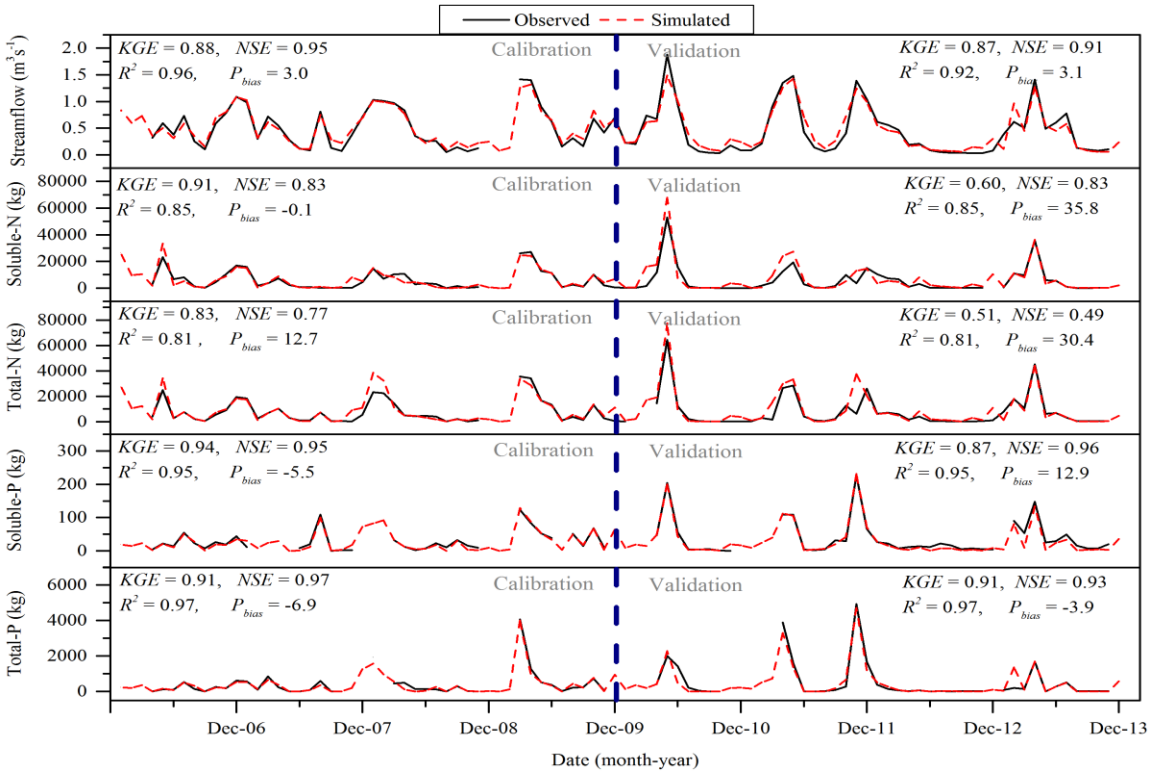


Figure 4.2. Observed and simulated monthly streamflow, soluble N, total N, soluble P and total P at the AXL watershed.

### 4.4.5 Representing Conservation Practices in SWAT

Simulation of BMPs such as grassed waterways, vegetative filter strips, no-tillage, and nutrient management in SWAT involves the adjustment of recommended model parameters. Other BMPs including the blind inlet can be represented by modifying the necessary algorithms found in the SWAT subroutine files. The SWAT parameters (including file extensions or subroutines) and the conservation practices they affect are presented in Table 4.4.

Table 4.4. Representation of conservation practices in SWAT.

| Conservation practices (BMPs) | Variable (input file) | Description | Value before BMPs | Value after BMPs |
|---|---|---|---|---|
| No-Till | ITNUM (till.dat) | Tillage implement code (4 = zero till, 60 = chisel plow, 80 = disk chisel) | 60, 85 | 4 |
| | EFFMIX (till.dat) | Mixing efficiency of tillage operation (%) | 30, 60 | 5 |
| | DEPTIL (till.dat) | Depth to mixing caused by the tillage operation (mm) | 150, 100 | 25 |
| | CNOP (.mgt) | SCS runoff curve number for moisture condition II | 0[b] | Adjusted CN2 |
| Vegetative filter strips (VFS) | VFSCON(.ops) | Fraction of total runoff from HRU entering most concentrated 10% of VFS | - | 0.75 |
| | VFSRATIO(.ops) | Field area to VFS ratio | - | 40 |
| | VFSCH(.ops) | Fraction of flow through most concentrated 10% of fully channelized VFS | - | 0 |
| Grassed waterways | CH_N2 (.rte) | Manning's roughness (adjusted based on cover in waterway) | varies by reach | 0.3 |
| | CH_COV2 (.rte) | Channel cover factor | 0[a] | 0.001 |
| | CH_COV1 (.rte) | Channel erodibility factor | 0[a] | 0.001 |
| Blind Inlet | TILEO (pothole.f subroutine) | Flow from surface inlet tile ($m^3$ $H_2O$) | varies by HRU | -45% |
| | DRCLA (pothole.f subroutine) | Delivery ratio for pothole sediment | varies by HRU | -38% |
| Nutrient management | FERT_ID (.mgt) | $P_2O_5$ as MAP/DAP (kg/ha) for corn and soybeans | varies | 0[c] |
| | FERT_ID (.mgt) | $P_2O_5$ as DAP (kg/ha) | 45 | 22] |

[a] Indicates that when the variable is set to zero, the default value is used for SWAT simulations.
[b] Indicates that when the variable value is set to zero, the CN2 value is used for the initial SWAT simulations.
[c] Indicates that $P_2O_5$ application rate for corn and soybean is set to zero when soil tests showed P > 40 mg $kg^{-1}$

*No-Till*: Representing no-till in SWAT requires the modification of till.dat and management files. In the till.dat file, the numeric code (ITNUM) is used to identify the tillage practice that will be modeled (#4 for no-till), and EFFMIX (mixing efficiency) specifies the fraction of residue on the soil surface that are mixed uniformly through the soil depth specified by DEPTIL. The mixing efficiency for no-till is typically five percent, while the mixing depth is approximately 25 mm (Srinivasan, unpublished). The management file specifies the month and date that the no-till operation takes place, as well the SCS curve number for soil moisture condition II (CN2). Based on available literature, curve numbers should be reduced to reflect the impacts of conservation tillage or no-till (Chung et al., 1999; Feyereisen et al., 2008; Rawls et al., 1980; Rawls and Richardson, 1983).

No-till operations increase the amount of residue on the surface after crop harvest and before planting the next crop. Using CN change/residue relationships developed by Rawls et al. (1980) as a guide, changes in CN2 values were estimated based on the amount of residue on the ground or a certain percentage of the surface covered with-residue. A study on crop rotation and residue cover shows that average percent residue cover at planting (no-till) is 69, 58 and 31 percent following corn, wheat and soybeans, respectively (Roth, 1996). Therefore, by applying Rawls et al. (1980) method, the CN2 values were adjusted (CNOP) for corn, soybeans and wheat cultivation (Table 4.5).

Table 4.5. Percentage change in CN2 values based on estimated residue cover after no-till planting.

| Previous Crop | Residue cover (%) | Change in CN2 (%) |
|---|---|---|
| Corn | 69 | -10.5 |
| Soybeans | 31 | -6.0 |
| Wheat | 58 | -9.0 |

*Vegetative filter strips*: The SWAT conservation practice-modeling guide provides a specific method for representing *vegetative filter strips (VFS)* in SWAT. This method includes adjusting the fraction of total runoff from a field entering the most concentrated 10% of a VFS (*VFSCON*); field area to VFS ratio (*VFSRATIO*); and the fraction of flow through the most concentrated 10% of fully channelized VFS (VFSCH). As recommended in the SWAT conservation practice-modeling guide, a *VFSCON* of 0.5, *VFSRATIO* of 40, and a *VFSCH* of zero were used to represent vegetative filter strips at optimal conditions.

*Grassed waterways*: Representing grassed waterways in SWAT include adjusting the channel Manning's roughness (*CH_N2*), channel cover factor (*CH_COV2*) and the channel erodibility factor (*CH_COV1*). As recommended by Fiener and Auerswald (2006), the Manning's roughness coefficient was adjusted to 0.3 to represent grassed waterways at optimal conditions, a channel cover factor of 0.001 was used to represent fully protected channels, and a channel erodibility factor of 0.001 was used to represent channels with zero erodibility (Bracmort et al., 2004, 2006). Other parameters associated with grassed waterways include channel width (*CH_W2*) and channel depth (*CH_D*), typically specified in the channel design phase.

*Blind Inlets*: Blind inlets are a new technology currently being developed by researchers attached to the ARS-NSERL-CEAP project (Smith and Livingston, 2013; Smith et al., 2008), and are not currently represented in SWAT. Being able to represent this technology in SWAT should enhance conservation efforts to protect surface water quality. At present,

SWAT assumes that once sediment, nutrients or pesticides enter a water body (e.g. potholes) they are instantaneously mixed throughout the volume (a well-mixed system) (Neitsch, 2002). Blind inlets were represented in SWAT by modifying the pothole.f subroutine. First, the flow from surface inlet tile to the main channel (tileo) was adjusted to reflect flow from the blind inlet, with blind inlets reducing flow from potholes by approximately 45%. Secondly, based on the results of field experiments (Smith et al., 2008; Feyereisen et al., 2015), reduction in suspended sediment leaving the potholes was accounted for by decreasing the delivery ratio for sediment fines (*drcla*) by 64%, Equation (4.1). Complete settling was assumed for all other particle sizes (e.g. *dr* = zero for sand, gravel etc.). Based on SWAT nutrient loss equations, particulate nitrogen and phosphorus are attached to sediment fines. Therefore, adjusting *drcla* decreased particulate forms of nitrogen and phosphorus by approximately 50%. Additionally, since the ranges for blind inlet's effectiveness on soluble N and P losses were wide (1% to 78% and 34% to 94%, respectively), the time it takes for a certain amount of soluble N and soluble P to be reduced by half were adjusted until total N and total P losses reached the 55% reduction reported by Feyereisen et al. (2015).

$$drcla = \left(\frac{1-0.5*V_{fall}}{pot_{depth}}\right) * 0.36 \quad (4.1)$$

where $V_{fall}$ is the particle size fall velocity (mm/d), and $pot_{depth}$ is the pothole depth (m). The effectiveness of blind inlets in reducing pesticide losses is uncertain and therefore, was not accounted for in this study.

Blind inlets were simulated on all potholes identified as farmed-closed depressions in the watershed, which had a contributing area of approximately 4.2 $km^2$ (10.0% of watershed area) (Figure 4.3). Using ArcGIS, farmed closed depressions were defined as sink features identified in a 1-meter resolution DEM that met a certain criteria (i.e. features with area >0.2ha, depth > 0.5m, features > 100m from drainage network and occurs in croplands only).

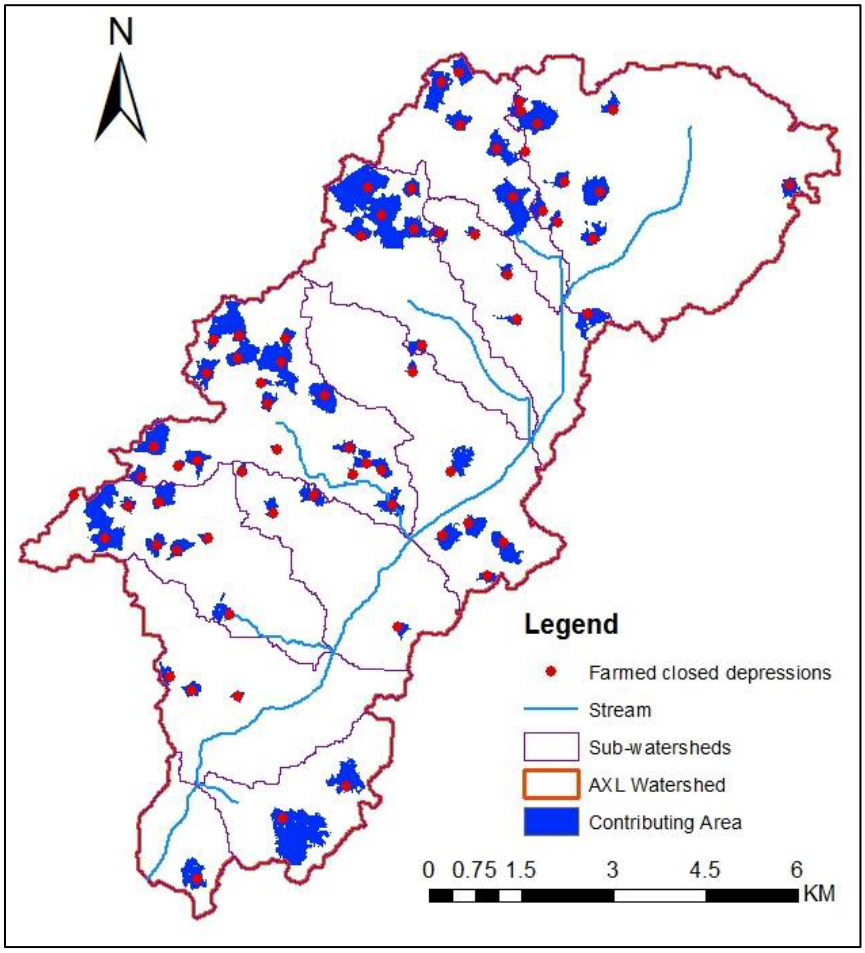


Figure 4.3. Map of AXL watershed showing the farmed closed depressions and their contributing areas.

*Nutrient management*: Based on the NRCS guidelines, nutrient management recommendations should be based on optimal crop agronomic requirements that would not reduce crop yields. For this study, nutrient management was considered concerning phosphorus (P) fertilizer reduction. Soil test data for northeastern Indiana (2001 to 2013) showed average phosphorus content ranging from 46 mg $kg^{-1}$ to 53 mg $kg^{-1}$. Therefore, based on the Tri-State fertilizer recommendations for soil P > 40 mg $kg^{-1}$ (Vitosh et al., 1995), no additional fertilizer was required for corn and soybeans, while a reduced application rate for wheat was recommended.

For the simulation of long-term nutrient management effects, modifying the application rate of P over time is desired to account for possible changes to soil P levels. For this study, however, changes in P application rate were based solely on current Tri-State fertilizer recommendations for soil P > 40 mg $kg^{-1}$ in order to assess the effect of climate change on P losses if reduced application rates are held constant over a long period of time. A future research opportunity would be to explore changes in P application rate for long-term simulations since in reality soil P would drop over time if P application rate were held at zero.

### 4.4.6 BMP Simulation Scenarios

Fourteen BMP scenarios related to surface flow, tile flow, tillage operations and nutrient management were assessed in this study. Five of the scenarios correspond to individual BMPs with existing management practices; five additional scenarios correspond to individual BMPs without existing management practices (as a control), while the other

four scenarios consist of combinations of the five individual BMPs with existing-management practices. A summary of the BMP simulation scenarios is presented in Table 4.6.

Table 4.6. Description of BMP simulation scenarios.

| | Simulation scenario | Scenario description |
|---|---|---|
| Baseline | Existing condition | Simulations performed using existing cropping and management practices. |
| Individual BMPs scenarios | 1 | Simulations performed using existing cropping and management practices within the watershed, but with all cropping done by no-tillage (for corn, soybeans, and wheat). |
| | 2 | Simulations performed using the existing cropping and management practices within the watershed, but with vegetative filter strips (VFS) added at the edge of all fields. |
| | 3 | Simulations performed using the existing cropping and management practices within the watershed, but with grassed waterways added to all secondary channels. |
| | 4 | Simulations performed using the existing cropping and management practices within the watershed, but with blind inlets added on all potholes in corn, soybeans and wheat cultivation. |
| | 5 | Simulations performed using the existing cropping and management practices within the watershed, except there was no application of fertilizer |
| Control | Worst case | Simulations performed with no conservation practices implemented (no VFS, no grassed waterways, conventional tillage practices, and no blind inlets) |
| Individual BMPs scenarios | 6 | Simulations performed with no conservation practices implemented, except cropping done with no-till |
| | 7 | Simulations performed with no conservation practices implemented, except VFS were added at the edge of all fields. |
| | 8 | Simulations performed with no conservation practices implemented, except grassed waterways added to all secondary channels |
| | 9 | Simulations performed with no conservation practices implemented, except blind inlets were added on all potholes in corn, soybeans and wheat cultivation. |
| | 10 | Simulations performed with no conservation practices implemented, except fertilizer application to fields was reduced or eliminated |
| Combined BMPs scenarios | 11 | BMP implementation consisted of VFS along the sides of 100% of the main channels, grassed waterways in 100% of secondary channels, no-till for 100% of corn, soybean crops and wheat, blind inlets on all potholes. |
| | 12 | Using scenario 11, fertilizer application to fields was eliminated |
| | 13 | BMP implementation consisted of VFS placed randomly along the sides of 50% of the main channels. Grassed waterways placed on 50% of randomly selected secondary channels; no-till for 80% of the soybeans and 50% of the corn and wheat crops (randomly selected); conservation tillage (mulch-till) for 20% of the soybeans and 50% of the corn and wheat crops; blind inlets on 50% of the potholes (randomly selected). |
| | 14 | Using scenario 13, fertilizer application to fields was eliminated |

### 4.4.7 Evaluation of BMP Scenarios

The effects of BMP implementation on water quality are presented as percent change in average annual surface runoff, sediment loss, atrazine loss, soluble N loss, total N loss, soluble P loss and total P loss for each decade relative to the baseline period. Reductions include cumulative load reductions for the watershed, considering overland transport and routing through the stream network (Tuppad et al., 2010). The calibrated model with existing management practices was used to establish baseline conditions against which to evaluate individual and combined BMP effects. Additionally, a SWAT model set-up without existing management practices (non-calibrated) was used to establish a control against which the individual BMPs effectiveness was contrasted. Both individual and combined BMP scenarios were simulated independently for the baseline period (1961-90) and for each decade of future climate (i.e. 2020s, 2030s….2090s). The percent change was calculated as:

$$Percent\ change = \left(\frac{Load_{post} - Load_{pre}}{Load_{pre}}\right) * 100 \quad (4.2)$$

where $Load_{pre}$ is the load before BMP implementation, and $Load_{post}$ is the load after BMP implementation (negative values indicate decrease). A paired t-test ($\alpha = 0.05$) was used to assess the significance in percent change for streamflow, sediment loss, atrazine loss, soluble N loss, total N loss, soluble P loss and total P loss before and after BMP implementation.

## 4.5 Results and Discussion

This study evaluated the performance of alternative conservation practices and determined their effectiveness for use in future watershed implementation plans. Average annual surface runoff, sediment loss, atrazine loss, soluble N loss, total N loss, soluble P loss and total P loss simulated under existing baseline conditions (1961-90, calibrated) were 100 mm, 0.71 t $ha^{-1}$, 1.55 g $ha^{-1}$, 10.1 kg $ha^{-1}$, 12.8 kg $ha^{-1}$, 0.05 kg $ha^{-1}$, and 0.6 kg $ha^{-1}$, respectively (Table 4.7). The baseline scenario, which involves simulations, performed using existing cropping and management practices, provided the basis for evaluating the individual and combined BMP scenarios under future climate conditions. Table 4.7 also shows the average annual metrics for uncalibrated SWAT simulation performed for 1961-90 (control). The large differences in average annual metrics between baseline and control simulations were because the control simulation was performed without existing management practices and were uncalibrated. Management practices such as no-tillage and VFS that were widely implemented in the AXL watershed reduced surface runoff, sediment and agricultural chemical losses.

Table 4.7. Average annual surface runoff, sediment, and chemical losses for existing baseline conditions (pre BMP, calibrated) and the control (pre BMP, uncalibrated), under baseline climate (1961-1990).

| | Baseline | Control |
|---|---|---|
| Surface runoff (mm) | 100 | 182 |
| Sediment loss (t $ha^{-1}$ $yr^{-1}$) | 0.71 | 1.62 |
| Atrazine loss (g $ha^{-1}$ $yr^{-1}$) | 1.55 | 2.41 |
| Soluble N loss (kg $ha^{-1}$ $yr^{-1}$) | 10.1 | 26.5 |
| Total N loss (kg $ha^{-1}$ $yr^{-1}$) | 12.8 | 33.3 |
| Soluble P loss (kg $ha^{-1}$ $yr^{-1}$) | 0.05 | 0.11 |
| Total P loss (kg $ha^{-1}$ $yr^{-1}$) | 0.60 | 1.65 |

### 4.5.1 Individual BMP scenarios

The effect of individual BMPs (no-till, VFS, grassed waterways, blind inlets, and nutrient management) in mitigating surface runoff, sediment loss, atrazine loss, soluble N loss, total N loss, soluble P loss, and total P loss, under baseline and future climate conditions are summarized in Figures 4.4 and 4.5 on a decadal basis. Summary of the long-term average annual percent reduction at the watershed outlet, and the statistical analysis is presented in Table 4.8. Summaries of magnitude change in surface runoff, sediment and chemical losses relative to the baseline scenario (existing management and cropping practices simulated under MarkSim baseline climate) are presented in Appendix C.

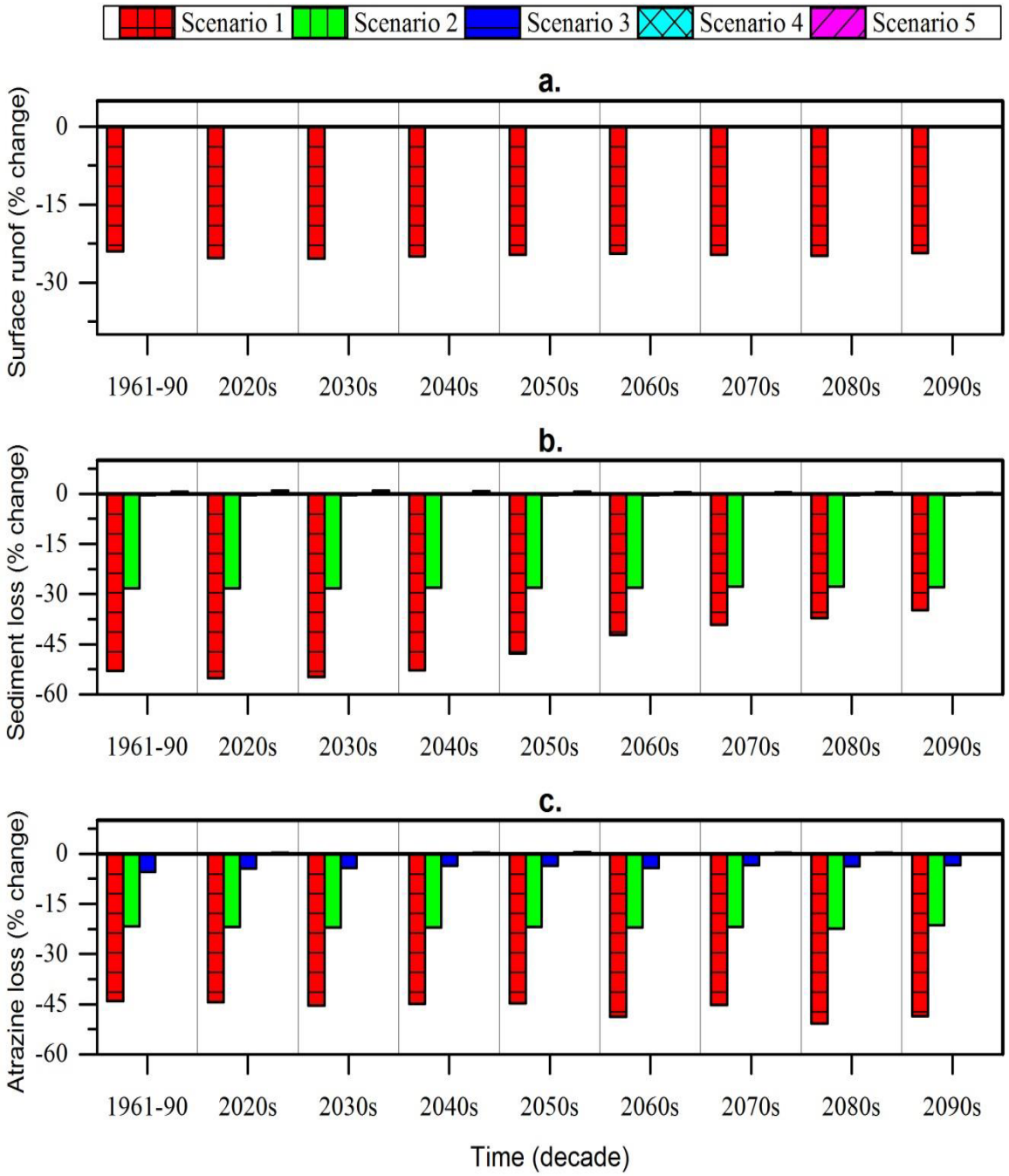


Figure 4.4. The effect of Individual BMP scenarios on a.) surface runoff, b.) sediment loss and c.) atrazine loss for the baseline climate (1961 to 1990) and each decade of future climate conditions (2020 to 2099).

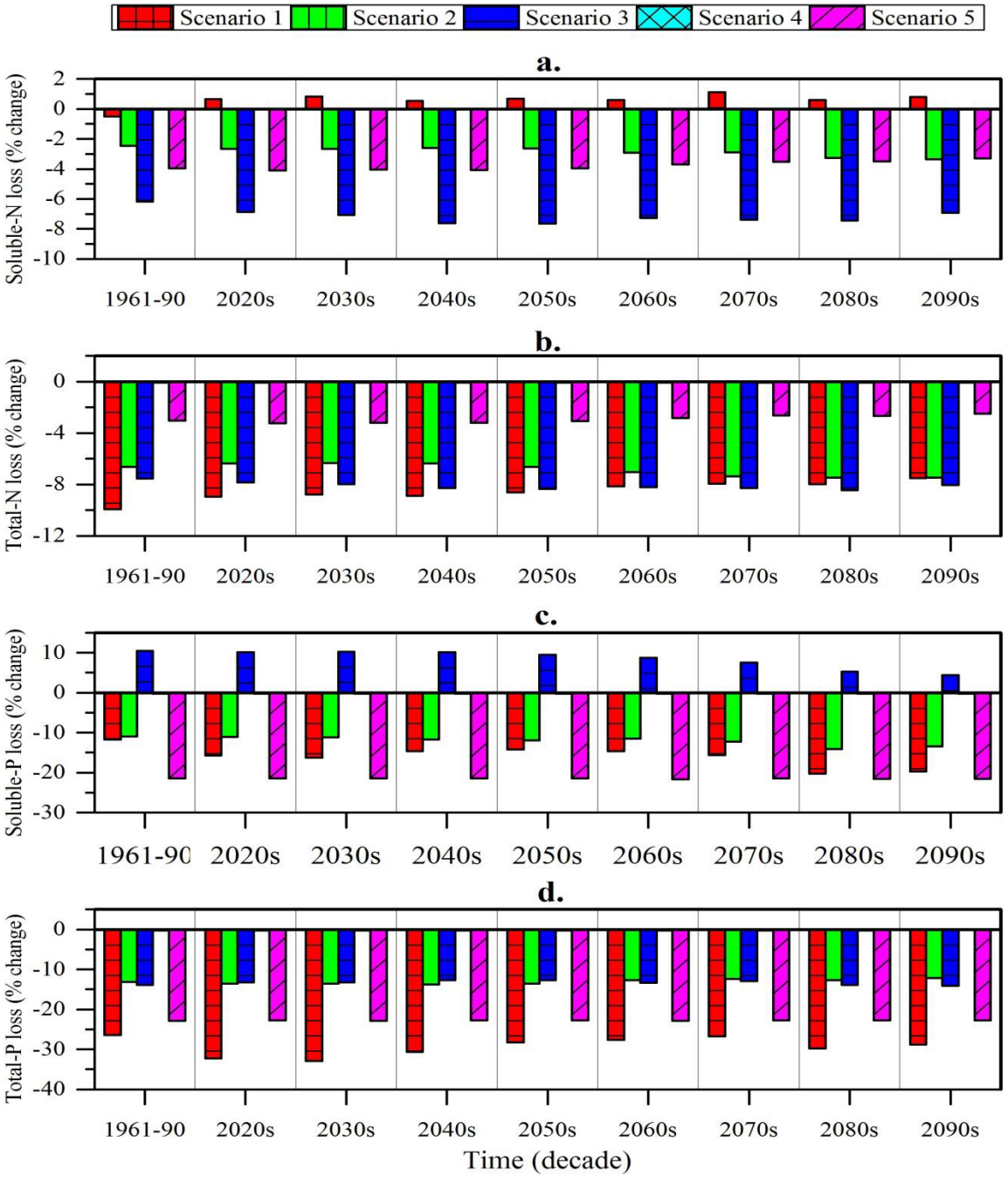


Figure 4.5. The effect of Individual BMP scenarios on a.) soluble N loss, b.) total N loss, c.) soluble P loss and d.) total P loss for the baseline climate (1961 to 1990) and each decade of future climate conditions (2020 to 2099).

Table 4.8. Long-term annual average percent change in surface runoff, sediment, atrazine, soluble N, total N, soluble P, and total P loadings at the watershed outlet, with respect to baseline simulations.

| | Surface runoff | | Sediment | | Atrazine | | Soluble N | | Total N | | Soluble P | | Total P | |
|---|---|---|---|---|---|---|---|---|---|---|---|---|---|---|
| BMPs Implementation | % change | p-value | % change | p-value | % changed | p-value | % change | p-value | % change | p-value | % change | p-value | % change | p-value |
| No-Till | -24.8 | 0.000 | -43.3 | 0.006 | -46.7 | 0.000 | 0.7 | 0.835 * | -8.3 | 0.029 | -16.3 | 0.000 | -29.4 | 0.000 |
| VFS | 0.0 | 1.000 | -28.0 | 0.050 | -22.0 | 0.001 | -2.9 | 0.304 * | -6.9 | 0.053 | -12.1 | 0.000 | -13.0 | 0.000 |
| Grassed Waterways | 0.0 | 1.000+ | -1.0 | 0.984 * | -3.8 | 0.515 * | -7.3 | 0.015 | -8.2 | 0.027 | 8.3 | 0.007 | -13.3 | 0.011 |
| Blind Inlets | -0.2 | 1.000 | -0.2 | 0.999 * | 0.0 | 1.000 * | 0.0 | 0.991 * | -0.1 | 0.982 * | -0.3 | 0.912 * | -0.2 | 0.960 * |
| Nutrient management | 0.0 | 1.000 | 0.5 | 0.972 * | 0.3 | 0.967 * | -3.8 | 0.194 * | -2.9 | 0.42* | -21.5 | 0.000 | -23.0 | 0.016 |
| Combined BMPs (scenario#11) | -24.8 | 0.000 | -57.0 | 0.001 | -56.5 | 0.000 | -9.5 | 0.002 | -20.3 | 0.000 | -28.0 | 0.000 | -52.6 | 0.000 |
| Combined BMPs (scenario#12) | -24.8 | 0.000 | -56.8 | 0.001 | -56.4 | 0.000 | -13.0 | 0.002 | -23.0 | 0.000 | -35.6 | 0.000 | -57.4 | 0.000 |
| Combined BMPs (scenario#13) | -15.2 | 0.000 | -37.7 | 0.014 | -38.2 | 0.000 | -5.4 | 0.064 * | -12.8 | 0.001 | -12.1 | 0.000 | -34.7 | 0.000 |
| Combined BMPs (scenario#14) | -15.2 | 0.000 | -37.4 | 0.015 | -38.0 | 0.000 | -6.6 | 0.029 | -13.7 | 0.001 | -16.5 | 0.000 | -39.0 | 0.000 |

Note:
The p-values are used to identify whether the reductions realized by the BMPs implementation are significant at $\alpha = 0.05$ level.
* indicates insignificant difference at $\alpha = 0.05$
Combined BMPs implementation consisted of:
# 11 VFS along 100% of the main channels, grassed waterways in 100% of secondary channels, no-till for 100% of corn, soybean and wheat, blind inlets on all farmed potholes
# 12 VFS along 100% of the main channels, grassed waterways in 100% of secondary channels, no-till for 100% of corn, soybean and wheat, blind inlets on all farmed potholes, nutrient mgt.
# 13 VFS along 50% of the main channels, grassed waterways in 50% of secondary channels, no-till for 50% of corn, 80% of soybean and 50% of wheat, blind inlets on 50% of farmed potholes
# 14 VFS along 50% of the main channels, grassed waterways in 50% of secondary channels, no-till for 50% of corn, 80% of soybean and 50% of wheat, blind inlets on 50% of farmed potholes, nutrient mgt.

#### 4.5.1.1 No-Tillage (Scenarios 1 and 6 in Table 4.6)

Results from this study, which is based on each decade of future climate (2020-2099), show that applying no-tillage to all crops in the watershed reduced average annual surface runoff in the range of 22% to 25% (approximately 20 mm). The reduction in surface runoff resulted in increasing average annual tile flow (5 mm), and seepage into the soil profile (10 mm). An additional 5 mm of rainfall is accounted for by increasing lateral flow, ET, percolation out of the soil, and aquifer recharge. Statistical analysis showed that the long-term annual average reduction in runoff due to no-till implementation was significant with $p = 0.000$ at $\alpha = 0.05$ (Table 4.8).

No-tillage also reduced average annual sediment (34.9% to 55.2%), atrazine (44.5% to 50.8%), total N (7.5% to 8.9%), soluble P (14.2% to 20.2%) and total P (26.7% to 32.9%) losses, with respect to existing baseline conditions (Figures 4.4 and 4.5). However, there was a slight increase in soluble N loss (0.5% to 1%). The control simulations also confirm that no-tillage will reduce surface runoff (23.2% to 25.0%), sediment (44.6% to 46.3%), atrazine (39.3% to 44.3%), and total N (2.9% to 4.4%), soluble P (1.0% to 8.7%) and total P (14.7% to 23.3%), but increase soluble N loss (2% to 4%) for the same period.

The long-term annual average reduction in sediment, atrazine, total N, soluble P and total P losses due to no-till implementation were significant at $\alpha = 0.05$ (Table 4.8). Several studies conducted using SWAT have shown similar results in terms of percent reduction in surface runoff, sediment and chemical losses due to the application of no-tillage or some other form of conservation tillage implementation at the watershed scale (Dalzell et

al., 2004; Tuppad et al., 2010; Dechmi and Skhiri, 2013). Shipitalo (2013) evaluated the effect of no-till on surface runoff, sediment and nutrient losses in seven sub-watersheds in the North Appalachian Watershed near Coshocton, Ohio under a corn/soybean rotation and concluded that no-till was more effective in minimizing surface runoff, sediment (25%), nitrogen (33%), and phosphorus (6%) losses when compared to chisel.

The soluble N loss from surface runoff decreased by approximately 0.13 kg/ha/yr while soluble N loss through tile flow increased by 0.24 kg/ha/yr, which resulted in a slight increase in overall soluble N loading. The slight increase in long-term annual average soluble N loss due to no-till implementation was not significant at $\alpha = 0.05$ (Table 4.8). Other studies (Sharpley and Smith, 1994; Dechmi and Skhiri, 2013) also reported similar increases in soluble N loss, which is attributed to the increasing surface crop residue resulting from no-tillage operations (Wang et al., 2008). The application of a no-tillage system increased soil surface residue in the range of 9.4% to 22.1% with respect to existing baseline conditions. With increased residue cover, surface runoff is often reduced while infiltration is increased. Therefore, because more water is allowed to enter the soil profile, there is potential for increased nitrate transport through subsurface tile drainage. Because nitrate is water-soluble and is negatively charged, it is easily leached and not held by the negatively charged soil particles. The AXL watershed is heavily drained using subsurface tiles that collect much of the leachate and deposit it directly to the stream reach; therefore, as the soil surface residue and infiltration increased, nitrate loss through

subsurface tiles also increased while the nitrate loss through surface runoff decreased (Figure 4.6).

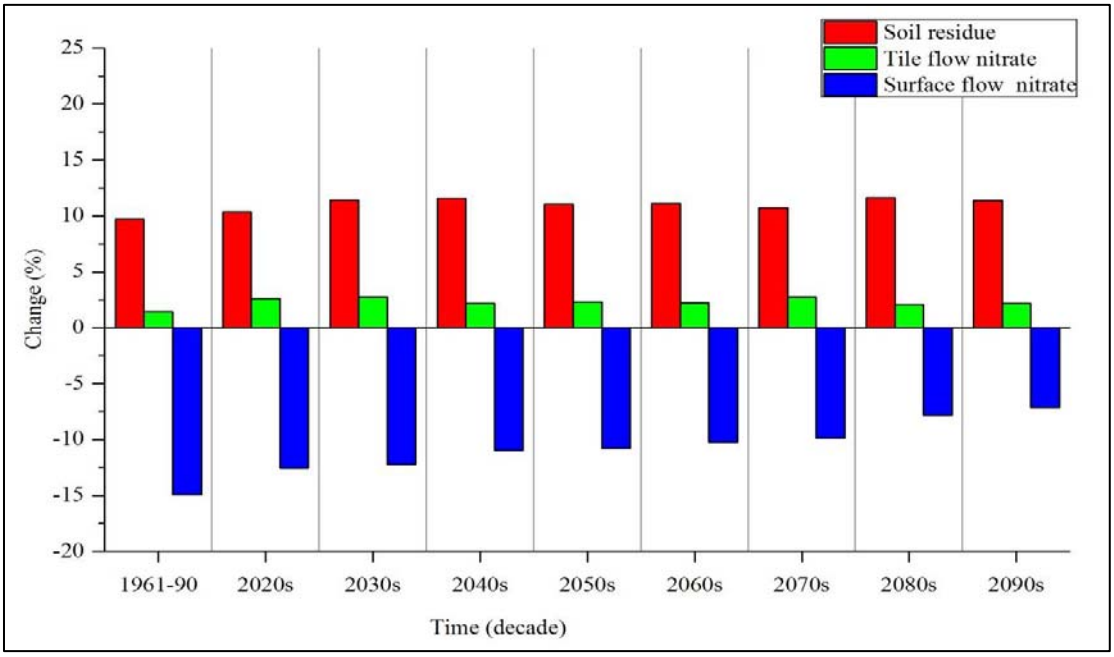


Figure 4.6. The effect of no-till (percent changes) on soil residue cover, nitrate lost through tile flow, and nitrate lost through surface flow for baseline climate and each decade of future climate simulations.

#### 4.5.1.2 Vegetative filter strips (VFS) (scenarios 2 and 7 in Table 4.6)

Vegetative filter strips were simulated at the edge-of-fields for all cropland under corn, soybeans and wheat cultivation, amounting to 67% of the watershed area. VFS are used to intercept and slow surface runoff thereby allowing more sediment and sediment-bound nutrients to settle out before flow enters stream channels. Results from this study show that VFS were effective at reducing sediment loss by approximately 28% ($p = 0.050$) (Table 4.8).

Atrazine sorbed to sediment is trapped in VFS thus resulting in atrazine loss being reduced by approximately 21% ($p = 0.001$), with respect to the existing baseline conditions (Figures 4.4 and 4.5). VFS reduced soluble N loss and total N loss by approximately three percent ($p = 0.304$) and seven percent ($p = 0.053$), respectively. Based on the control simulations, VFS will have negligible effects on the total surface runoff volume in the AXL watershed, but will be effective at reducing sediment by approximately 28%, atrazine by 23%, soluble P by 12% and total P by 13% given future clime conditions. Tuppad et al. (2010) predicted that VFS applied at the edge of all fields reduced sediment 25% to 63%, and total N and total P by 62% and 64%, respectively, at the HRU level in the Bosque River Watershed, Texas. At the sub-watershed and watershed levels, Parajuli et al. (2008) predicted that application of VFS in the 950 $km^2$ Upper Wakarusa Watershed, Kansas reduced sediment by 46% and 12%, respectively.

#### 4.5.1.3 Grassed waterways (scenarios 3 and 8 in Table 4.6)

Grassed waterways were simulated on the secondary channels within the watershed and are used to protect the soil from concentrated flows and to reduce gully erosion, thus reducing sediment loading to the main channels. Results from this study show that the effectiveness of grassed waterways in reducing surface runoff volume, sediment and atrazine losses was not significant, with $p = 1.000$, 0.984 and 0.515, respectively, at $\alpha = 0.05$. The control simulations also suggest grassed waterways will have negligible effects on surface runoff volume, but will reduce sediment and atrazine losses by approximately 2% and 4%, respectively.

The implementation of grassed waterways, however, were effective in reducing soluble N loss by approximately 7% ($p = 0.015$), total N loss by approximately 8% ($p = 0.027$), and total P loss by approximately 13% ($p = 0.011$) (Figures 4.4 and 4.5). But despite a significant reduction in total P loss due to grassed waterway implementation, soluble P loss increased by approximately 8% ($p = 0.007$). This phenomenon indicates that the way grassed waterways are represented in SWAT did not quite capture the physical processes the way they would be in reality. Here, the grassed waterways seem to be capturing sediment that it should not be, and by capturing sediment, it acts as sink for total P and a source for soluble P during runoff events. Grassed waterways were represented in SWAT by increasing the Manning's roughness coefficient for the channels, and by modifying the channel cover factor and the channel erodibility factor to reflect a fully covered non-erosive channel (Bracmort et al., 2004, 2006). There is a built-in function for representing grassed waterways in SWAT; however, this built-in function did not work with the version of SWAT used in this study and therefore, the procedure suggested by Bracmort et al. (2004, 2006) was used.

While other studies using SWAT have determined that grassed waterways were effective in reducing sediment, total nitrogen and total losses (Bracmort et al., 2006; Kaini et al., 2012), very few examined its effect on soluble forms of nutrient (soluble N and soluble P) losses. Based on the unexpected results obtained for soluble P in this study, further research is required to determine whether the representation of grassed waterways in SWAT needs to be improved or whether grassed waterways have unintended

consequences and implications for sustainable management as suggested by Dodd and Sharpley (2015).

#### 4.5.1.4 Blind inlet (scenario 4 and scenario 9 in Table 4.6)

At the HRU level, blind inlets were effective in reducing sediment loss in the range of 42% to 69% and total N loss in the range of 35% to 55%. However, at the watershed level, the percentage change in surface runoff, sediment and atrazine losses for the baseline climate and each decade of future climate were not significant, with p-values of 1.000, 0.999 and 1.000, respectively. The effectiveness of blind inlets in reducing soluble N, total N, soluble P and total P at the watershed level were also not significant, with p-values of 0.991, 0.982, 0.912, and 0.960, respectively.

The negligible effect of blind inlets at the watershed level is most likely due to the relatively small watershed area contributing to the closed depression as shown in Figure 4.3. The contributing area simulated in SWAT was limited to the number of selected farmed-closed depressions that were based on a set of criteria using best professional judgment. This method of identifying and representing closed depressions in SWAT adds a level of uncertainty to the simulation process that may be alleviated once precise representation procedures are developed for closed depressions in agricultural watersheds.

#### 4.5.1.5 Nutrient management (scenario 5 and scenario 10 in Table 4.6)

The implementation of a nutrient management scenario (Table 4.4) was aimed at reducing excess phosphorus in the soil, and consequently reducing the phosphorus transport induced by surface runoff. Results from this study show that the nutrient management scenario had no impact on surface runoff, while its impact on sediment loss, atrazine loss, soluble N loss and total N loss was insignificant with p-values of 0.972, 0.972, 0.194 and 0.420, respectively.

The effectiveness of a nutrient management scenario was evident in its reduction of soluble P and total P losses by approximately 22% ($p = 0.000$) and 23% ($p = 0.016$), respectively. The control simulations also confirm the reduction in soluble P and total P losses by approximately 23.0%. These results were similar to those in other studies evaluating the impact of reduced-P nutrient management on soluble P and total P loss (Santhi et al., 2001; Santhi et al., 2006; Dechmi and Skhiri, 2013b; Dodd and Sharpley, 2015; Francesconi et al., 2015). In a study that evaluated the impacts of BMP in an agricultural watershed using SWAT, Dechmi and Skhiri (2013) predicted that a reduced nutrient management implementation was effective in reducing soluble P and total P losses by 5.8 and 5.1%, respectively. Santhi et al. (2006) evaluated the impacts of BMP (including nutrient management) on sediment and nutrient loadings in the West Fork Watershed of Trinity River Basin in Texas and reported reductions of 10% to 12% from sediment, 3% to 18% for total N, and 5% to 29% for total P.

In this study, reduced P nutrient management was simulated for the entire simulation period (2020s to 2090s). Since P application rate is based on the current Tri-State Fertilizer Recommendations for Corn, Soybeans and Wheat (Vitosh et al., 1995), it is recommended that for future studies, the P application rate is adjusted over time, should the soil P levels fall below the suggested agronomic levels.

### 4.5.2 Combined BMP scenarios (scenarios 11-14 in Table 4.6)

The effect (percent change) of combined BMP scenarios (scenarios 11 through 14) in mitigating surface runoff, sediment, atrazine, soluble N, total N, soluble P, and total P losses, under baseline climate and each decade of future climate conditions are summarized in Figures 4.7 and 4.8. Summaries of the magnitude change in atrazine, soluble N, total N, soluble P, and total P losses relative to the baseline scenario (existing management and cropping practices simulated under MarkSim baseline climate) are presented in Appendix C.

The combined BMPs scenarios were significantly more effective in reducing surface runoff, sediment, atrazine, soluble N, total N, soluble P, and total P losses when compared to the individual BMPs, except for scenario 1 (no-till) that resulted in surface runoff reductions similar to scenarios 11 and 12 but greater than scenarios 13 and 14. This was because the no-till BMP was simulated for 100% of corn, soybeans, and wheat in scenarios 1, 11 and 12, but only 50% of corn, 80% of soybeans, and 50% of wheat in scenarios 13 and 14. The largest percent reductions were achieved by scenarios 11 and

12, which represented the application of 100% of the individual BMPs (except nutrient management was only included in scenario 12). Sediment and total P were the pollutants that were reduced the most in all four combined BMPs scenarios because more of the individual BMPs affect sediment loss and sediment-bound phosphorus than other pollutants.

The percent reductions achieved by scenario 12 were similar to those of scenario 11, but with an average of 3% more reduction in soluble N and total N losses, and 5% more reduction in soluble P and total P losses because of the inclusion of a nutrient management scheme. More specifically, the implementation of scenario 11 resulted in percent reductions ranging from 24% to 26% for surface runoff, 50% to 68% for sediment, 55% to 60% for atrazine, 9% to 10% for soluble N, 20% to 21% for soluble P and 51% to 55% for total P losses. The implementation of scenario 12 resulted in identical changes on surface runoff, sediment, atrazine loss, but predicted reductions ranging from 13% to 14% for soluble N, 23% to 24% for total N, 31% to 41% for soluble P, and 55% to 60% for total P.

Scenarios 13 and 14 represented a more realistic and balanced case of BMP implementation, because they do not require 100% implementation of the individual BMPs in order to be effective in reducing surface runoff, sediment and agricultural chemical losses. They may also be more cost effective and attractive for farmers to implement. Both scenarios resulted in similar reductions for surface runoff, sediment and atrazine loss, ranging from 15% to 16%, 32% to 45%, and 37% to 41%, respectively. The

implementation of scenario 13 resulted in reductions ranging from 5% to 6% for soluble N, 12% to 13% for total N, 9% to 16% for soluble P and 33% to 36% for total P losses. Scenario 14 produced similar results, but with an average of 1% to 4% more reduction in soluble N and total N losses, and 4% to 5% more reduction in soluble P and total P losses because of the inclusion of nutrient management.

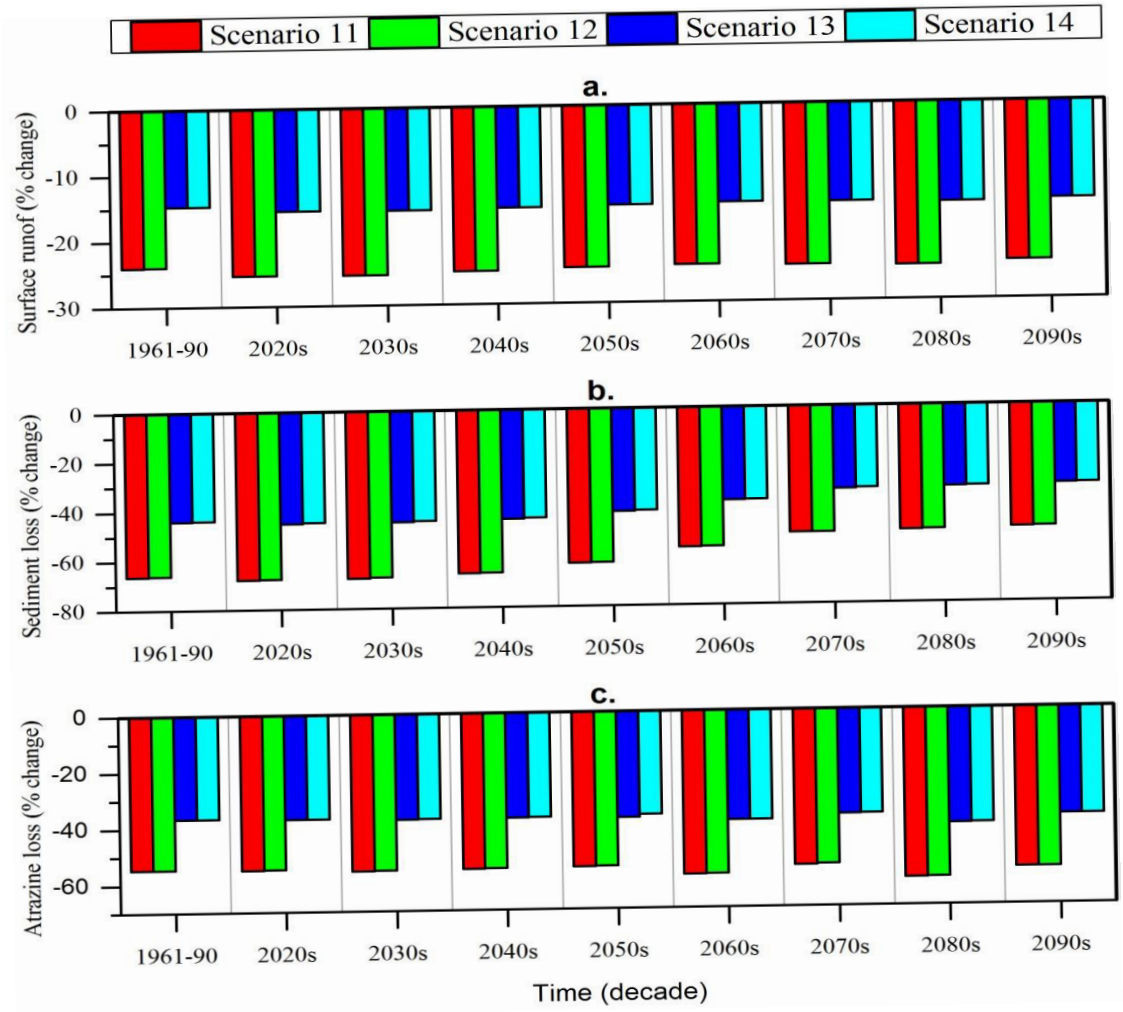


Figure 4.7. The effect of combined BMPs scenarios on a.) surface runoff, b.) sediment loss and c.) atrazine loss for the baseline climate (1961 to 1990) and each decade of future climate conditions (2020 to 2099).

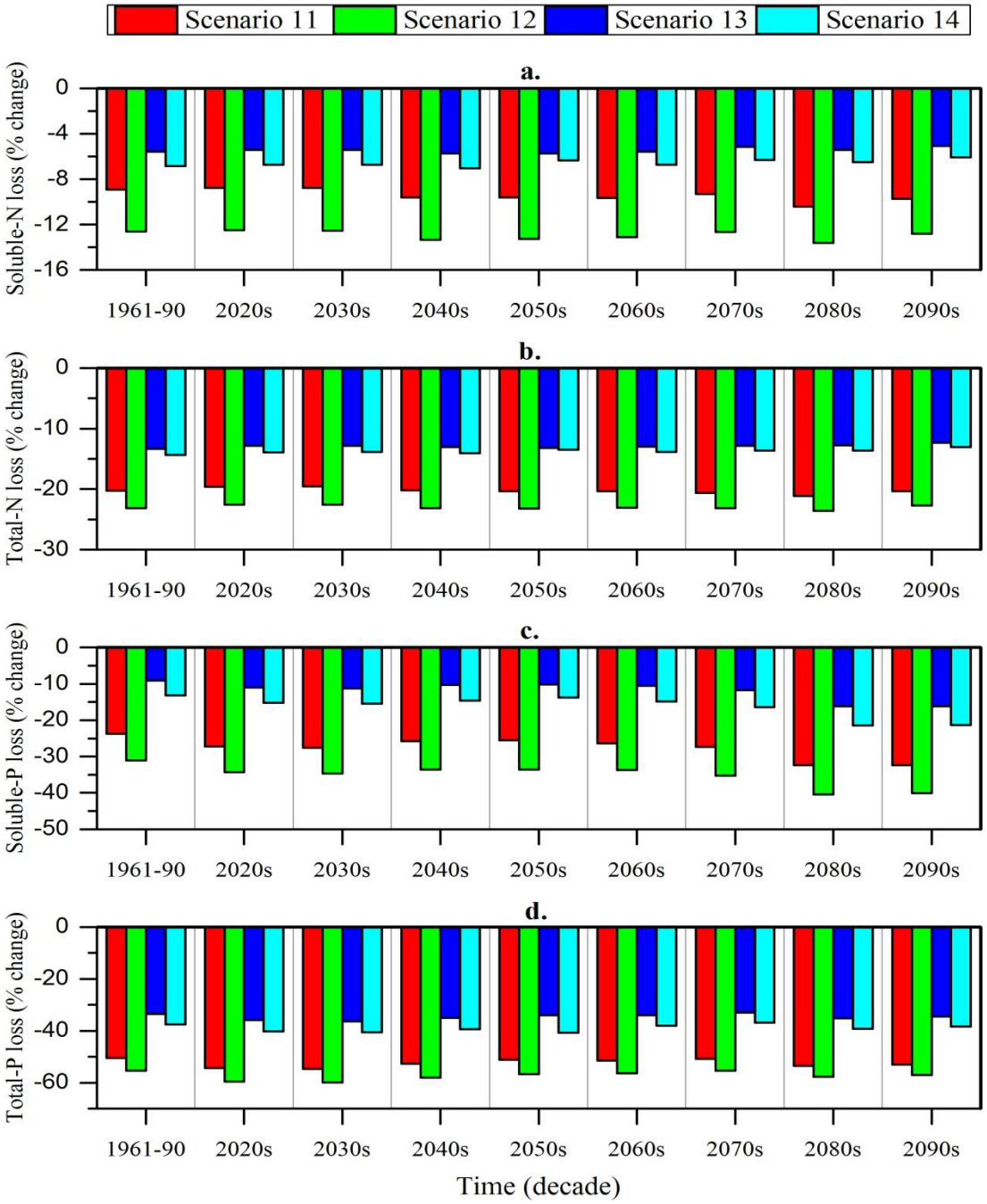


Figure 4.8. The effect of combined BMPs scenarios on a.) soluble N loss, b.) total N loss, c.) soluble P loss and d.) total P loss for the baseline climate (1961 to 1990) and each decade of future climate conditions (2020 to 2099).

## 4.6 Summary and Conclusions

SWAT with future climate data downscaled using the MarkSim weather file generator was used to quantify the long–term effects of different conservation practice implementation on surface runoff, sediment and agricultural chemical losses in the Matson Ditch (AXL) Watershed, Northeastern Indiana. Average annual surface runoff, sediment and atrazine losses showed reductions ranging from 0% to 25%, 0% to 68%, and 0% to 60% respectively, with no-till or combined BMPs (including 100% no-till) being the most effective. Implementing grassed waterways, VFS, blind inlets and nutrient management individually had insignificant effects on surface runoff at the watershed outlet. Predicted changes in average annual soluble N and total N losses ranged from -5% to 14%, and 0.1% to 24%, respectively, with grassed waterways or combined BMPs (including grassed waterways on 100% of secondary channels) being the most effective in reducing soluble N loss, while no-till or combined BMPs (including 100% no-till) being the most effective in reducing total N loss. Changes in average annual soluble P and total P losses ranged from -10% to 41%, and 0.2% to 60%, respectively, with nutrient management or combined BMPs (including 100% no-till and VFS along the sides of 100% of the main channels) being the most effective in reducing soluble P loss. No-till or combined BMPs (including 100% no-till and VFS along the sides of 100% of the main channels) were the most effective in reducing total P loss.

Based on these results, the implementation of individual conservation practices may be effective in addressing a specific sediment or nutrient concern in agricultural watersheds,

but may not be as effective in mitigating the loads of unintended pollutants that could impair water quality. The combined BMPs, however, were the most effective in reducing surface runoff, sediment, atrazine, and nutrient loadings simultaneously under current and future climate scenarios. This study therefore, helps to highlight the importance of combined implementation of different conservation practices in addressing the environmental concerns surrounding agricultural watersheds. Given the availability of several other conservation practices and the costs associated with implementing them at the watershed scale, a detailed assessment would be useful in determining the most cost effective combination of BMPs that will achieve optimum results based on current and future climate scenarios, and the design life of each BMP.

# CHAPTER 5. OVERALL CONCLUSIONS AND RECOMMENDATIONS

## 5.1 Summary and Conclusions

The Soil and Watershed Assessment Tool (SWAT) was used to study four watersheds in northeastern Indiana. SWAT is a hydrologic model developed by the USDA-ARS to predict the impact of land management practices on water, sediment and agricultural chemical losses in large watersheds. The major objective of the research was to evaluate the effect of different agricultural practices on runoff, sediment and chemical losses under current baseline and future climate conditions.

SWAT was first used to evaluate the influence of watershed sizes on model calibration parameters in four watersheds (CCW = 680 $km^2$, F34 = 183 $km^2$, AXL = 42 $km^2$ and ALG = 20 $km^2$) located in Northeastern Indiana. SWAT model parameters were optimized in each of the four watersheds independently and then applied to the other watersheds of different sizes to determine whether calibrating the model at one size watershed would yield satisfactory results when applied to different watersheds. The results showed that calibrating SWAT at one size and applying the optimized parameters at different watersheds of varying sizes with similar physiographic features yielded satisfactory results. The size at which the model was calibrated had little effect on streamflow simulations. The prediction of soluble nitrogen loss was improved when

calibration was performed at the larger CCW watershed. Calibrating SWAT at the smaller AXL and ALG watersheds produced improved NSE, $R^2$ and PBIAS values for soluble and total P when applied to the larger watersheds. SWAT coupled with downscaled climate projections obtained using the MarkSim weather file generator was used to evaluate the impact of climate change on runoff, sediment, atrazine, soluble N, total N, soluble P and total P at the four calibrated watersheds. Based on the results obtained, there will be a significant decrease in surface flow, while tile flow will increase significantly by the end of this century. Average annual sediment loss is expected to increase, though the overall magnitude will be small for the watershed considered here. There will be no significant changes in atrazine, soluble N, total N, and total P losses between the baseline period and the end of the century, while soluble P losses might be larger at the CCW and F34 watersheds.

Finally, the AXL watershed was selected and used to evaluate the long-term impact of BMPs on surface runoff, sediment, atrazine, nitrogen and phosphorus losses. The performance of individual and combined BMPs was simulated under current and baseline climate conditions. Based on the results obtained, individual conservation practices were effective in reducing only a targeted pollutant load, but combined practices were more effective in reducing multiple pollutant loadings simultaneously. Of the individual BMPs assessed, no-till was the most effective in reducing multiple pollutant loads. When individual BMPs were combined, pollutant loads were reduced significantly (at $\alpha = 0.05$) for all pollutants, both under baseline and future climate scenarios. The percent change

for each decade of future climate ranged from 15% to 25% for surface runoff, 32% to 68% for sediment, 37% to 60% for atrazine, 5% to 13% for soluble N, 12% to 35% for total N, 9% to 41% for soluble P, and 33% to 60% for total P.

The overall results of the study will contribute to the Conservation Effects Assessment Project's (CEAP) efforts to quantify the effects of conservation practices on water quality and other environmental parameters as part of its mission to provide oversight as to how the millions of dollars being spent on conservation projects is benefiting the environment.

## 5.2 Recommendations for future work

An assessment of the MarkSim weather file generator to determine whether the ensemble of climate models resulted in a larger proportion of rainfall occurring in small events for future climate compared to baseline climate, future studies could compare individual climate model results with the ensemble mean of multiple climate model results. In addition, other climate change models and downscaling approaches could be considered.

The pothole representation in SWAT needs to be enhanced. The method of identifying and representing closed depressions in SWAT adds a level of uncertainty to the simulation process that may be alleviated once precise representation procedures are developed for closed depressions in agricultural watersheds.

Potholes are numerous within some landscapes and therefore should be properly represented in SWAT setup especially in regions where they are drained with tile risers to increase the cultivation acreage. Therefore, an automated procedure is needed to input

pothole information in SWAT. This would save time and minimize the modeling uncertainty errors.

The reduced P nutrient management scenario used in this study was solely based on the Tri-State fertilizer recommendation for corn, soybeans and wheat without taking into account possible changes in soil P levels over time. Therefore, it is recommended that in future studies, the P application rate be adjusted over time, should the soil P levels be determined to fall below the suggested agronomic levels.

In order to control the number of variables involved in this study and to make the study more manageable, the impact of possible changes in future $CO_2$ levels that are important to crop growth and water usage was not considered. SWAT provides an option to represent the effects of increased CO2 explicitly therefore, with future CO2 concentrations projected to increase (between 550ppm and 950ppm) it is recommended that future climate change studies consider these effects.

# REFERENCES

# REFERENCES

Abbaspour, K. C., M. Vejdani, S. Haghighat, L. Oxley, and D. Kulasiri. 2007. SWAT-CUP calibration and uncertainty programs for SWAT. *Modsim 2007: International Congress on Modelling and Simulation* 1603-1609.

Abbaspour, K. C. 2012. SWAT calibration and uncertainty programs - A user manual. Dübendorf, Switzerland: Swiss Federal Institute of Aquatic Science and Technology, Eawag.

Almendinger, J.E., and J. S. Ulrich. 2010. Constructing a SWAT model of the Sunrise River watershed, eastern Minnesota. Final report to the National Park Service and Minnesota Pollution Control Agency. *St. Croix Watershed Research Station, Science Museum of Minnesota* 63 pp.

Arnold, J., and P. Allen. 1999. Automated methods for estimating baseflow and ground water recharge from streamflow records. *Journal of the American Water Resources Association* 35(2):411-424.

Arnold, J., and N. Fohrer. 2005. SWAT2000: current capabilities and research opportunities in applied watershed modelling. *Hydrological Processes* 19(3):563-572.

Arnold, J., D. Moriasi, P. Gassman, K. Abbaspour, M. White, R. Srinivasan, C. Santhi, R. Harmel, A. van Griensven, M. Van Liew, N. Kannan, and M. Jha. 2012. SWAT: model use, calibration and validation. *Transactions of the ASABE* 55(4):1491-1508.

Arnold, J., R. Srinivasan, R. Muttiah, and J. Williams. 1998. Large area hydrologic modeling and assessment - Part 1: Model development. *Journal of the American Water Resources Association* 34(1):73-89.

Baker, D., and R. Richards. 2002. Phosphorus budgets and riverine phosphorus export in northwestern Ohio watersheds. *Journal of Environmental Quality* 31(1):96-108.

Bharati, L., P. Gurung, P. Jayakody, V. Smakhtin, and U. Bhattarai. 2014. The projected impact of climate change on water availability and development in the Koshi Basin, Nepal. *Mountain Research and Development* 34(2):118-130.

Bingner, R. L., J. Garbrecht, J. G. Arnold and R. Srinivasan. 1997. Effect of watershed subdivision on simulation runoff and fine sediment yield. No. 5. *American Society of Agricultural Engineers*, St. Joseph, MI, ETATS-UNIS.

Bouraoui, F., B. Grizzetti, K. Granlund, S. Rekolainen, and G. Bidoglio. 2004. Impact of climate change on the water cycled and nutrient losses in a Finnish catchment. *Climate Change* 66(1-2): 109-126.

Bracmort, K. S., B. A. Engel, and J. R. Frankenberger. 2004. Evaluation of structural best management practices 20 years after installation: Black Creek watershed, Indiana. *Journal of Soil and Water Conservation.* 59(5): 191-196.

Bracmort, K. S., M. Arabi, J. R. Frankenberger, B. A. Engel and J. G. Arnold. 2006. Modeling long-term water quality impact of structural BMPs. *Transactions of the ASABE* 49(2): 367-374.

Chung, S., P. Gassman, L. Kramer, J. Williams, and R. Gu. 1999. Validation of EPIC for two watersheds in southwest Iowa. *Journal of Environmental Quality* 28(3):971-979.

Cibin, R., K. Sudheer, and I. Chaubey. 2010. Sensitivity and identifiability of stream flow generation parameters of SWAT. *Hydrological Processes* 24(9):1133-1148.

Cohen, B., R. Wiles, and E. Bondoc. 1995. Weed killers by the glasss - A citizens' tapwater monitoring project in 29 cities. Available at: http://www.ewg.org/research/weed-killers-glass. Accessed 12 January 2016.

Dalzell, B. J., P. H. Gowda, and D.J. Mulla. 2004. Modeling sediment and phosphorus losses in an agricultural watershed to meet TMDLs. *Journal of the American Water Resources Association* 40: 533–543.

Dechmi, F., and A. Skhir. 2013. Evaluation of best management practices under intensive irrigation using SWAT model. *Agricultural Water Management* 123: 55–64.

DeKalb SWCD. 2014. DeKalb County Indiana Soil & Water Conservation District Available at: http://dekalbswcd.org/. Accessed 1 November 2014.

Diamond, H. J., T. R. Karl, M. A. Palecki, C. B. Baker, J. E. Bell, R. D. Leeper, D. R. Easterling, J. H. Lawrimore, T. P. Meyers, M. R. Helfert, G. Goodge, and P. W. Thorne, 2013: U.S. Climate Reference Network after one decade of operations: status and assessment. *Bulletin of the American Meteorological Society* 94, 489-498.

Dodd, R. J., and A. N. Sharpley. 2015. Conservation practice effectiveness and adoption: unintended consequences and implications for sustainable management. *Nutrient Cycling in Agroecosystems* (2008) DOI: 10.1007/s10705-015-9748-8.

Dolan, D. 1993. Point-Source loadings of phosphorus to Lake Erie -1986-1990. *Journal of Great Lakes Research* 19, 212-223.

Du, B., J. Arnold, A. Saleh, and D. Jaynes. 2005. Development and application of SWAT to landscapes with tiles and potholes. *Transactions of the ASAE* 48(3):1121-1133.

Du, B., A. Saleh, D. Jaynes, and J. Arnold. 2006. Evaluation of SWAT in simulating nitrate nitrogen and atrazine fates in a watershed with tiles and potholes. *Transactions of the ASABE* 49(4):949-959.

Farm Bill Act. 2002. Farm Security and Rural Investment ACT of 2002. *US House of Representatives*: 1–408.

Farm Bill Act. 2014. Agricultural Act of 2014. *US House of Representatives*: 1–575.

Feyereisen, G., T. Strickland, D. Bosch, C. Truman, J. Sheridan, and T. Potter. 2008. Curve number estimates for conventional and conservation tillages in the southeastern Coastal Plain. *Journal of Soil and Water Conservation* 63(3):120-128.

Feyereisen, G. W., W. Francesconi, D. R. Smith, S. K. Papiernik, E. S. Krueger, and C. D. Wente. 2015. Effect of replacing surface inlets with blind or gravel inlets on sediment and phosphorus subsurface drainage losses. *Journal of Environmental Quality* 44(2):594-604.

Ficklin, D., Y. Luo, E. Luedeling, and M. Zhang. 2009. Climate change sensitivity assessment of a highly agricultural watershed using SWAT. *Journal of Hydrology* 374(1-2):16-29.

Fiener, P., and K. Auerswald. 2009. Effects of hydrodynamically rough grassed waterways on dissolved reactive phosphorus loads coming from agricultural watersheds. *Journal of Environmental Quality* 38 (2): 548-559.

FitzHugh, T. W., and D. S. Mackay. 2000. Impacts of input parameter spatial aggregation on an agricultural nonpoint source pollution model. *Journal of Hydrology* 236(1–2):35-53.

Fitzsimmons, E. G. 2014. Tap water ban for Toledo residents. The New York Times. Available at: http://www.nytimes.com/2014/08/04/us/toledo-faces-second-day-of-water-ban.html?_r=0. Accessed 12 January 2016.

Francesconi, W., D. R. Smith, D. C. Flanagan, C. Huang, and X. Wang. 2015. Modeling conservation practices in APEX : from the field to the watershed. *Journal of Great Lakes Research* 41 (3): 760–769.

Gassman, P. W., M. R. Reyes, C. H. Green, and J. G. Arnold. 2007. The Soil and Water Assessment Tool: Historical development, applications, and future research directions. *Transactions of the ASABE* 50 (4): 1211–1250.

Ginting, D., J. Moncrief, and S. Gupta. 2000. Runoff, solids, and contaminant losses into surface tile inlets draining lacustrine depressions. *Journal of Environmental Quality* 29(2):551-560.

Gosain, A., S. Rao, and D. Basuray. 2006. Climate change impact assessment on hydrology of Indian river basins. *Current Science* 90(3):346-353.

Green, W. H., and G. A. Ampt. 1911. Studies on soil physics: 1. The flow of air and water through soils. *Journal of Agricultural Science* 4: 11-24.

Haddad, O. B., M. Jahandideh-Tehrani, and M. A. Marino. 2013. Discussion of 'Assessments of Impacts of Climate Change and Human Activities on Runoff with SWAT for the Huifa River Basin, Northeast China' by Aijing Zhang; Chi Zhang; Guobin Fu; Bende Wang; Zhenxin Bao; and Hongxing Zheng. *Water Resources Management* 27 (7): 2071–2073.

Hartkamp, A., J. White, and G. Hoogenboom. 2003. Comparison of three weather generators for crop modeling: a case study for subtropical environments. *Agricultural Systems* 76(2):539-560.

Heathman, G., M. Larose, and J. Ascough. 2009. Soil and Water Assessment Tool evaluation of soil and land use geographic information system data sets on simulated stream flow. *Journal of Soil and Water Conservation* 64(1):17-32.

Heathman, G., M. Larose, L. Oxley, and D. Kulasiri. 2007. Influence of scale on SWAT model calibration for streamflow. *Modsim 2007: International Congress on Modelling and Simulation* 2747-2753.

Hoang, L., A. van Griensven, P. van der Keur, J. Refsgaard, L. Troldborg, B. Nilsson, and A. Mynett. 2014. Comparison and evaluation of model structures for the simulation of pollution fluxes in a tile-drained river basin. *Journal of Environmental Quality* 43(1):86-99.

IPCC (Intergovernmental Panel on Climate Change). 2014. Climate Change 2014: Impacts, Adaptation, and Vulnerability. Part A: Global and Sectoral Aspects. Contribution of Working Group II to the Fifth Assessment Report of the Intergovernmental Panel on Climate Change [Field, C.B., V.R. Barros, D.J. Dokken, K.J. Mach, M.D. Mastrandrea, T.E. Bilir, M. Chatterjee, K.L. Ebi, Y.O. Estrada, R.C. Genova, B. Girma, E.S. Kissel, A.N. Levy, S. MacCracken, P.R. Mastrandrea, and L.L. White (eds.)]. Cambridge University Press, Cambridge, United Kingdom and New York, NY, USA.

Jeppesen, E., B. Kronvang, M. Meerhoff, M. Sondergaard, K. Hansen, H. Andersen, T. Lauridsen, L. Liboriussen, M. Beklioglu, A. Ozen, and J. Olesen. 2009. Climate change effects on runoff, catchment loading and lake ecological state, and potential adaptations. *Journal of Environmental Quality* 38(5):1930-1941.

Jha, M., P. W. Gassman, S. Secchi, R. Gu, and J. Arnold. 2004. Effect of watershed subdivision on SWAT flow, sediment, and nutrient predictions. *Journal of the American Water Resources Association* 40(3):811-825.

Jones Jr.,. J. B. 2002. *Agronomic Handbook: Management of Crops, Soils and Their Fertility.* CRC press.

Jones, P., and P. Thornton. 2013. Generating downscaled weather data from a suite of climate models for agricultural modelling applications. *Agricultural Systems* 114:1-5.

Jones, P., and P. Thornton. 2000. MarkSim: Software to generate daily weather data for Latin America and Africa. *Agronomy Journal* 92(3):445-453.

Jones, P., and P. Thornton. 1999. Fitting a third-order Markov rainfall model to interpolated climate surfaces. *Agricultural and Forest Meteorology* 97(3):213-231.

Jones, P. G., and P. K. Thornton. 1993. A rainfall generator for agricultural applications in the tropics. *Agricultural and Forest Meteorology* 63(1-2):1-19.

Kaini, P., A. Kim, and J. W. Nicklow. 2012. Optimizing structural best management practices using SWAT and genetic algorithm to improve water quality goals. *Water Resources Management* 26:1827–1845

Khoi, D. N., and T. Suetsugi. 2012. Hydrologic response to climate change: a case study for the Be River Catchment, Vietnam. *Journal of Water and Climate Change* 3 (3): 207–224.

Kim, J., J. Choi, C. Cho, S. Park. 2013. Impacts of changes in climate and land use/land cover under IPCC RCP scenarios on streamflow in the Hoeya River Basin, Korea. *Science of the Total Environment* 452: 181–195.

King, K. W., J. G. Arnold, and R. L. Bingner. 1999. Comparison of Green-Ampt and curve number methods on Goodwin Creek watershed using SWAT. *Transactions of the ASAE* 42(4): 919-925.

Kirsch, K., A. Kirsch, and J. Arnold. 2002. Predicting sediment and phosphorus loads in the Rock River basin using SWAT. *Transactions of the ASAE* 45(6):1757-1769.

Kling, H. and H. Gupta. 2009. On the development of regionalization relationships for lumped watershed models: the impact of ignoring sub-basin scale variability. *Journal of Hydrology* 373, 337–351.

Knisel, W. G., ed. 1980. CREAMS: A field-scale model for chemicals, runoff, and erosion from agricultural management systems. Conservation Research Report No. 26. Washington D.C.: USDA Science and Education Administration.

Kunkel, K. E., L. E. Stevens, S. E. Stevens, L. Sun, E. Janssen, D. Wuebbles, S. D. Hilberg, M. S. Timlin, L. Stoecker, N. E. Westcott, and J. G. Dobson. 2013: Regional Climate Trends and Scenarios for the U.S. National Climate Assessment: Part 3. Climate of the Midwest U.S. NOAA Technical Report NESDIS 142-3. 103 pp., National Oceanic and Atmospheric Administration, National Environmental Satellite, Data, and Information Service, Washington, D.C.

Kumar, S., and V. Merwade. 2009. Impact of watershed subdivision and soil data resolution on SWAT model calibration and parameter uncertainty. *Journal of the American Water Resources Association* 45(5):1179-1196.

Lake Erie LAMPs (Lake Erie Lakewide Action and Management Plans). 2011. Status of Nutrients in the Lake Erie Basin. Available at: http://www.epa.gov/sites/production/files/2015-10/documents/status-nutrients-lake-erie-basin-2010-42pp.pdf. Accessed 12 October 2015.

Larose, M., G. Heathman, L. Norton, and B. Engel. 2007. Hydrologic and atrazine simulation of the Cedar Creek Watershed using SWAT. *Journal of Environmental Quality* 36(2):521-531.

Lee, M., G. Park, M. Park, J. Park, J. Lee, S. Kim. 2010. Evaluation of nonpoint source pollution reduction by applying Best Management Practices using a SWAT model and QuickBird high resolution satellite imagery. *Journal of Environmental Sciences-China* 22 (6): 826–833 DOI: 10.1016/S1001-0742(09)60184-4

Legates, D., and G. McCabe. 1999. Evaluating the use of "goodness-of-fit" measures in hydrologic and hydroclimatic model validation. *Water Resources Research* 35(1):233-241.

Leonard, R., W. Knisel, and D. Still. 1987. GLEAMS - Groundwater Loading Effects of Agricultural Management-Systems. *Transactions of the ASAE* 30(5):1403-1418.

Lim, K., B. Engel, Z. Tang, J. Choi, K. Kim, S. Muthukrishnan, and D. Tripathy. 2005. Automated web GIS based hydrograph analysis tool, WHAT. *Journal of the American Water Resources Association* 41(6):1407-1416.

Lobell, D., and M. Burke. 2010. On the use of statistical models to predict crop yield responses to climate change. *Agricultural and Forest Meteorology* 150(11):1443-1452.

Mausbach, M., and A. Dedrick. 2004. The length we go - Measuring environmental benefits of conservation practices. *Journal of Soil and Water Conservation* 59(5):96A-103A.

Mavromatis, T., and J. Hansen. 2001. Interannual variability characteristics and simulated crop response of four stochastic weather generators. *Agricultural and Forest Meteorology* 109(4):283-296.

Mishra, S., M. Jain, R. Pandey, and V. Singh. 2005. Catchment area-based evaluation of the AMC-dependent SCS-CN-based rainfall-runoff models. *Hydrological Processes* 19(14):2701-2718.

Mishra, S., M. Jain, and V. Singh. 2004. Evaluation of the SCS-CN-based model incorporating antecedent moisture. *Water Resources Management* 18(6):567-589.

Monteith, J. 1995. Accomodation between transpiring vegetation and the convective boundary-layer. *Journal of Hydrology* 166(3-4):251-263.

Moriasi, D. N., J. G. Arnold, M. W. Van Liew, R. L. Bingner, R. D. Harmel, and T. L. Veith. 2007. Model evaluation guidelines for systematic quantification of accuracy in watershed simulations. *Transactions of the ASABE* 50(3):885-900.

Muleta, M., and J. Nicklow. 2005. Sensitivity and uncertainty analysis coupled with automatic calibration for a distributed watershed model. *Journal of Hydrology* 306(1-4):127-145.

Narsimlu, B., A. Gosain, and B. Chahar. 2013. Assessment of future climate change impacts on water resources of Upper Sind River Basin, India using SWAT model. *Water Resources Management* 27(10):3647-3662.

Nash, J. E., and J. V. Sutcliffe. 1970. River flow forecasting through conceptual models part I - A discussion of principles. *Journal of Hydrology* 10(3): 282–290.

Neitsch, S. L., J.G. Arnold, J.R. Kiniry, and J.R. Williams. 2002. Soil and Water Assessment Tool (SWAT): User's Manual. http://swat.tamu.edu/media/1294/swatuserman.pdf: Grassland, Soil & Water Research Laboratory, and Blackland Research and Extension Center, Temple, Texas.

Pappas, E. A., and D. R. Smith. 2007. Effects of dredging an agricultural drainage ditch on water column herbicide concentration, as predicted by fluvarium techniques. *Journal of Soil and Water Conservation* 62(4):262-268.

Parajuli, P. B., K. R. Mankin, and P. L. Barnes. 2008. Applicability of targeting vegetative filter strips to abate fecal bacteria and sediment yield using SWAT. *Agricultural Water Management* 95 (10): 1189–1200.

Park J. Y., G. A. Park, and S. J. Kim. 2013. Assessment of future climate change impact on water quality of chungju lake, South Korea, using WASP coupled with SWAT. *Journal of the American Water Resources Association* 49 (6): 1225–1238.

Parker, R., J. Arnold, M. Barrett, L. Burns, L. Carrubba, S. Neitsch, N. Snyder, and R. Srinivasan. 2007. Evaluation of three watershed-scale pesticide environmental transport and fate models. *Journal of the American Water Resources Association* 43(6):1424-1443.

Pfister, L., J. Kwadijk, A. Musy, A. Bronstert, and L. Hoffmann. 2004. Climate change, land use change and runoff prediction in the Rhine-Meuse basins. *River Research and Applications* 20(3):229-241.

Ponce, V., and R. Hawkins. 1996. Runoff curve number: has it reached maturity? *Journal of Hydrologic Engineering* 1(1):11-19.

Pryor, S. C., D. Scavia, C. Downer, M. Gaden, L. Iverson, R. Nordstrom, J. Patz, and G. P. Robertson. 2014: Ch. 18: Midwest. Climate Change Impacts in the United States: The Third National Climate Assessment, J. M. Melillo, Terese (T.C.) Richmond, and G. W. Yohe, Eds., U.S. Global Change Research Program, 418-440.

Raneesh, K. Y., and G. T. Santosh. 2011. A study on the impact of climate change on streamflow at the watershed scale in the humid tropics. *Hydrological Sciences Journal-Journal Des Sciences Hydrologiques* 56 (6): 946–965.

Rao, B., R. Kurothe, P. Mishra, G. Kumar, and V. Pande. 2015. Climate change impact on design and costing of soil and water conservation structures in watersheds. *Current Science* 108(5):960-966.

Rawls, W. J., C. Onstad, and H. H. Richardson. 1980. Residue and tillage effects on SCS runoff curve numbers. *Transactions of the ASAE* 23(2):357-361.

Rawls, W. J., and H. H. Richardson. 1983. Runoff curve numbers for conservation tillage. *Journal of Soil and Water Conservation* 38(6):494-496.

Richards, R., F. Calhoun, G. Matisoff., 2002. The Lake Erie agricultural systems for environmental quality project: An introduction. *Journal of Environmental Quality* 31, 6-16.

Roth, G.W. 1996. Crop Rotations and Conservation Tillage. *PennState University Conservation Tillage Series: 4.*

Running, S., and C. Reid. 1980. Soil-temperature influences on root resistance of Pinus-Contorta seedlings. *Plant Physiology* 65(4):635-640.

Runkel, R. L., C. G. Crawford, and T. A. Cohn. 2004, Load Estimator (LOADEST): A FORTRAN program for estimating constituent loads in streams and rivers, U.S. Geological Survey Techniques Methods. Book 4, Chap. A5, 69 pp.

Santhi C., J. G. Arnold, J. R. Williams, L. M. Hauck, W. A. Dugas. 2001. Application of a watershed model to evaluate management effects on point and nonpoint source pollution. *Transactions of the ASABE* 44 (6): 1559–1570.

Santhi, C., J. Arnold, J. Williams, W. Dugas, R. Srinivasan, and L. Hauck. 2001. Validation of the SWAT model on a large river basin with point and nonpoint sources. *Journal of the American Water Resources Association* 37(5):1169-1188.

Secchi, S., P. Gassman, M. Jha, L. Kurkalova, H. Feng, T. Campbell, and C. Kling. 2007. The cost of cleaner water: Assessing agricultural pollution reduction at the watershed scale. *Journal of Soil and Water Conservation* 62(1):10-21.

Sharpley A. N., S. J. Smith. 1994. Wheat tillage and water-quality in the southern plains. *Soil & Tillage Research* 30 (1): 33–48.

Sharpley A. N., L. Bergström, H. Aronsson, M. Bechmann, C. H. Bolster, K. Börling, F. Djodjic, H. P. Jarvie, O. F. Schoumans, C. Stamm. 2015. Future agriculture with minimized losses to waters: Research needs and direction. *Ambio* 44 (S2): 163–179.

Shipitalo M. J. 2013. Effect of no-till and extended rotation on nutrient losses in surface runoff soil & water management & conservation. *Soil Science Society of America Journal* 77 (July 2013): 1329–1337.

SJRWI (St. Joseph River Watershed Initiative). 2005. Cedar Creek watershed management plan. ARN01-383. Available at: http://www.sjrwi.org/cp_5. Accessed January 12 2014.

Smith, D. R., and S. J. Livingston. 2013. Managing farmed closed depressional areas using blind inlets to minimize and nitrogen losses. *Soil Use and Management* 29:94-102.

Smith, D. R., S. J. Livingston, B. W. Zuercher, M. Larose, G. C. Heathman, and C. Huang. 2008. Nutrient losses from row crop agriculture in Indiana. *Journal of Soil and Water Conservation* 63(6):396-409.

Southworth, J., R. Pfeifer, M. Habeck, J. Randolph, O. Doering, J. Johnston, and D. Rao. 2002. Changes in soybean yields in the midwestern United States as a result of future changes in climate, climate variability, and $CO_2$ fertilization. *Climatic Change* 53(4):447-475.

Spruill, C., S. Workman, and J. Taraba. 2000. Simulation of daily and monthly stream discharge from small watersheds using SWAT. *Transactions of the ASAE* 43(6):1431-1439.

Srinivasan, R., T. S. Ramanarayanan, J. G. Arnold, and S. T. Bednarz. 1998. Large area hydrologic modeling and assessment part II. Modeling application. *Journal of the American Water Resources Association* 34(1):91-101.

Sun, G., D. Amatya, S. McNulty, R. Skaggs, and J. Hughes. 2000. Climate change impacts on the hydrology and productivity of a pine plantation. *Journal of the American Water Resources Association* 36(2):367-374.

Thampi, S., K. Raneesh, and T. Surya. 2010. Influence of scale on SWAT model calibration for streamflow in a river basin in the humid tropics. *Water Resources Management* 24(15):4567-4578.

Thornton, P., P. Jones, G. Alagarswamy, J. Andresen, and M. Herrero. 2010. Adapting to climate change: Agricultural system and household impacts in East Africa. *Agricultural Systems* 103(2):73-82.

Tolson, B., and C. Shoemaker. 2007. Cannonsville reservoir watershed SWAT2000 model development, calibration and validation. *Journal of Hydrology* 337(1-2):68-86.

Tomer, M., C. Wilson, T. Moorman, K. Cole, D. Heer, and T. Isenhart. 2010. Source-pathway separation of multiple contaminants during a rainfall-runoff event in an artificially drained agricultural watershed. *Journal of Environmental Quality* 39(3):882-895.

Trotochaud, J., D. C. Flanagan, and B. A. Engel. 2016. A simple technique for obtaining future climate data inputs for natural resource models. Applied Engineering in Agriculture (In press).

Tuppad P., N. Kannan, R. Srinivasan, C. G. Rossi and J. G. Arnold. 2010. Simulation of agricultural management alternatives for watershed protection. *Water Resources Management* 24 (12): 3115–3144.

USDA NRCS (United States Department of Agriculture, Natural Resources Conservation Service). 2014. NRCS Conservation Practices Available at: http://www.nrcs.usda.gov/wps/portal/nrcs/detailfull/national/technical/cp/ncps/?cid=nrcs143_026849. Accessed 1 November 2014.

USDA (United States Department of Agriculture). 2014. Soil Survey Geographic (SSURGO) Database. Natural Resources Conservation Service, National Soil Survey Center. Washington, D.C. Available at http://datagateway.nrcs.usda.gov/GDGOrder.aspx. Accessed 10 January 2014.

USDA (United States Department of Agriculture). 2011. National Agricultural Statistics Service (NASS). Available at https://nassgeodata.gmu.edu/CropScape/. Accessed 10 January 2014.

USDA (United States Department of Agriculture). 2011b. National Elevation Dataset (NED). Natural Resources Conservation Service, National Soil Survey Center. Washington, D.C.. Available at http://datagateway.nrcs.usda.gov/GDGOrder.aspx. Accessed 10 January 2014.

USDA-SCS (United States Department of Agriculture, Soil Conservation Service). 1986. Urban hydrology for small watersheds. SCS Technical release 55. US Government Printing Office, Washington, D. C.

USEPA (U.S. Environmental Protection Agency). 2014. Climate impacts in the Midwest. Available at: https://www3.epa.gov/climatechange/impacts/midwest.html. Accessed: 15 March, 2016.

USEPA (U.S. Environmental Protection Agency). 2014. Great Lakes Monitoring. Available at: http://www.epa.gov/greatlakes/glindicators/water/. Accessed: 28 October, 2014.

USEPA (U.S. Environmental Protection Agency). 2011. Healthy Watersheds Initiative. Available at: https://www.scgcorp.com/docs/EPA_HWI_2011_FINAL.pdf. Accessed: 12 January 2016.

USEPA (U.S. Environmental Protection Agency). 2002. Federal water pollution control act: 234.

USEPA (U.S. Environmental Protection Agency). 1994. National Water Quality Inventory. 1992 Report to Congress. EPA-841-R-94-001. Office of Water, Washington, DC. Available at: http://www.fao.org/docrep/w2598e/w2598e04.htm. Accessed: 12 January 2016.

USGCRP (United States Global Change Research Program). 2009. Climate Change Impacts on the United States: The Potential Consequences of Climate Variability and Change and associated documents. Available at https://downloads.globalchange.gov/usimpacts/pdfs/climate-impacts-report.pdf. Accessed: 7 November 2014.

Vache K. B., J. M. Eilers and M.V. Santelmann. 2002. Water quality modeling of alternative agricultural scenarios in the US corn belt. Journal of the American Water Resources Association 38 (3): 773–787.

Van Liew, M., J. Arnold, and J. Garbrecht. 2003. Hydrologic simulation on agricultural watersheds: Choosing between two models. *Transactions of the ASAE* 46(6):1539-1551.

Van Liew, M., and J. Garbrecht. 2003. Hydrologic simulation of the Little Washita River experimental watershed using SWAT. *Journal of the American Water Resources Association* 39(2):413-426.

Vitosh M. L., J. W. Johnson, and D. B. Mengel. 1995. Tri-State Fertilizer Recommendations for Corn, Soybeans, Wheat and Al. *Time* 2567 (July).

Walsh, J., D. Wuebbles, K. Hayhoe, J. Kossin, K. Kunkel, G. Stephens, P. Thorne, R. Vose, M. Wehner, J. Willis, D. Anderson, S. Doney, R. Feely, P. Hennon, V. Kharin, T. Knutson, F. Landerer, T. Lenton, J. Kennedy, and R. Somerville, 2014. Ch. 2: Our Changing Climate. Climate Change Impacts in the United States: The Third National Climate Assessment, J. M. Melillo, Terese (T.C.) Richmond, and G. W. Yohe, Eds., U.S. Global Change Research Program, 19-67.

Wang, R., L. C. Bowling, and K. A. Cherkauer. 2016. Estimation of the effects of climate variability on crop yield in the Midwest USA. *Agricultural and Forest Meteorology* 216: 141-156.

Wang X., P. W. Gassman, J. R. Williams, S. R. Potter, and A. R. Kemanian. 2008. Modeling the impacts of soil management practices on runoff, sediment yield, maize productivity, and soil organic carbon using APEX. *Soil and Tillage Research* 101 (1-2): 78–88.

White, K., and I. Chaubey. 2005. Sensitivity analysis, calibration, and validations for a multisite and multivariable SWAT model. *Journal of the American Water Resources Association* 41(5):1077-1089.

Williams, J.R. and R.W. Hann. 1978. Optimal operation of large agricultural watersheds with water quality constraints. Texas Water Resources Institute, Texas A & M University, TR-96, 152 pp.

Williams, J., K. Renard, and P. Dyke. 1983. EPIC - A new method for assessing erosion's effect on soil productivity. *Journal of Soil and Water Conservation* 38(5):381-383.

Winkler, J.A., R.W. Arritt, S.C. Pryor. 2012: Climate Projections for the Midwest: Availability, Interpretation and Synthesis. In: U.S. National Climate Assessment Midwest Technical Input Report. Available from the Great Lakes Integrated Sciences and Assessment (GLISA) Center, http://glisa.msu.edu/docs/NCA/MTIT_Future.pdf.

Woznicki S. A,, and P.A. Nejadhashemi. 2014. Assessing uncertainty in best management practice effectiveness under future climate scenarios. *Hydrological Processes* 28 (4): 2550–2566.

Wright J., and G. Sands. 2001. Planning an agricultural subsurface drainage system in agricultural drainage. Publication No. BU-07685. Minnesota Extension Service, University of Minnesota, St. Paul, MN, USA.

Wuebbles, D. J., and K. Hayhoe. 2004. Climate Change Projections for the United States Midwest. *Mitigation Adaptation. Strategies Global Change* 9: 335–363.

Yang, B., P. Blackwell, and D. Nicholson. 1996. A numerical model of heat and water movement in furrow-sown water repellent sandy soils. *Water Resources Research* 32(10):3051-3061.

Yu, C., W. Northcott, and G. McIsaac. 2004. Development of an artificial neural network for hydrologic and water quality modeling of agricultural watersheds. *Transactions of the ASAE* 47(1):285-290.

Zahabiyoun B., M. R. Goodarzi, A. R. M. Bavani, and H. M. Azamathulla. 2013. Assessment of climate change impact on the Gharesou River Basin using SWAT hydrological model. *Clean-Soil Air Water* 41 (6): 601–609.

Zhang X., R. Srinivasan, and F. Hao. 2007. Predicting hydrologic response to climate change in the Luohe River basin using the SWAT model. *Transactions of the ASABE* 50 (3): 901–910.

Zhang X., R. Srinivasan, and M. Van Liew. 2008. Multi-site calibration of the SWAT model for hydrologic modeling. *Transactions of the ASABE* 51 (6): 2039–2049.

Zhang X.S., R. Srinivasan, K.G. Zhao, and M. Van Liew. 2009. Evaluation of global optimization algorithms for parameter calibration of a computationally intensive hydrologic model. *Hydrological Processes* 23 (3): 430–441.

Zhang, L., W. Lu, Y. An, D. Li, and L. Gong. 2013. Evaluation of non-point source pollution reduction by applying best management practices in Dongliao River Watershed using SWAT model. *Fresenius Environmental Bulletin* 22(2A):531-536

# APPENDICES

# APPENDICES

Appendix A: Simulated and observed monthly time series for calibration and validation.

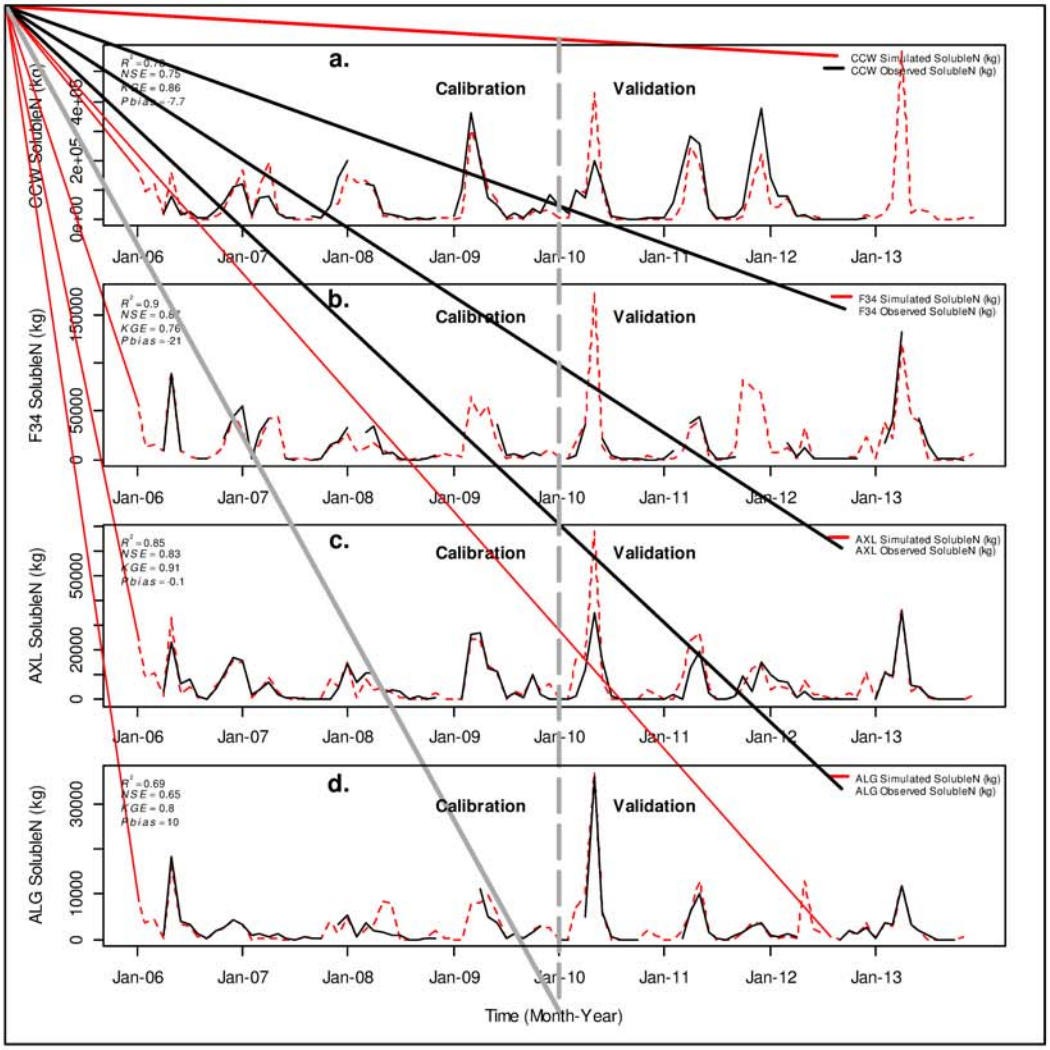


Figure A 1. Monthly time series of simulated and observed nitrate+nitrite for CCW, F34, AXL and ALG. Calibration period was from January 2006 to December 2009 and validation.

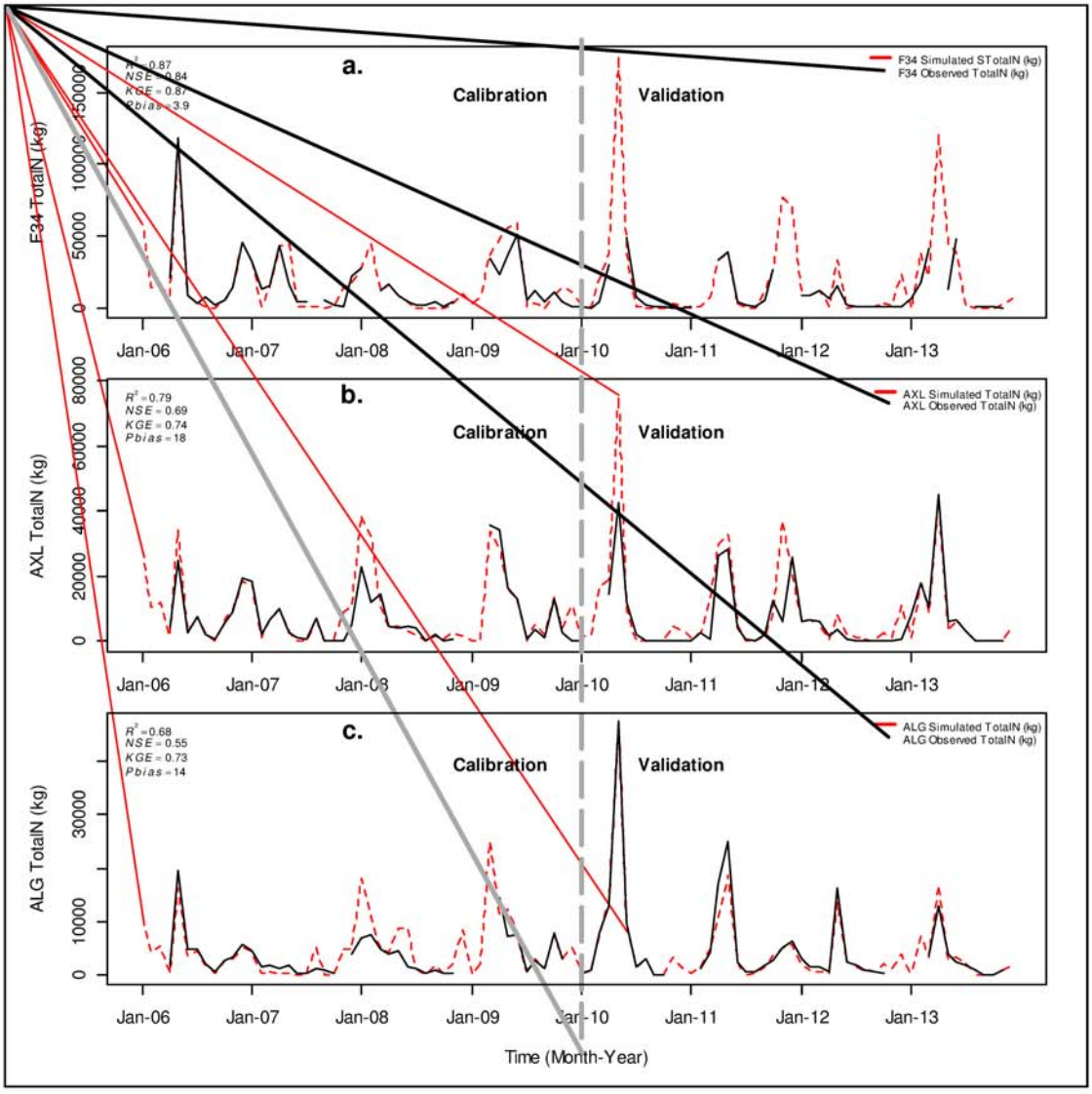


Figure A 2. Monthly time series of simulated and observed total nitrogen for CCW, F34, AXL and ALG. Calibration period was from January 2006 to December 2009 and validation period from January 2010 to December 2013.

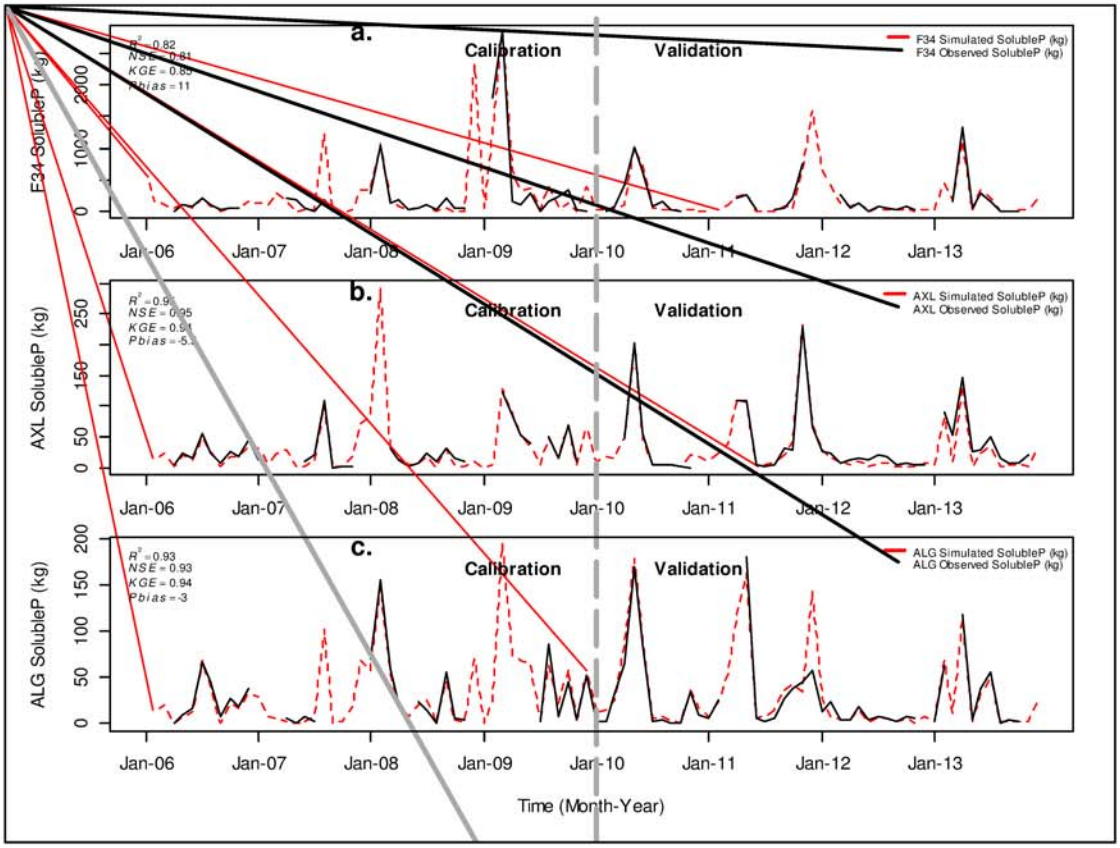


Figure A 3. Monthly time series of simulated and observed Orthophosphate (soluble P) for F34, AXL and ALG. Calibration period was from January 2006 to December 2009 and validation period from January 2010 to December 2013.

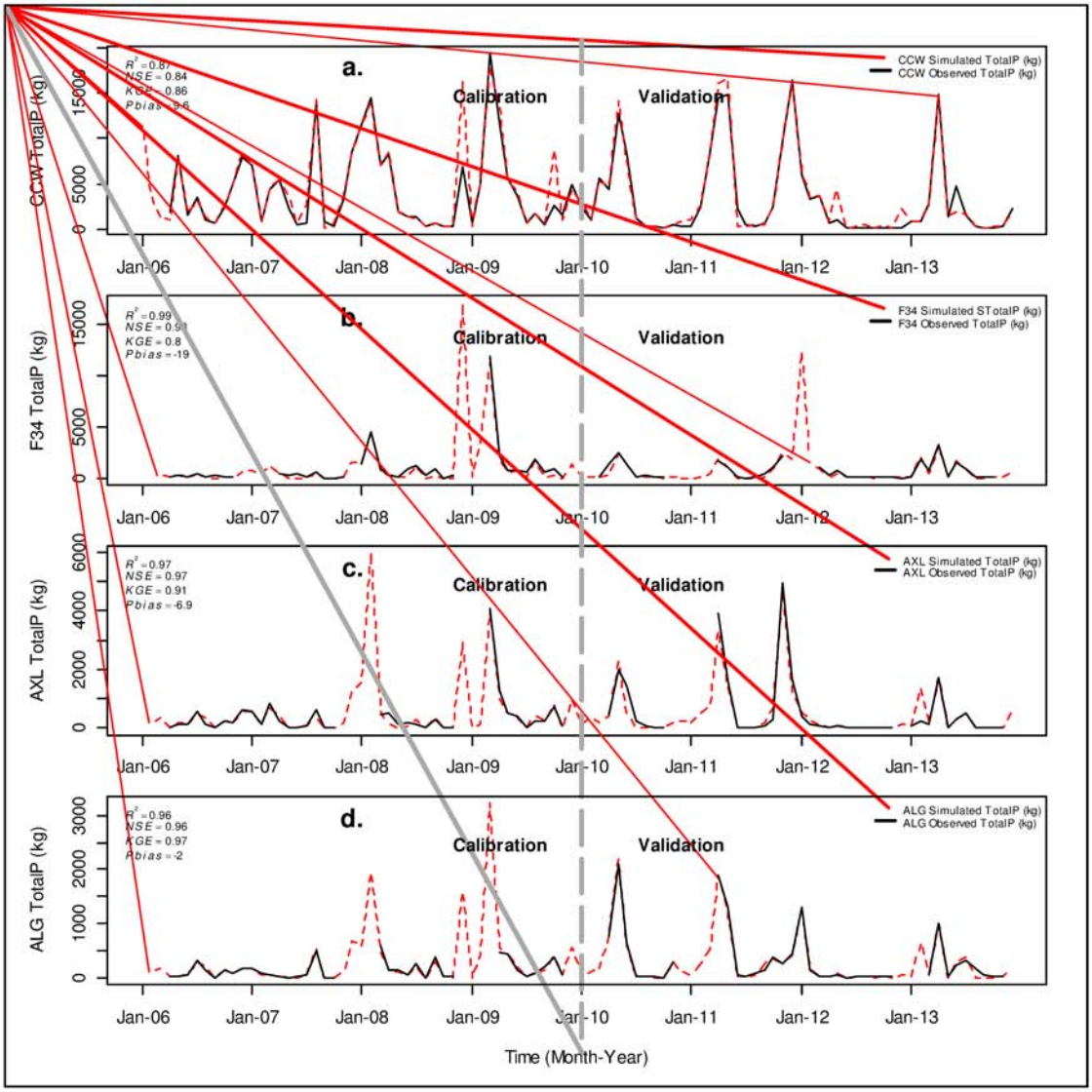


Figure A 4. Monthly time series of simulated and observed Orthophosphate (soluble P) for CCW, F34, AXL and ALG. Calibration period was from January 2006 to December 2009 and validation period from January 2010 to December 2013.

Appendix B: Nutrients load calculated using LOADEST.

| | |
|---|---|
| Site Name : | _CEDAR_CREEK_NEAR_CEDARVILLE,_IN_ |
| Parameter Name : | **Phosphorus** |
| Watershed Area : | **167833.97** ac |

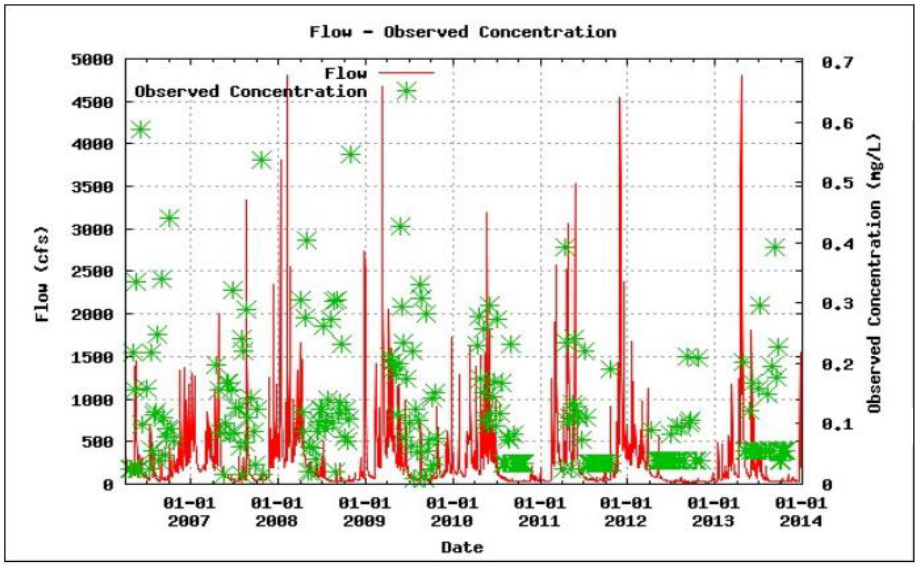


Figure B. 1. Observed total P concentration at Cedar Creek Watershed outlet.

| | Total | Per acre |
|---|---|---|
| Estimated Annual Load : | **46,238** Kg/yr | **0.3** Kg/ac/yr |
| Maximum Annual Load to Meet Target : | **19,074** Kg/yr | **0.1** Kg/ac/yr |
| Load Reduction Needed to Meet Target : | **27,164** Kg/yr | **0.2** Kg/ac/yr |

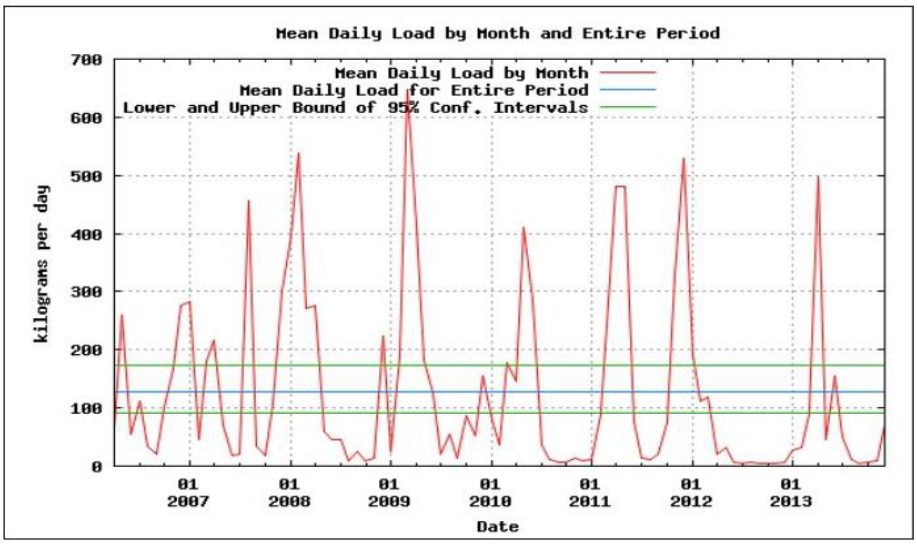


Figure B. 2. Web-based Total phosphorus Load Calculation using LOADEST.

| | |
|---|---|
| Site Name : | _CEDAR_CREEK_NEAR_CEDARVILLE, IN_ |
| Parameter Name : | Nitrate_Nitrite |
| Watershed Area : | 167833.97 ac |

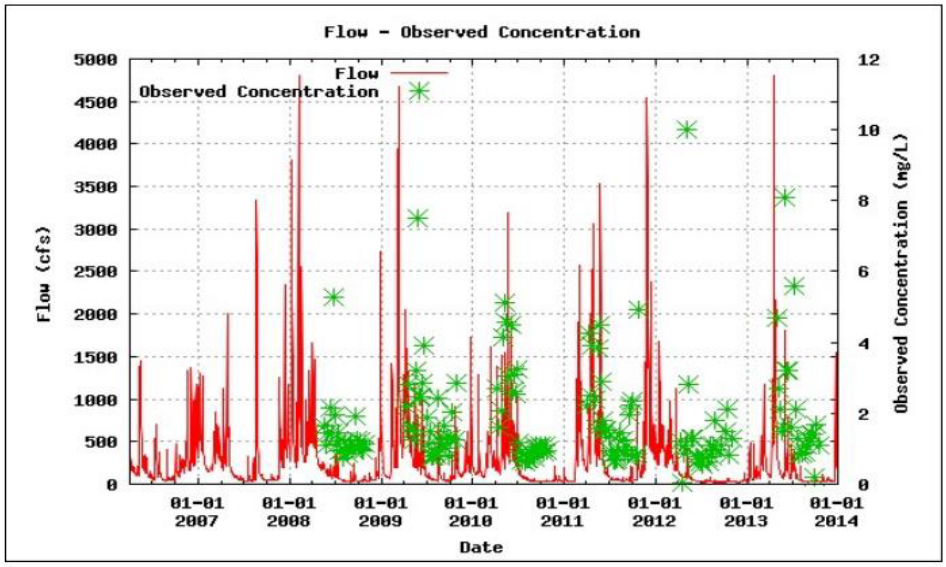


Figure B. 3. Observed total P concentration at Cedar Creek Watershed outlet.

| | Total | Per acre |
|---|---|---|
| Estimated Annual Load : | **1,132,230** Kg/yr | **6.7** Kg/ac/yr |
| Maximum Annual Load to Meet Target : | **381,481** Kg/yr | **2.3** Kg/ac/yr |
| Load Reduction Needed to Meet Target : | **750,748** Kg/yr | **4.5** Kg/ac/yr |

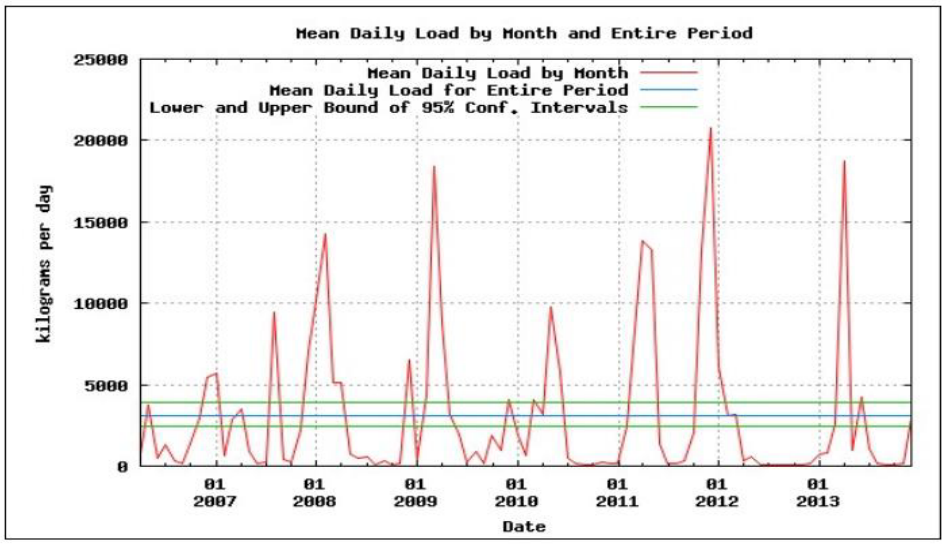


Figure B. 4. Web-based Nitrate+Nitrite Load Calculation using LOADEST.

Appendix C: Changes in surface runoff and constituent loadings.

Figures in this section contain summaries of the changes in surface runoff, sediment and chemical losses relative to the baseline scenario (existing management and cropping practices simulated under MarkSim baseline climate). The simulated BMPs include scenario 1 (no-till), scenario 2 (VFS), scenario 3 (grassed waterways), scenario 4 (blind inlets), scenario 5 (nutrient management), scenario 11 (combined BMPS – w/o nutrient management), scenario 12 (combined BMPS – w/ nutrient management)), scenario 13 (scenario 11 applied at 50%) and scenario 14 (scenario applied at 50%).

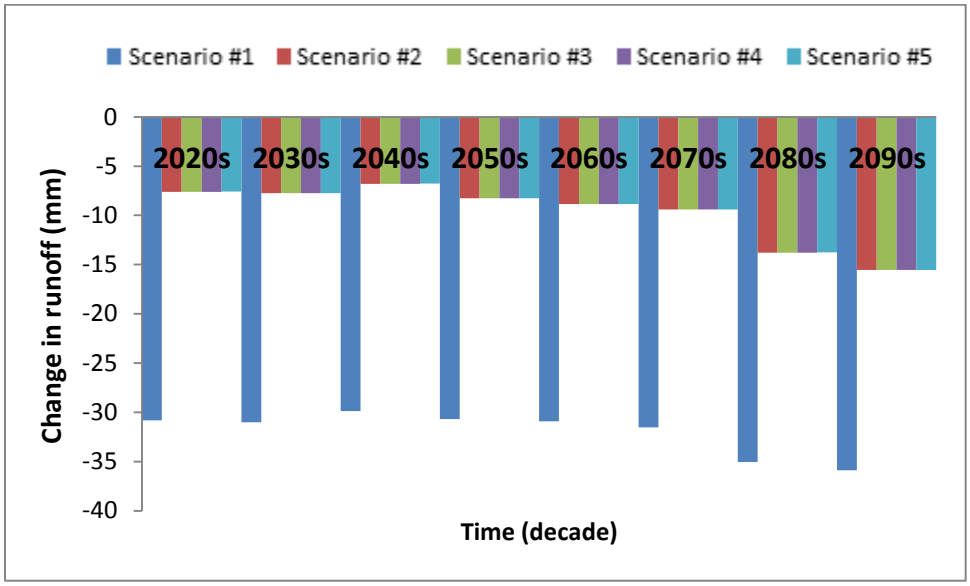


Figure C. 1. Change in average annual surface runoff (with respect to baseline simulation) resulting from individual BMP implementation and climate change.

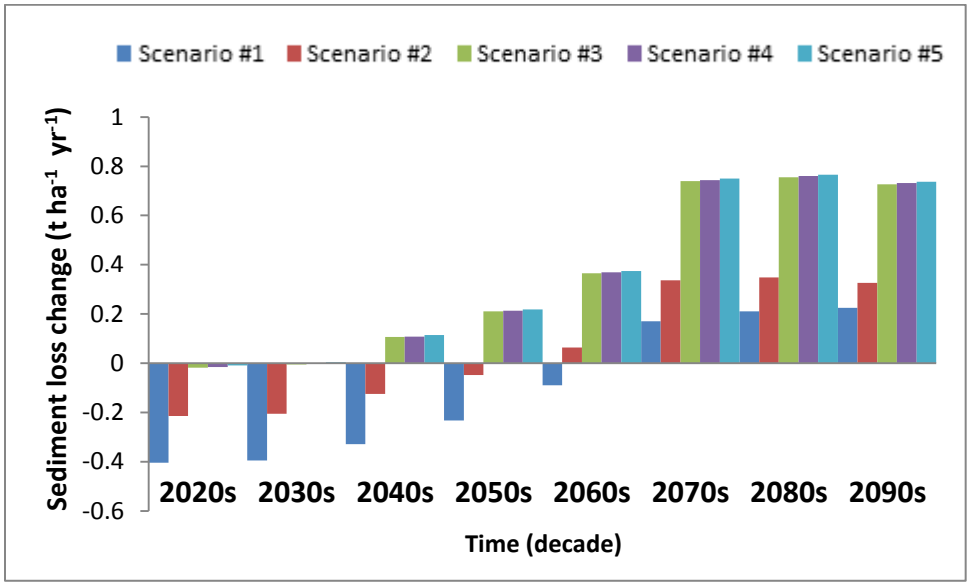


Figure C. 2. Change in average annual sediment loss (with respect to baseline simulation) resulting from individual BMP implementation and climate change.

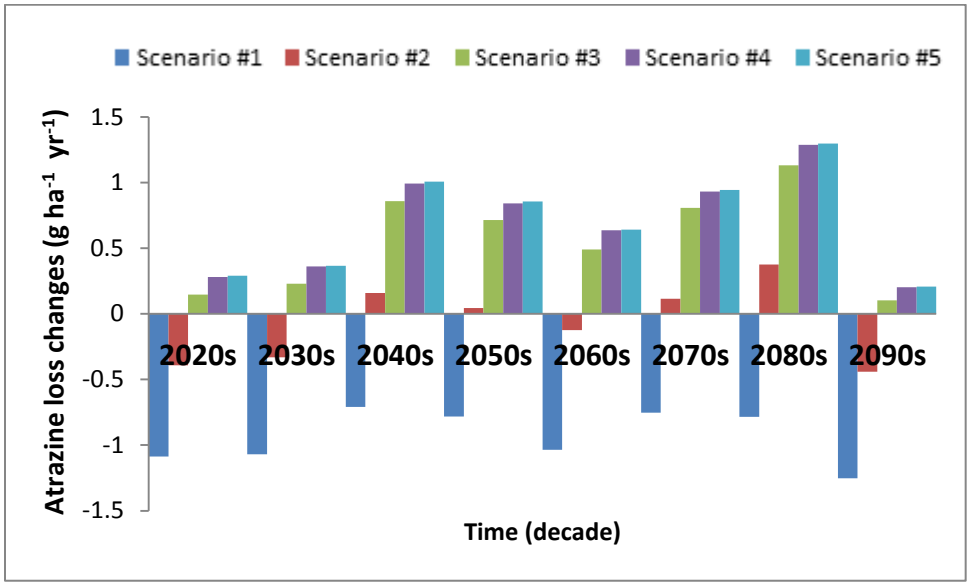


Figure C. 3. Change in average annual atrazine loss (with respect to baseline simulation) resulting from individual BMP implementation and climate change.

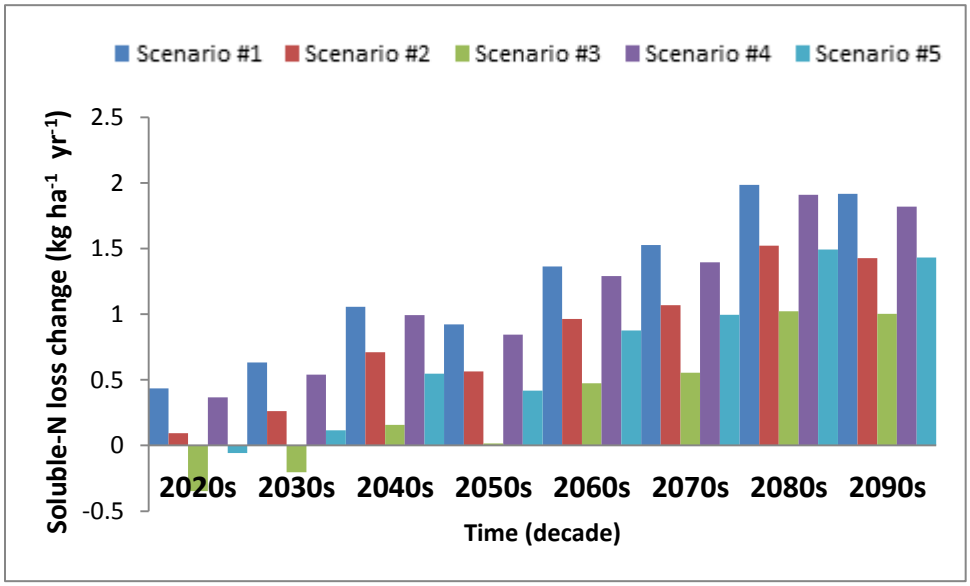


Figure C. 4. Change in average annual soluble N loss (with respect to baseline simulation) resulting from individual BMP implementation and climate change.

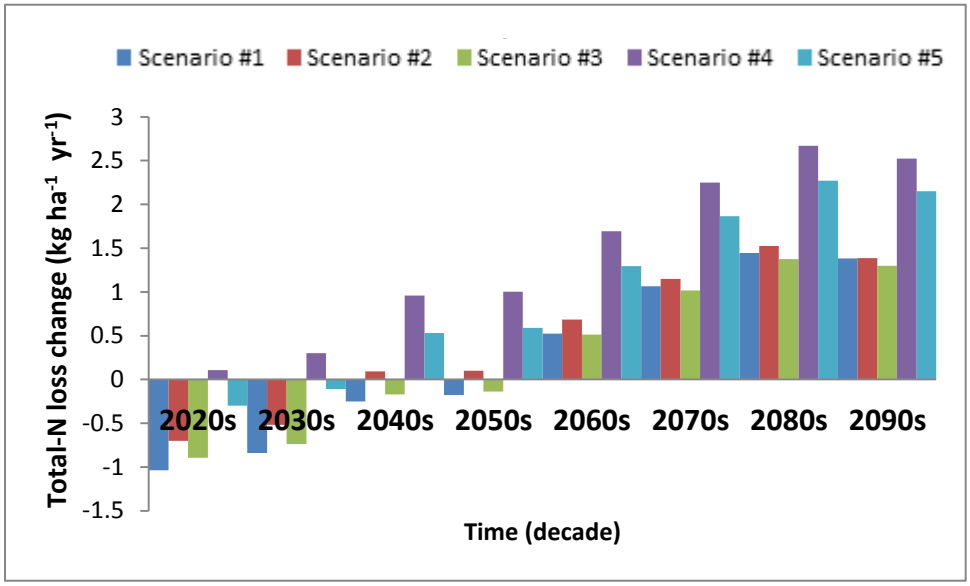


Figure C. 5. Change in average annual total N loss (with respect to baseline simulation) resulting from individual BMP implementation and climate change.

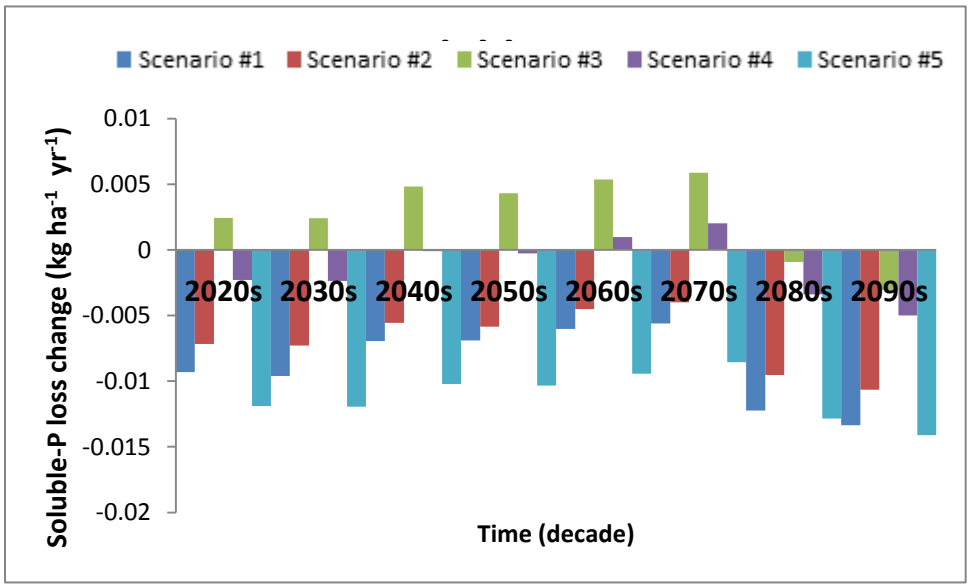


Figure C. 6. Change in average annual soluble P loss (with respect to baseline simulation) resulting from individual BMP implementation and climate change.

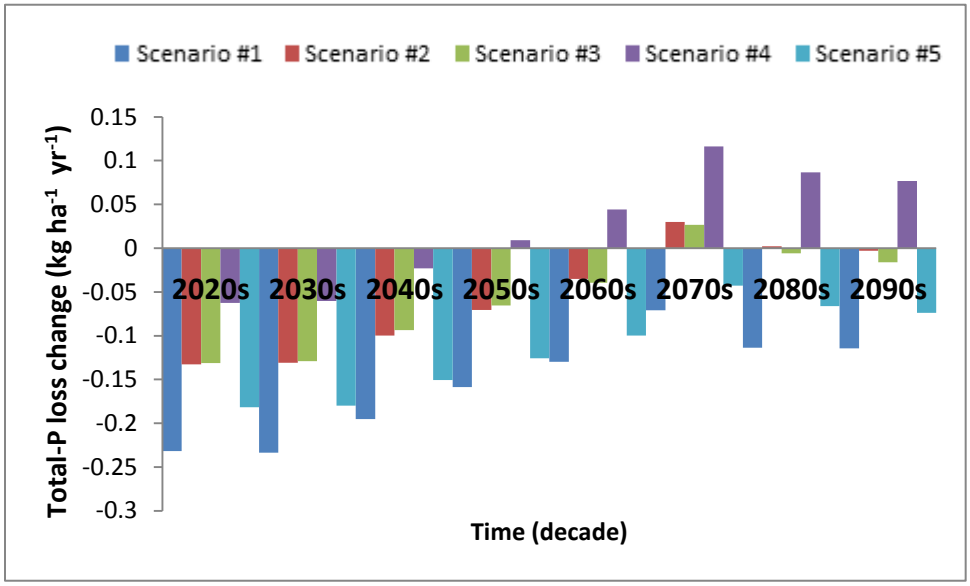


Figure C. 7. Change in average annual total P loss (with respect to baseline simulation) resulting from individual BMP implementation and climate change.

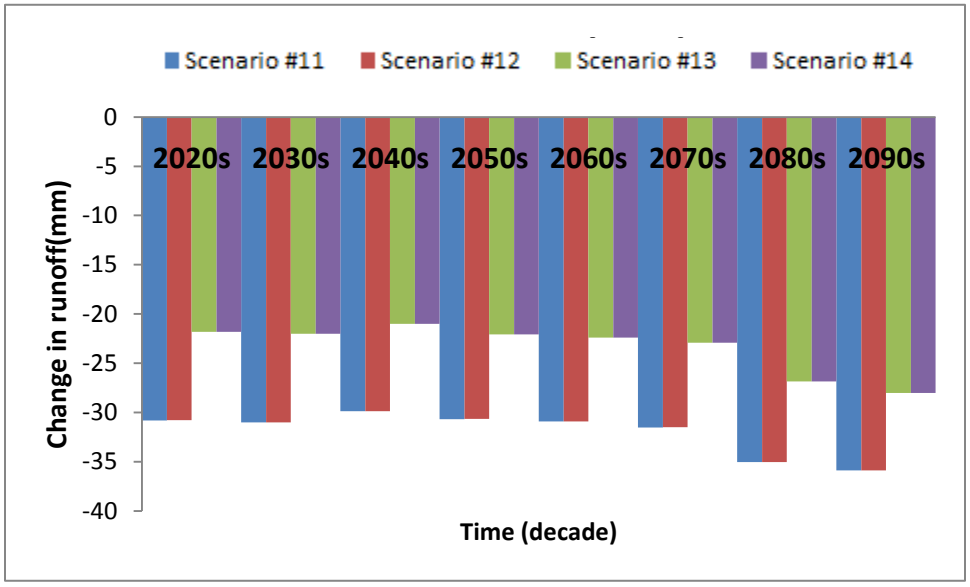


Figure C. 8. Change in average annual surface runoff (with respect to baseline simulation) resulting from combined BMPs implementation and climate change.

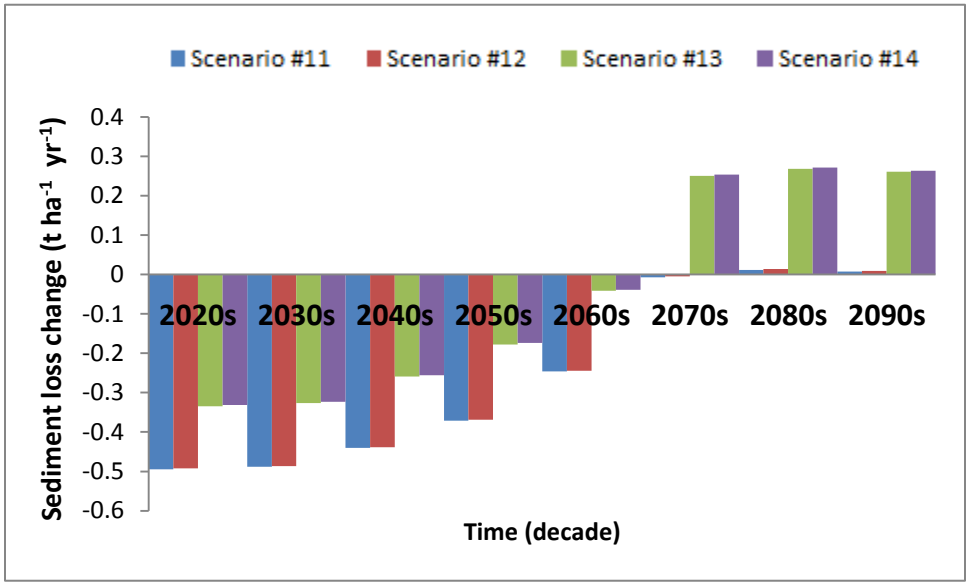


Figure C. 9. Change in average annual sediment loss (with respect to baseline simulation) resulting from combined BMPs implementation and climate change.

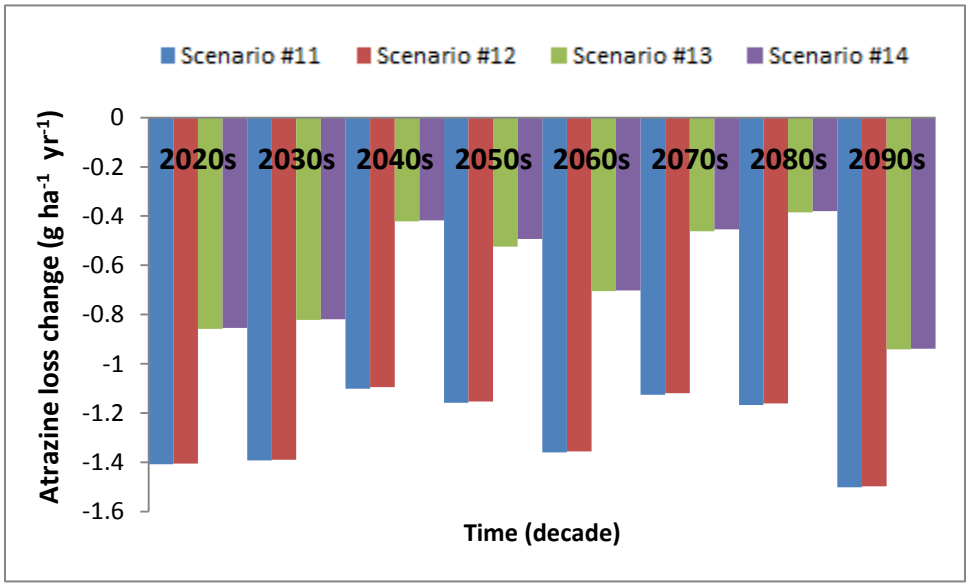


Figure C. 10. Change in average annual atrazine loss (with respect to baseline simulation) resulting from combined BMPs implementation and climate change.

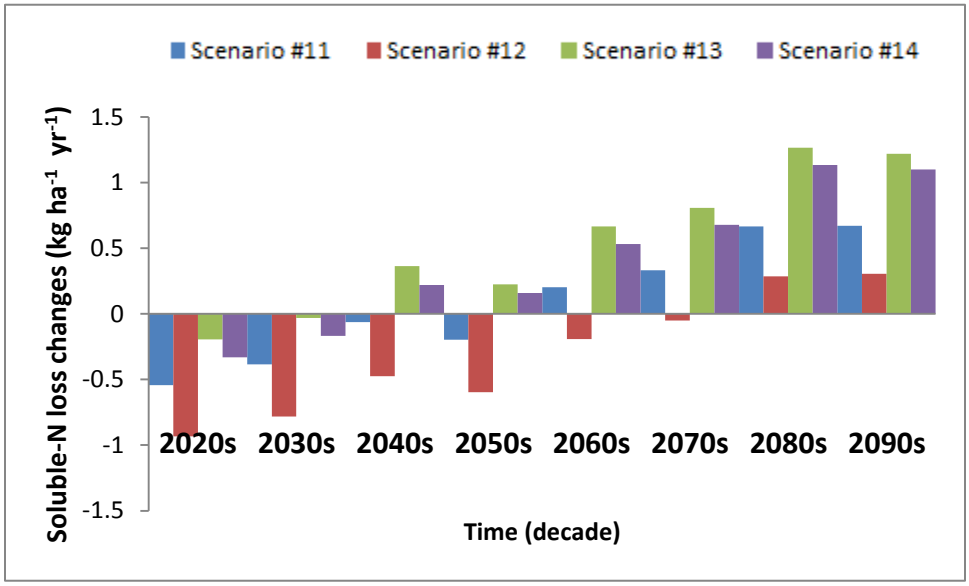


Figure C. 11. Change in average annual soluble N loss (with respect to baseline simulation) resulting from combined BMPs implementation and climate change.

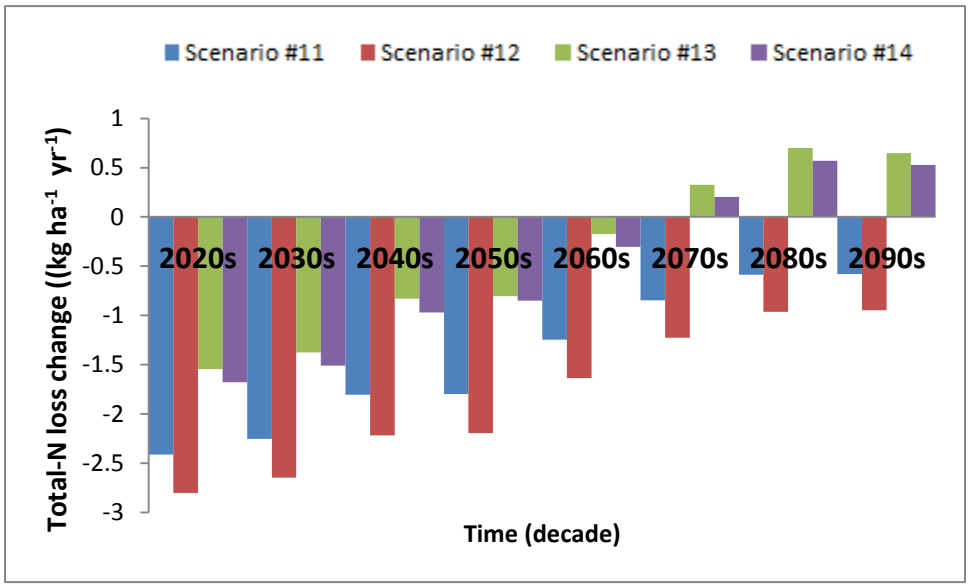


Figure C. 12. Change in average annual total N loss (with respect to baseline simulation) resulting from combined BMPs implementation and climate change.

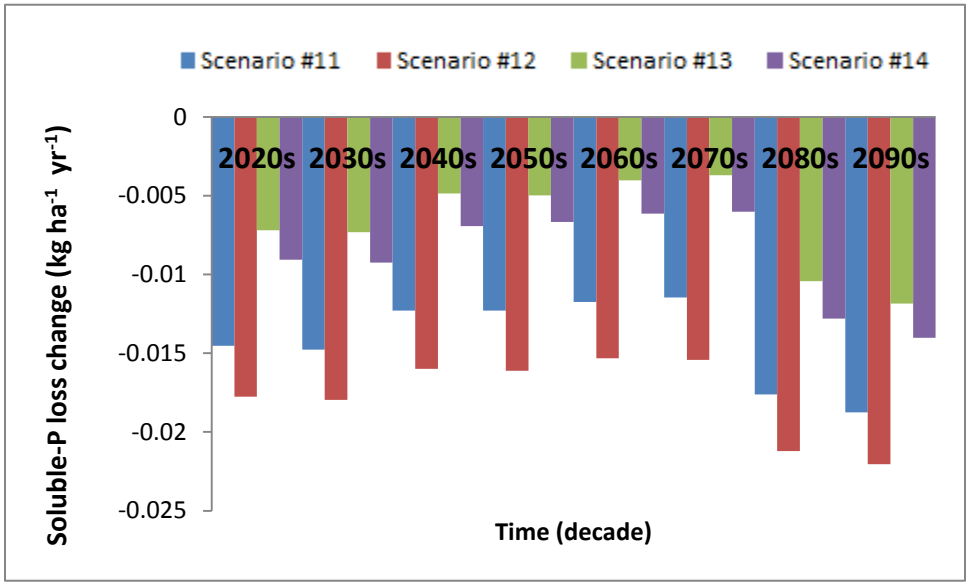


Figure C. 13. Change in average annual soluble P loss (with respect to baseline simulation) resulting from combined BMPs implementation and climate change.

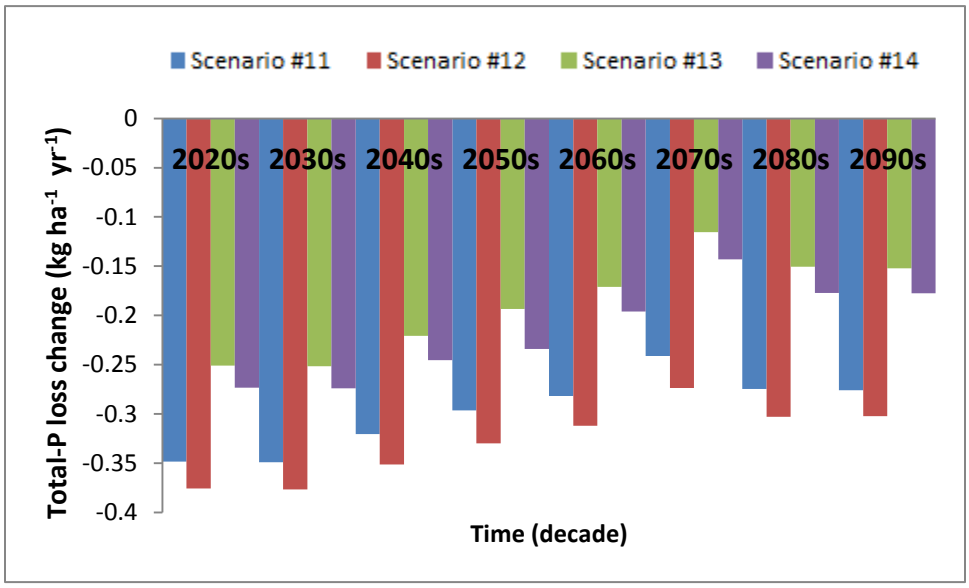


Figure C. 14. Change in average annual total P loss (with respect to baseline simulation) resulting from combined BMPs implementation and climate change.

VITA

# VITA

Carlington Wallace was born in the small Maroon village of Accompong, St. Elizabeth, Jamaica. He received his Bachelor of Science (BS) degree in Biological Engineering from North Carolina Agricultural and Technical State University (NCATSU), Greensboro, North Carolina, USA in 2010. He graduated with a Master of Science (MS) in Biological Systems Engineering from Virginia Tech University, Blacksburg, Virginia, USA in 2012. He then joined the Agricultural and Biological Engineering Department's Ph.D. program at Purdue University in August 2012.